From Data Gaps to Forest Futures: Mapping Current Conditions and Estimating Carbon Vulnerabilities in Southeast Alaska and Coastal British Columbia

by

James Lamping

A dissertation accepted and approved in partial fulfillment of the

requirements for the degree of

Doctor of Philosophy

in Geography

Dissertation Committee:

Dr. Melissa Lucash, Chair

Dr. Dan Gavin, Core Member

Dr. Mark Fonstad, Core Member

Dr. Lucas Silva, Institutional Representative

University of Oregon

Summer 2024

© 2024 James Lamping
This work is openly licensed via CC BY 4.0



DISSERTATION ABSTRACT

James Lamping

Doctor of Philosophy in Geography

Title: From Data Gaps to Forest Futures: Mapping Current Conditions and Estimating Carbon Vulnerabilities in Southeast Alaska and Coastal British Columbia

The temperate rainforests of Southeast Alaska and Coastal British Columbia are globally significant for their role in carbon storage and cycling, hosting some of the highest aboveground carbon densities in the world and large reserves of late-seral forest. Recent shifts in forest management practices have transitioned the region towards the conservation of late-seral forest, with the Tongass National Forest implementing young-growth management and British Columbia setting large areas aside for conservation. However, this region lacks estimates of forest composition and structure that are spatially complete across political boundaries. There is also uncertainty in how the interaction among young-growth management, climate change, and wind, the main driver of natural disturbance, will affect the future carbon storage capacities of these forests.

The research presented is divided into three primary chapters. The first chapter utilizes a GNN modeling approach, integrating regional forest plot data with environmental predictors to estimate aboveground biomass, species-level biomass, basal area, and three other structural attributes across a vast and ecologically diverse landscape. The study identifies key environmental variables influencing forest structure and provides comprehensive maps highlighting spatial patterns of forest attributes. The second chapter focuses on the conservation of old-growth and mature forests, employing the GNN method to classify forest seral stages. It

examines the distribution and extent of old growth and mature forests, contextualizing them within various protected areas and assessing their vulnerability to management policies. The third chapter models future carbon and species vulnerabilities under various scenarios of management and climate change using the LANDIS-II landscape model. Potential shifts in forest composition and carbon storage are quantified.

ACKNOWLEDGMENTS

First and foremost, I would like to express my deepest gratitude to my advisor, Dr. Melissa Lucash, for her unwavering support, guidance, and encouragement throughout my research and dissertation process. Her expertise and dedication have been invaluable. I extend my heartfelt thanks to my committee members, Dr. Dan Gavin, Dr. Mark Fonstad, and Dr. Lucas Silva, for their insightful feedback, constructive criticism, and continuous support. Their combined knowledge and encouragement have significantly enriched my work.

Special thanks to Dr. Brian Buma and Dr. Trevor Carter for their collaboration and guidance in our joint work in the temperate rainforest of North America. Their expertise and support have been crucial in advancing this research. I would also like to extend my gratitude to the team at the Landscape Ecology, Modeling, Mapping & Analysis (LEMMA) lab at Oregon State University and the Pacific Northwest Research Station. The endless help and support I received from Dr. Dave Bell, Dr. Matt Gregory, Dr. Harold Zald, and Dan Irvine gave me the resources and understanding needed to work in this space.

I am also deeply grateful to my family for their love and support. To my wife, Leslie Neu-Lamping, thank you for your endless patience, understanding, and encouragement (especially as we planned a wedding, had the wedding, and moved to a new city all while preparing to defend this dissertation). To my mother, thank you for always believing in me and supporting me in every step of my life. Finally, I would like to acknowledge everyone who has supported me throughout this journey, including friends, colleagues, and mentors. Your encouragement and support have made this achievement possible.

DEDICATION

This dissertation and the work therein are dedicated to William E. Lamping (1951 - 2023). Thanks for the always picking up the never-ending phone calls and always believing I would make it.

TABLE OF CONTENTS

Chapter Page

DISSERTATION ABSTRACT **3**

ACKNOWLEDGMENTS **5**

DEDICATION **6**

TABLE OF CONTENTS **7**

LIST OF FIGURES **9**

LIST OF TABLES **12**

CHAPTER 1 - INTRODUCTION **13**

STUDY REGIONS 14
STUDY THEMES 15

CHAPTER 2 - GRADIENT NEAREST NEIGHBOR MODELING OF FOREST STRUCTURE **17**

INTRODUCTION 17
METHODS 20
Study area *20*
Forest plot data *21*
GRADIENT NEAREST NEIGHBOR PREDICTIONS 23
Mapped explanatory data *24*
MODEL EVALUATION 26
RESULTS 28
Explanatory variables relation to plot data *28*
Forest structural attribute predictions *31*
Imputed maps of individual species *34*
Model uncertainty *35*
DISCUSSION 37
Aboveground biomass, age, and species composition across the landscape *37*
Uses of GNN prediction results *39*
Uncertainty in model results *41*

CHAPTER 3 – CROSS BORDER MAPPING OF OLD GROWTH AND MATURE FORESTS **45**

INTRODUCTION 45
Conservation of old growth *45*
Complexities in defining mature and old growth forests *48*
METHODS 50
Study area *50*
Gradient nearest neighbor and explanatory variables *50*
Mapped categorical variables *50*
RESULTS 55
Dominant species maps *55*

Old growth and mature classifications *56*
DISCUSSION 60
Dominant Species Extent Maps *60*
Multiple regional definitions *61*
Future vulnerabilities to late-successional forests. *62*
Implications *63*
CHAPTER 4 – MODELING FUTURE CARBON VULNERABILITIES WITH NATURAL DISTURBANCE, MANAGEMENT AND CLIMATE CHANGE 64
INTRODUCTION 64
Natural disturbance and succession *65*
Future climate and vegetation *67*
METHODS 69
Study area *69*
LANDIS-II landscape model *69*
Description of NECN extension *70*
Natural Disturbance *71*
Biophysical inputs *72*
Climate scenarios *73*
Management scenarios *74*
RESULTS 75
DISCUSSION 82
Patterns of natural disturbance *82*
Harvest interactions with natural disturbance *83*
The future of aboveground biomass and climate change *85*
Limitations *87*
CONCLUSION 88
REFERENCES 90

LIST OF FIGURES

Figure Page

Figure 1. Landscape for GNN forest structural mapping (grey) and LANDIS-II landscape model (orange). 15

Figure 2. GNN modeling region of the temperate rainforests of North America separated into five sub-modeling regions..... 21

Figure 3. Plot location by country of origin, with FIA plot locations labeled in green and FAIB plot locations in yellow. FIA plot locations are shown here using the publicly available fuzzed coordinates. 22

Figure 4. Associations between vegetation and explanatory variables from canonical correspondence analysis for the Tongass modeling region. The arrow length represents the strength of the correlation between the environmental variables and the plot forest structure. ... 28

Figure 5. Regressions of aboveground live biomass (top) and age of dominant species (bottom) to environmental variables shown to have strong influence on model outcomes based on CCA results. 30

Figure 6. Comparison of predicted to observed data from the leave-one-out cross-validation analysis. Displayed is the 1:1 line with the GMFR line plotted in red. Data points are colorized by density to surrounding points, with yellow illustrating areas of highest point density..... 31

Figure 7. Mapped results of GNN imputation model for the full modeling region. The four variables selected here represent the main categories of predicted structural metrics..... 32

Figure 8. Comparison of observed versus predicted aboveground biomass predictions by country. 33

Figure 9. Map of mean nearest-neighbor distances for the k = 5 nearest neighbor predictions. Values in this map represent the mean Euclidean distance from the environmental gradients a pixel represents to the nearest-neighbor imputed by GNN..... 35

Figure 10. Mapped results of GNN imputation model for the full modeling region of species biomass (gm-2) and extent. The four species select show the spatial constraints around areas of observed presence. 36

Figure 10. Examples of forest structural predictions. Rows are representative of different places within the study region, with Juneau on top, Zarembo Island in the middle, and Vancouver on the bottom. Columns represent the satellite imagery, structural attribute, and a select individual species prediction. 38

Figure 12. Protected areas of the northern temperate rainforests in Alaska and coastal British Columbia. 54

Figure 13. Dominant species classification map. Percent of total area by species is also displayed on the left of the map. 58

Figure 14. Map showing the spatial predictions of old growth and mature forests. 59

Figure 15. Average annual minimum and maximum aboveground air temperature across the perhumid forests of southeast Alaska and British Columbia from the years 1979 to 2016. Dashed lines are linear regressions fitted to monthly temperature records and show a general increase in both minimum and maximum temperatures. Historical data obtained from CHELSA (Karger and Zimmermann 2018) 68

Figure 16. Annual rain and snow precipitation at the Juneau International Airport weather station from 1970 – 2022. Dashed lines are linear regressions fitted to monthly temperature records and show a general increase in both minimum and maximum temperatures. Historical data obtained from Climate Data Online *(NOAA 2023)*. 68

Figure 17. Schematic diagram of the NECN succession extension for LANDIS-II. In the top panel, species and age cohorts with leaf, wood, fine root, and coarse root components are represented. Following mortality, this biomass is transferred to one of the detrital pools. Foliage is transferred to the surface residue pool; fine roots to the soil residue pool. As decay progresses, carbon and nitrogen are transferred to and among the fast, slow, and passive soil organic matter (SOM) pools, with some loss to the atmosphere and through leaching. (Scheller et al., 2011) ... 71

Figure 18. Conceptual diagram of the Biomass Hurricane extension in LANDIS-II used in this study. Simulated coastline is represented as a linear line with a fixed axis. Simulated wind speed (increasing brightness of blue color), mean and deviations of the storm track, and biomass removed (red) in each cell are also shown. 72

Figure 19. Simulated climate scenarios. 74

Figure 20. Maps of unconstrained, wind-protected, and wind-exposed management areas used in LANDIS-II. 75

Figure 21. Comparison of simulated and observed maximum sustained wind speed and wind direction: A. Simulated MSWS, B. Observed (Sitka airport) MSWS, C. Simulated wind direction by windspeed, D. Observed (Sitka airport) wind direction by windspeed. 76

Figure 22. Two simulated storms and associated biomass mortality: 1. Severe storm from the southeast with widespread tree mortality, 2. moderate storm from the southwest with more localized tree mortality. 77

Figure 23. Boxplots showing biomass removed ($g \cdot m^{-2}$) from ETC events across all management and climate scenarios. Outliers which represent larger blowdown events are not shown. 77

Figure 24. Aboveground biomass trajectories in stands of high, medium, and low wind exposure. Sites shown here had similar aboveground starting conditions but different exposure levels to large regional storm events. 78

Figure 25. Summarized results from unconstrained, wind-protected, and wind-exposed harvest scenarios under historical, moderate, and severe climate change. 79

Figure 26. Mean biomass per species, within the young-growth management area of Zarembo Island, under simulated management and climate scenarios. The first bar in each climate scenario represents the initial starting conditions, followed by the end scenario species biomass of each harvest scenario. 80

Figure 27. Density plot showing age distribution within the young-growth management area of Zarembo Island under simulated management and climate scenarios. 81

Figure 28. Annual net primary productivity (ANPP) of the three different management scenarios by climate scenario. 82

Figure 29. Modelled wind disturbance from a moderate storm using the Biomass Hurricane extension in LANDIS-II (left). Modelled windthrow probabilities and areas of identified windthrow from aerial observations (Kramer et al., 2001) 83

Figure 30. Mean slope and wind exposure class of historical harvest boundaries on Zarembo Island. 84

LIST OF TABLES

Table Page

Table 1. Forest composition and structural data obtained from forest plot observations. 23

Table 2. Environmental predictor variables that will be used in GNN mapping. 26

Table 3. Distribution of imputed GNN structural data for AGB, stand age, BA, snag biomass, TPH, and live volume. Distributions are shown for both the Alaska modeling regions and the British Columbian modeling regions separately, as well as the full modeling region. 29

Table 4. Dominant tree species. 51

Table 5. Definitions for old growth and mature classification based on dominant species forest type. 52

Table 6. Dominant overstory species extent and percent cover of total study region. 56

Table 7. Administrative protective areas with the total area (ha) of old growth and mature forest contained within each. Mean aboveground biomass (gm^{-2}) within each protected area is also reported. 57

CHAPTER 1 - INTRODUCTION

The temperate rainforests of the Pacific coast of North America include nearly half of all temperate rainforests on Earth. These forests are globally significant for their role in storing and cycling carbon and are home to some of the highest aboveground carbon densities in the world (Alaback, 1996; Yatskov et al., 2019). Regionally and locally, they are valued for their cultural significance by indigenous communities, their ability to provide ecosystem services and their economic importance (DellaSala et al., 2022; Suttles et al., 1997). They are described as being among the most intact tracts of coastal temperate rainforests in the world (Alaback, 1996; DellaSala et al., 2011). Yet despite their global and regional significance, there is a relative lack of consistent spatial data and modeling of future conditions to help inform management decisions affecting this region which spans jurisdictional boundaries.

Spatially complete data that describes the composition and structure of forests can be used for a variety of monitoring and management objectives. Regional vegetation maps are used to assess changes in how we use land and classify land (e.g. Wulder et al., 2004), estimate total carbon storage and sequestration rates (e.g. Loudermilk et al., 2017; Lucash et al., 2023; McNicol et al., 2019; Smithwick et al., 2002), estimate timber volume (e.g. Falkowski et al., 2010), predict suitable wildlife habitat (e.g. Lorenz et al., 2021), and predict fire behavior (e.g. Pierce et al., 2009). Monitoring how vegetation may change over time can enable the assessment of resilience after disturbance (e.g.Weiss et al., 2023), of trends in natural disturbances (e.g.Kramer et al., 2004), and impacts from specific land management policies or legislation (e.g.Davis et al., 2022)

Recent shifts in land management policies, with Alaska moving to sustainable young-

growth management (USDA Forest Service, 2022) and British Columbia putting large areas into conservation (Al Gorley and Garry Merkel, 2020), create uncertainties regarding future conditions under a changing climate. These policy shifts are recent and have largely gone understudied in this carbon-dense region; little is known about how they will impact local ecosystems in terms of carbon storage and species shifts.

Study Regions

The study area for this project will span nearly 29.9 million hectares of coastal regions of coastal British Columbia up through southeast Alaska to Kodiak Island (Fig. 1). It is composed of large climatic, geologic, and vegetation gradients with latitudinal of 48°N to 61°N and a longitudinal gradient of 121°W to 154°W. The temperate rainforests in this region experience a maritime climate characterized by mild temperatures, high humidity, and abundant precipitation throughout the year, supporting some of the highest amounts of above- and belowground biomass in the world (Buma et al., 2016a; Carter and Buma, 2024; McNicol et al., 2019). Winters are mild, with temperatures ranging from 0°C to 10°C, accompanied by substantial rainfall and occasional snowfall in the southern extents, with increasing amounts of snow with increasing latitude. Springs bring increasing temperatures and abundant rain showers, while summers remain cool with temperatures ranging from 15°C to 25°C and persistent fog and mist (Hennon et al., 2012; Shanley et al., 2015). A smaller modeling region, consisting of Zarembo Island, will be used for modeling future forest conditions using a spatially-explicit forest landscape model (Figure 1).

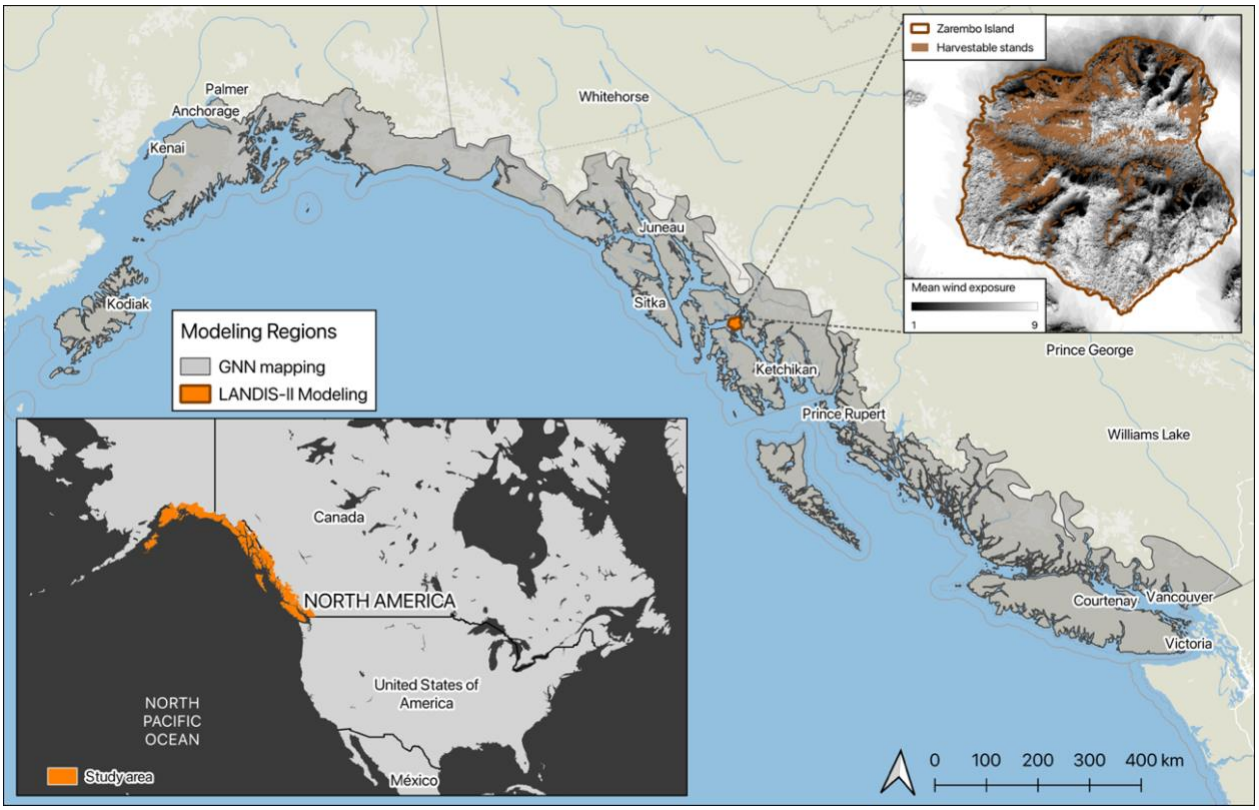


Figure 1. Landscape for GNN forest structural mapping (grey) and LANDIS-II landscape model (orange).

Study Themes

The first chapter uses a Gradient Nearest Neighbor (GNN) approach to produce high-resolution and spatially explicit predictions of aboveground biomass, forest structure, and composition spanning from Kodiak Island in Alaska down to the southern border of British Columbia. The second chapter will use the same GNN mapping approach, with a focus on vulnerabilities to old-growth and mature forests in the region. Finally, the third chapter examines how new forest management policies, natural disturbance, and future climate may influence the spatial distribution of forest carbon storage, structure, and composition. Through this analysis, this dissertation will address the following research questions:

RQ1: Which factors are most influential in driving spatial patterns in tree species composition, aboveground carbon, basal area, density, and volume of live and dead trees across the

temperate rainforest?

RQ2: How much of this region remains as old-growth and what is the spatial context in which we find forests of different successional stages?

RQ3: How does the combination of repeat natural disturbance and the spatial patterns of forest management affect the future vulnerability of carbon in the temperate rainforests of Southeast Alaska under climate change?

CHAPTER 2 - GRADIENT NEAREST NEIGHBOR MODELING OF FOREST STRUCTURE

Introduction

Today's most pressing challenges in natural resource management and conservation planning extend across vast spatial scales, often traversing land ownerships, administrative jurisdictions, and intricate ecological gradients. A multitude of interacting threats, such as wildfires, invasive species (Walsh, 2018), and climate change, alongside balancing various benefits like wildlife habitat preservation, watershed health, and timber supply (DeGayner et al., 2005; Shanley et al., 2015). Consequently, there is a growing demand among analysts and decision-makers for comprehensive, highly detailed, and spatially-complete data on vegetation and land cover across extensive and complicated landscapes. A spatial understanding of vegetation structure and composition is helpful to land managers in understanding where there is potential habitat for wildlife (Vogeler and Cohen, 2016), understanding natural disturbance regimes (Kennedy et al., 2014), estimating carbon stocks (Lucash et al., 2023b), and tracking changes in the environment due to climate change.

In the temperate rainforests of North America, particularly within the coastal forests of Southeast Alaska and British Columbia, there are numerous challenges in obtaining comprehensive spatial data due to their vast size, remote nature, complex terrain, and the spanning of political and managerial borders. These forests play crucial roles in various aspects, including supporting regional economies (e.g. timber), cultural significance (e.g. berry and salmon production), and in their ability to store large amounts of carbon (DellaSala et al., 2022; McNicol et al., 2019). Despite their significance both regionally and globally, this area lacks consistent spatial data, hindering informed management decisions. However, mapping efforts

can encounter obstacles such as limited observational datasets and difficulties with remote sensing instruments exacerbated by the region's unique environmental conditions.

Regional obstacles in the use of remote sensing stems from its high latitudes, intricate topography, and adverse weather patterns. Cloud cover, atmospheric haze, and cloud shadows frequently distort spectral values in remote sensing data, leading to inaccuracies and omissions (Braaten et al., 2015; Kennedy et al., 2014; Zhu and Woodcock, 2014). The steep relief, especially on northern slopes in higher latitudes, exacerbates terrain shading owing to the low angle of the sun (Beamish et al., 2020; Stow et al., 2004), influencing reflectance values and distorting surface features. Moreover, forests with intricate, multilayered canopies cast shadows that are critical for defining forest characteristics (Cohen and Spies, 1992), but they also complicate topographic shading interpretation (Kane et al., 2008), causing pixel saturation and making it challenging to differentiate between pixel features. Heterogeneity within and among stands further complicates matters when sensor pixel size exceeds typical forest patch dimensions (Ohmann et al., 2014).

Despite the numerous challenges, the northern temperate rainforests have seen several vegetation mapping endeavors. Starting in the 1970s, comprehensive mapping initiatives began in southeast Alaska, initially delineating timber volume classes using stereo-pair aerial photography. These efforts evolved over the years, with updates mandated by the Tongass National Forest Land Management Plan in 1997. Subsequent attempts involved advanced techniques such as artificial neural networks and multivariate analyses to predict forest characteristics and refine classification methods. Federal agencies collaborated on projects like the Multi-Resource Land Characteristics (MRLC), employing algorithms to classify Landsat pixels and create National Land Cover Database (NLCD) layers. Notable studies include

Blackard et al., 2008, which predicted forest biomass across Alaska, and Buma et al., 2016a, which mapped aboveground forest carbon in southeast Alaska. Recent efforts, such as Wang et al., 2019, have utilized Random Forest machine learning and remote sensing to classify vegetation cover over large regions. Additionally, projects like the Landscape Change Monitoring System have assessed land cover changes in specific areas.

An existing gap in research lies in the absence of a continuous spatial dataset depicting the structure and composition of forests in the temperate rainforests of southeast Alaska and coastal British Columbia, which can be essential for informing land management decisions. In this study, I seek to enhance previous mapping endeavors in the region by combining national-level field observations from the USDA Forest Service Forest Inventory and Analysis (FIA) program and the Forest Analysis Inventory Branch (FAIB) from British Columbia and creating a cloud-free and terrain corrected satellite composite of the entire region. The approach involves a Gradient Nearest Neighbor (GNN) imputation technique, which models forest attributes through Canonical Correspondence Analysis (CCA) and imputes results across the landscape based on weighted Euclidean distance. This method allows for the mapping of various forest attributes across a wide geographic area and enables the imputation of any forest attribute derived from field observations to similar pixels across the landscape. Environmental variables that show the strongest influence in the spatial patterns of aboveground carbon, basal area, density, and volume of live and dead trees across the temperate rainforest will be identified. This method will allow me to address my research question: which factors are most influential in driving spatial patterns in aboveground carbon, basal area, density, and volume of live and dead trees across the temperate rainforest?

Methods

Study area

The study area for this project spans nearly 29.9 million hectares of coastal regions of coastal British Columbia up through southeast Alaska to Kodiak Island (Fig. 1). It spans a large climatic, physiographic, geologic, and vegetation gradients with latitudinal of 48°N to 61°N and a longitudinal gradient of 121°W to 154°W. The temperate rainforests in this region experience a maritime climate characterized by mild temperatures, high humidity, and abundant precipitation throughout the year, supporting some of the highest amounts of above- and belowground biomass in the world (Buma et al., 2016a; McNicol et al., 2019). Winters are mild, with temperatures ranging from 0°C to 10°C, accompanied by substantial rainfall and occasional snowfall in the southern extents, with increasing amounts of snow with increasing latitude. Springs bring increasing temperatures and abundant rain showers, while summers remain cool with temperatures ranging from 15°C to 25°C and persistent fog and mist.

The study area was split into five separate modeling regions based on climatic differences and species composition. The western Kenai Peninsula and the Anchorage Bowl comprise portions of the Cook Inlet Basin and represent a transition to the boreal forest biome, characterized by cooler winters, warmer summers, and far less annual precipitation than the temperate maritime region (Nowacki et al., 2003). In contrast, modeling regions within the coastal rainforest are characterized generally by warmer winters and cooler summers, with substantial annual precipitation.

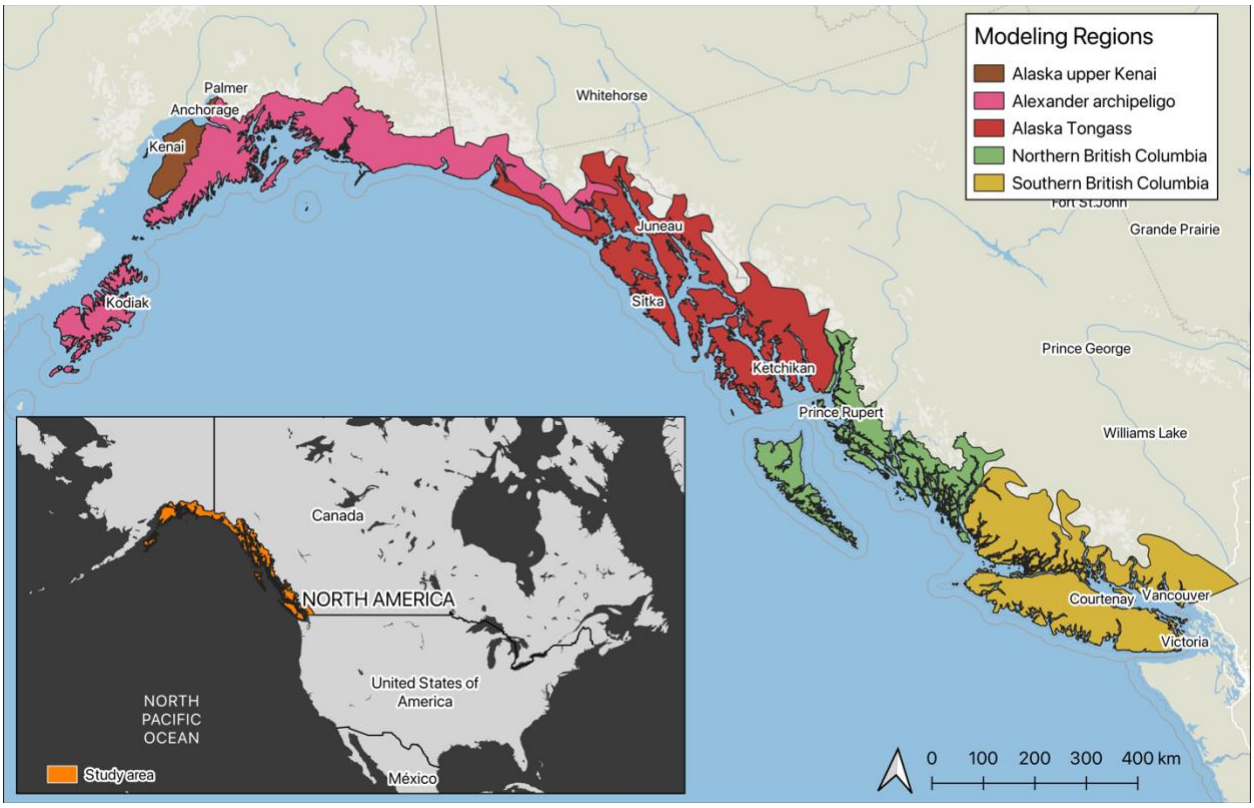


Figure 2. GNN modeling region of the temperate rainforests of North America separated into five sub-modeling regions.

Forest plot data

Forest inventory data was obtained and combined from both the United States and British Columbia (Figure 3). In British Columbia, we obtained utilized sample plots from the Forest Analysis and Inventory Branch (FAIB; William Bourgeois et al., 2018) while in Alaska plot data was obtained from the United States Forest Inventory and Analysis Program (FIA; Gray et al., 2012). FIA measures vegetation in permanent plots on forested lands across the United States while the FAIB database helps determine an appropriate annual allowable cut (AAC) for the timber harvest regions of British Columbia. For both datasets, plots were validated for accurate tree measurements and filtered to the latest remeasurement date. There were multiple plots

contained in FAIB that contained the same coordinates (n = 42) and these plots were also removed from analysis.

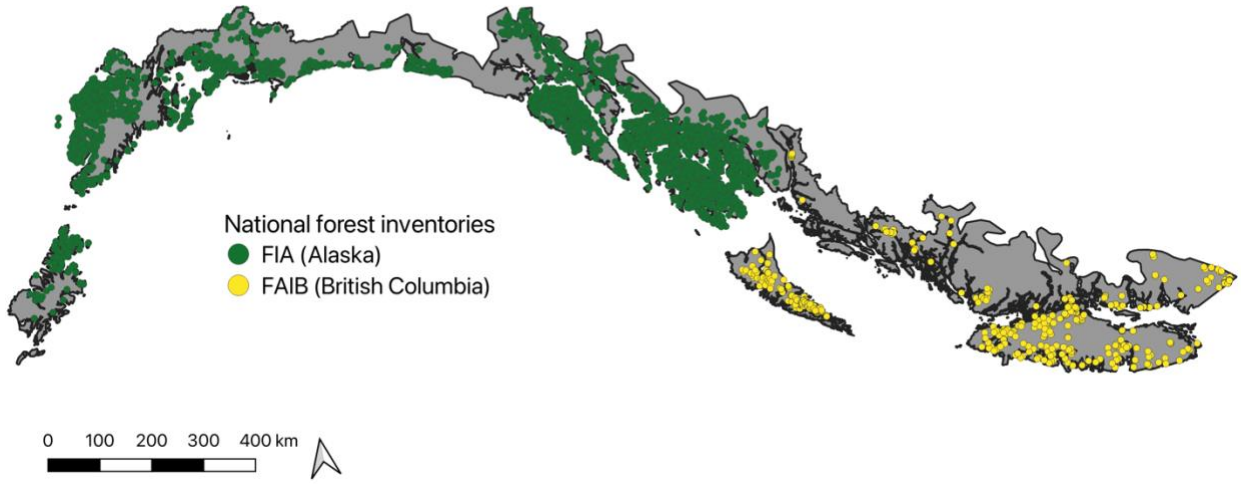


Figure 3. Plot location by country of origin, with FIA plot locations labeled in green and FAIB plot locations in yellow. FIA plot locations are shown here using the publicly available fuzzed coordinates.

To calculate individual tree-level biomass across both datasets, stem taper equations Kozak et al., 1969 were used to estimate the total volume of each standing stem. Tree stem volume was then converted to standing biomass with species-specific wood densities (Jenkins et al., 2003). After converting individual tree biomass to unit/area densities via the supplied expansion factors plot data was reassessed for erroneous species biomass densities at both the individual species and whole plot level. Plots that had biomass densities that were well outside the explainable range (n= 94) were omitted from the analysis (Buma et al., 2016b; Krumlik, 1974; Smithwick et al., 2002).

Table 1. Forest composition and structural data obtained from forest plot observations.

Variable code	Units	Description
total_bio	$g \cdot m^{-2}$	plot level biomass density
snag_bio	$g \cdot m^{-2}$	Plot level biomass of dead trees
*species*_gm2	$g \cdot m^{-2}$	species specific biomass densities $g \cdot m^{-2}$
BA_GE_3	$m^2 \cdot hectare^{-1}$	Basal area of live trees
BAC_GE_3	$m^2 \cdot hectare^{-1}$	Basal area of live conifers
BAH_GE_3	$m^2 \cdot hectare^{-1}$	Basal area of live hardwoods
TPH_live	$trees \cdot hectare^{-1}$	Density of live trees
TPH_dead	$trees \cdot hectare^{-2}$	Density of dead trees
TPH_Con	$trees \cdot hectare^{-3}$	Density of live conifers
TPH_Hw	$trees \cdot hectare^{-4}$	Density of live hardwoods
VPH_live	$m^3 \cdot hectare^{-1}$	Volume of live trees
VPH_dead	$m^3 \cdot hectare^{-1}$	Volume of dead trees
VPH_Con	$m^3 \cdot hectare^{-1}$	Volume of live conifers
VPH_Hw	$m^3 \cdot hectare^{-1}$	Volume of live hardwoods
AGE_DOM	years	95th percentil of tree ages
QMD_live	cm	Quadratic mean diameter of all live trees

Gradient nearest neighbor predictions

To model forest composition and structure across all forested land within the study area, we used Gradient Nearest Neighbor (GNN) imputation as described in Ohmann et al., 2011 and Ohmann and Gregory, 2002b. The selection of the nearest neighbor is based on the weighted Euclidean distance within multivariate gradient space determined using a constrained ordination method called canonical correspondence analysis (CCA; Ter Braak, 1986). This modeling method was chosen due to its robustness to the nonlinear responses expected of vegetation communities to environmental gradients and to the response matrices containing many null values and without normal distributions, which is common in plant community ecology. CCA is best suited to community datasets where (1) species responses to the environment are unimodal and (2) the important underlying environmental variables have been measured. Because CCA uses data on the environment to structure the community analysis, and CCA plots points in a

space defined by environmental variables, CCA can be considered a “direct gradient analysis” method.

Mapped explanatory data

The explanatory variables used in the GNN imputation were continuous raster layers describing observed satellite reflectance values, topography, climate, landcover, location, and disturbance (Table 2). All layers were sampled to the same resolution (30m) and extent using the terra package (Hijmans, 2023) in R (R Core Team, 2023). A cloud-free and terrain-corrected Landsat 8 composite was generated in Google Earth Engine (GEE; Gorelick et al., 2017) using a modified version of an image pre-processing tool developed by Hurni et al., 2017 that replaces SRTM elevation data with JAXA ALOS elevation data due to data availability at high latitudes (Tadono et al., 2016). The Landsat 8 image collection was filtered to months with minimal snow cover, and pixels chosen for the composite image were the highest quality available pixels captured between 2018 and 2021, with priority given to the most recently captured pixel.

In addition to individual spectral bands, Tasseled Cap transformations (TCT) were calculated, providing a set of spectral indices effective at capturing changes in the density and vigor of vegetative foliage (Tasseled Cap Greenness, TCG), surface reflectance from the particles that make up the bare earth (Tasseled Cap Brightness, TCB), and surface moisture (Tasseled Cap Wetness, TCW). TCT condenses the multidimensional spectral data into a few key components: brightness, greenness, and wetness. Brightness measures overall reflectance, indicating the presence of bare soil or urban areas; greenness highlights vegetation by emphasizing the contrast between the visible and near-infrared bands; and wetness indicates soil or canopy moisture content by combining information from shortwave infrared bands. These

components simplify the complex spectral information, facilitating the analysis of land cover changes, vegetation health, and ecosystem monitoring (Cohen and Goward 2004).

To constrain biomass predictions in areas of disturbance the Landsat-based detection of Trends in Disturbance and Recovery (LandTrendr) algorithm, implemented in GEE, was used (Kennedy et al., 2018). LandTrendr exploits time-series satellite imagery to detect and characterize land cover changes over time. It uses a pixel-based approach to identify temporal trends and abrupt changes in spectral characteristics and is particularly useful for assessing long-term trends and disturbances in large-scale ecosystems. To ensure disturbance from harvests were fully represented, historical harvest boundaries were added to the LandTrendr output of disturbed pixels providing a layer that represents the time since disturbance (2021 – *year of disturbance*) for both human and natural causes.

Climate, landcover, and topographic layers were also included due to their influence on observed vegetation patterns found in northwest forests (Ohmann and Spies, 1998). High-resolution climatologies were derived from CHELSA V2.1 (Karger et al., 2017) while topographic layers, such as elevation and slope, were developed from JAXA ALOS (Tadono et al., 2016). Landcover classes from the Multi-Resolution Land Characteristics (MRLC) Consortium were used as predictors of vegetation type while also as a tool to mask non-forested areas from this analysis.

Table 2. Environmental predictor variables that will be used in GNN mapping.

Predictor	Band name	Description
Landsat 8 Composite	blue	Landsat 8 blue band
	green	Landsat 8 green band
	red	Landsat 8 red band
	NIR	Landsat 8 near infrared band
	SWIR1	Landsat 8 shortwave infrared 2 band
	SWIR2	Landsat 8 shortwave infrared 1 band
Landsat 8 indices	R54	Landsat 8 near infrared band / Landsat 8 red band
	R65	Landsat 8 shortwave infrared 1 / Landsat 8 near infrared
	R67	Landsat 8 shortwave infrared 1 / Landsat 8 shortwave infrared 2
	NDVI	Landsat 8 normalized difference vegetation index
Landsat 8 Tasseled Cap	brightness	Axis 1 from tasseled cap transformation of Landsat 8 surface reflectance.
	greeness	Axis 2 from tasseled cap transformation of Landsat 8 surface reflectance.
	wetness	Axis 3 from tasseled cap transformation of Landsat 8 surface reflectance.
Landcover	landcov	National Land Cover Database (NLCD) Landcover classifications
Topography	elevation	Elevation (m)
	slope	Slope (degrees)
Location	latitude	northing based on EPSG:3338 (m)
	longitude	easting based on EPSG:3338 (m)
Climate	bio1	mean annual air tempurature
	bio4	temperature seasonality (°C/100)
	bio5	mean daily air temperature of the warmest month (°C)
	bio12	annual precipitation amount ($kg \cdot m^{-2}$)
	bio14	precipitation amount of the driest month ($kg \cdot m^{-2}$)
	bio15	precipitation seasonality ($kg \cdot m^{-2}$)
Disturbance	TSD	Time since disturbance obtained from Landtrendr (Kennedy et al., 2010)

Model evaluation

To evaluate CCA model performance at individual sites, we compared a subset of predicted values to observed values. This was done for each individual modeling region, and then again for all modeling regions to show overall agreement across the study area. For each of the compared vegetation attributes, the 6 nearest neighbors were predicted. The first nearest neighbor was omitted, being that it would represent the observed site we are comparing to, and the mean of the second- through fifth-nearest neighbor was calculated. This has been used in

previous studies as a computationally efficient method similar to leave-one-out-cross-validation (Janet L Ohmann and Gregory, 2002). Statistical comparisons were used to quantify how well the models predicted observed values and if there were any trends in systematic and unsystematic bias (Riemann et al., 2010).

Maps were generated based on the mean of the five nearest-neighbor distances. This allowed us to create a spatial representation of uncertainty in our model predictions. Shorter distances show areas of greater confidence, whereas greater distances represent areas of greater uncertainty and may be attributed to under sampled environmental conditions within the filed plot dataset (Moeur and Stage, 1995).

A map was also generated showing the mean of the 5 nearest-neighbor distances (Figure 9). This was used as an indicator of model uncertainty for all our GNN model prediction maps. Pixel values in this map represent the mean Euclidean distances from the environmental gradients a pixel represents to the nearest neighbor imputed by GNN. Higher Euclidean distances represent areas that had less association with the environmental gradients found at plot locations.

Results

Explanatory variables relation to plot data

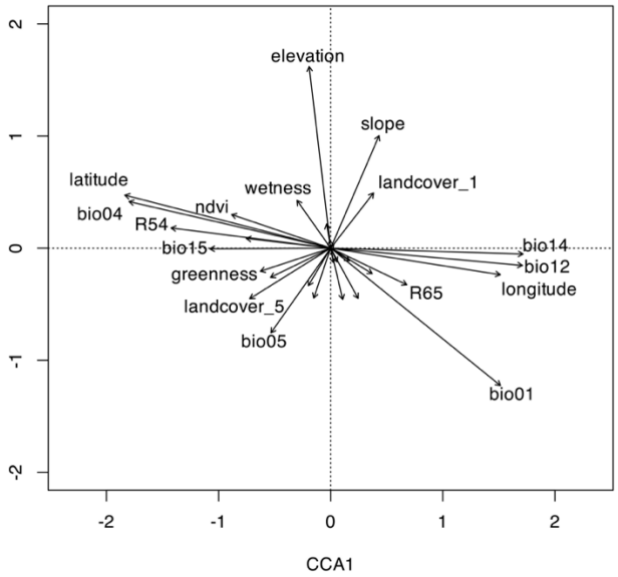


Figure 4. Associations between vegetation and explanatory variables from canonical correspondence analysis for the Tongass modeling region. The arrow length represents the strength of the correlation between the environmental variables and the plot forest structure.

Environmental variables, such as elevation, slope, location, and climate, had the strongest influence on forest species composition and structure (Figure 4). Climate variables had the largest overall importance, with mean annual temperature, temperature seasonality, annual precipitation, and precipitation seasonality together describing relations in observed structural metrics. Landsat 8 imagery had varying degrees of importance, with calculated indices of NDVI and tasseled-cap transformation bands having moderate influence. Individual bands from Landsat 8 had relatively little importance when predicting forest structural attributes. Landcover classification also showed moderate amounts of influence.

Environmental variables that strongly influence vegetation structure had an effect on structural prediction outcomes in different ways (Figure 5). For example, with increases in observed elevation, prediction results trended towards lower levels of aboveground biomass. Elevation had the opposite trend for stand age, with stands increasing in age with increasing elevation. Increases in mean annual temperature resulted in increases in aboveground biomass. However, this didn't hold true for stand age, where there seemed to be little effect. Spatial location also showed expected patterns of a decreasing ability to support large amounts of

aboveground biomass with increasing latitude. Increases in longitude also showed an increase in both aboveground biomass and stand age and may be an effect of distance from accessible coastal forest land. A multimodal pattern also emerges when looking at how spatial context affects stand age and biomass, which is likely due to multiple large islands in the region and are also evidence of younger forests being spatially located near coastlines that are easily accessed for the use of timber.

Table 3. Distribution of imputed GNN structural data for AGB, stand age, BA, snag biomass, TPH, and live volume. Distributions are shown for both the Alaska modeling regions and the British Columbian modeling regions separately, as well as the full modeling region.

	Variable	unit	Min	25th quartile	Median	Mean	75th quartile	Max
Alaska	AGB	$g \cdot m^{-2}$	79	7,584	22,844	30,084	47,646	170,245
	Stand age	years	14	52	83	95	122	570
	BA	$cm^2 \cdot h^{-1}$	0.3	11	25	27	41	99
	Snag bio	$g \cdot m^{-2}$	8	822	2,571	4,690	6,934	37,952
	TPH	$trees \cdot ha^{-1}$	14	205	342	345	464	1,407
	Live volume	$m^3 \cdot ha^{-1}$	2	191	577	755	1,194	4,247
British Columbia	AGB	$g \cdot m^{-2}$	68	21,327	37,184	37,668	52,108	180,101
	Stand age	years	14	51	71	93	109	529
	BA	$cm^2 \cdot h^{-1}$	0.3	33	49	50	66	158
	Snag bio	$g \cdot m^{-2}$	4	2,427	5,248	6,465	9,231	41,183
	TPH	$trees \cdot ha^{-1}$	20	430	598	720	831	4,775
	Live volume	$m^3 \cdot ha^{-1}$	3	887	1,728	2,551	2,737	28,546
Total	AGB	$g \cdot m^{-2}$	68	12,534	31,561	33,765	50,349	180,101
	Stand age	years	13	58	83	94	115	570
	BA	$cm^2 \cdot h^{-1}$	0.3	18	37	38	53	158
	Snag bio	$g \cdot m^{-2}$	4	1,376	3,869	5,552	8,231	38,453
	TPH	$trees \cdot ha^{-1}$	15	291	445	525	622	4,775
	Live volume	$m^3 \cdot ha^{-1}$	2	366	4,042	1,621	1,894	28,546

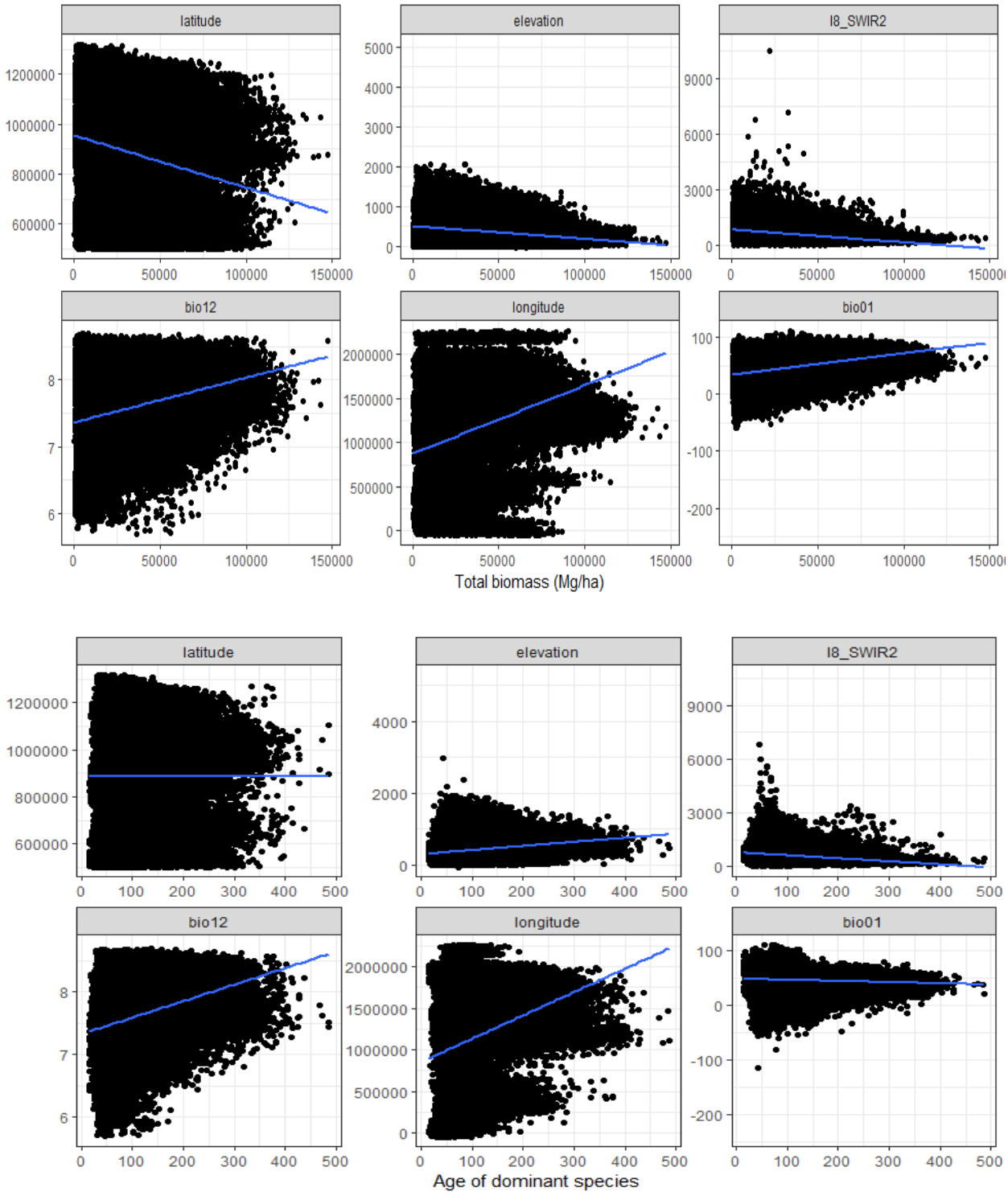


Figure 5. Regressions of aboveground live biomass (top) and age of dominant species (bottom) to environmental variables shown to have strong influence on model outcomes based on CCA results.

Forest structural attribute predictions

Our modeling efforts yielded thirty-nine individual maps of forest structure and composition. The resulting spatial predictions of forest structural attributes were moderately accurate across the study area. At the site level, predictions of aboveground live biomass (R^2 = 0.38), stand age (R^2 = 0.28), and QMD (R^2 = 0.36) demonstrated the highest agreement with plot observations, while spatial predictions of snag biomass (R^2 = 0.19) show the lowest levels of agreement (Figure 6). Results from the modified LOOCV analysis also showed a trend of overpredictions in the lower range of observed values while underpredicting in the upper range. This result was expected due to the use of the mean values across five nearest neighbor maps truncating observed extremes.

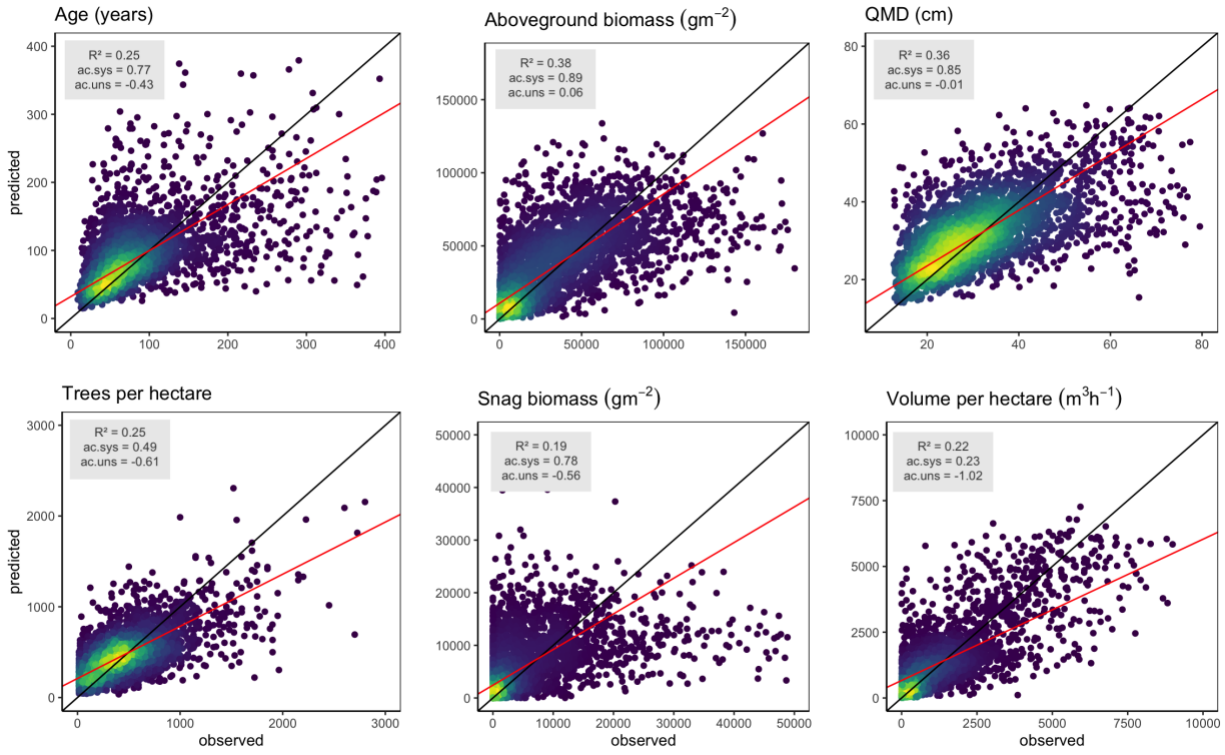


Figure 6. Comparison of predicted to observed data from the leave-one-out cross-validation analysis. Displayed is the 1:1 line with the GMFR line plotted in red. Data points are colorized by density to surrounding points, with yellow illustrating areas of highest point density.

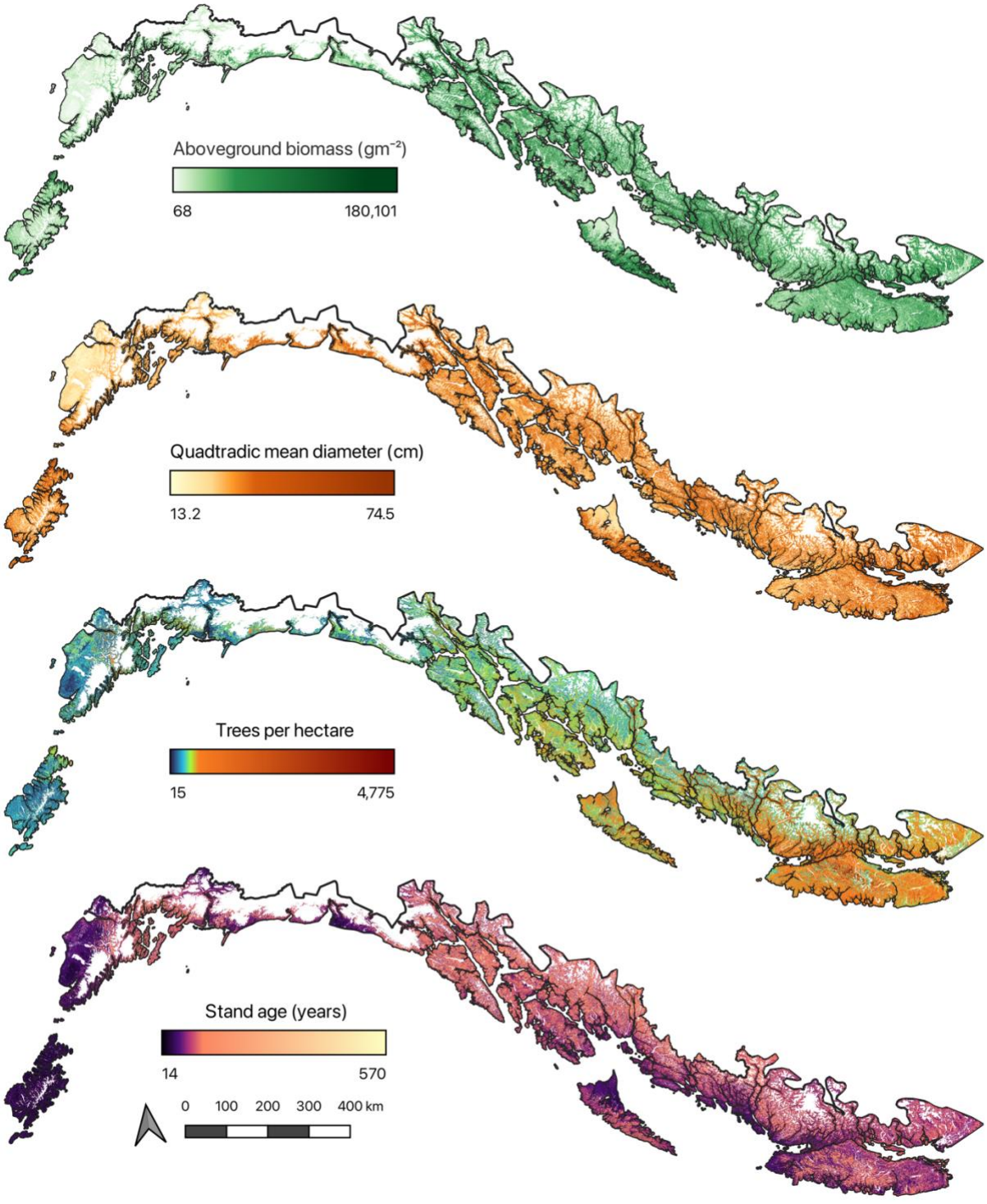


Figure 7. Mapped results of GNN imputation model for the full modeling region. The four variables selected here represent the main categories of predicted structural metrics.

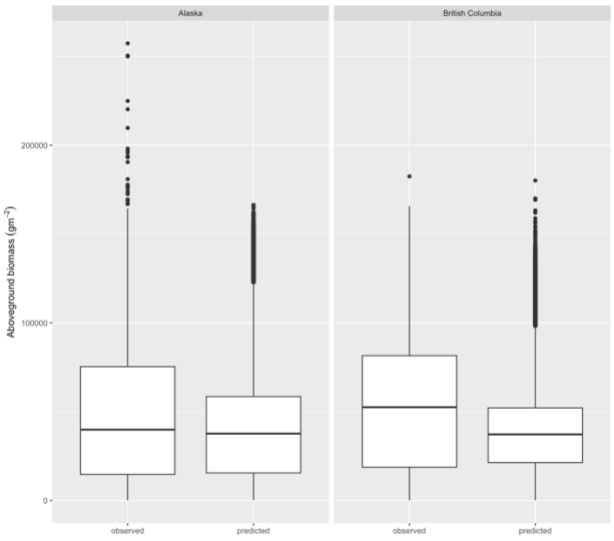


Figure 8. Comparison of observed versus predicted aboveground biomass predictions by country.

Regionally, the relative distributions of structural data exhibit similar patterns. While the predicted median values closely align with the observed values across all plots, the upper and lower quantiles in the predicted values are slightly condensed compared to the observed plot data (Figure 8). There were differences seen between the predicted and observed data in coastal British Columbia compared to the Alaska region, with predicted median values in the southern modeling regions being lower than the observed plot data. This observation may be due to the inclusion of biomass plots from FIA data in Alaska to estimate forest structure throughout the northern and southern regions of British Columbia. This decision was made both to lessen the effect of predicting structure using plot data across political borders but also due to a smaller coverage of plot data in the northern regions of coastal British Columbia. Being that the two national forest plot networks work on slightly different data collection protocols, it is difficult to determine if one is underestimating or overestimating forest structural attributes. However, the difference between the two was relatively minor.

British Columbia also tended to have higher median values across all structural predictions apart from stand age (Table 3). An example of this can be seen in predictions of aboveground biomass, with Alaska having a median value of 30,084 gm^{-2} and British Columbia showing a median of 37,668 gm^{-2}. Although stand-level biomass, volume, and basal area were slightly lower overall in the Alaska modeling region, it had higher stand ages compared to

forests in coastal British Columbia, with the median stand age being 83 years and 71 years respectively. However, the mean stand age between both regions showed only a difference of 2 years.

Imputed maps of individual species

Biomass density maps were created for significant overstory species in the region. These maps provide an estimate of species spatial extent and abundance and were compared to mapped plot locations where the species was observed (Figure 10). This comparison showed that the resulting GNN prediction of where species are within the study area matched that of observations in the plot data. Species spatial distributions along environmental gradients also matched those of published descriptions (Alaback, 1996; Alaback and Juday, 1989; Caouette et al., 2016; Harris and Farr, 1974).

When comparing the presence of predicted species to the observed plot data, levels of agreement varied significantly by species. Across all species, however, there was a large trend in errors of commission over omission. Commission errors were strongest in species that have expansive ranges and whose habitat is less constrained to environmental gradients, such as *Picea sitchensis* (Kappa = 0.1) and *Tsuga heterophylly* (Kappa = 0.2), compared to species such as *Pseudotsuga menziesii* (Kappa = 0.3) and *Populus trichocarpa* (Kappa = 0.3). Commission errors are most evident in species that have limited spatial extents on the landscapes but have representative environmental variables outside their current range, such as the presence of *Picea sitchensis* within the Kodiak Archipelago and the northern distribution of *Pseudotsuga menziesii* being artificially limited by modeling region.

Model uncertainty

A map of the mean Euclidian distance in gradient space was made to estimate the amount of uncertainty in our predictions (Figure 9). The lowest levels of uncertainty were seen in low-elevation areas of the Tongass, while higher amounts of uncertainty were observed in areas of high elevation. Patterns of uncertainty also seemed to be driven by the level of plot support for a particular region, with the lowest uncertainty in areas that were well represented by either FIA or FAIB plot data.

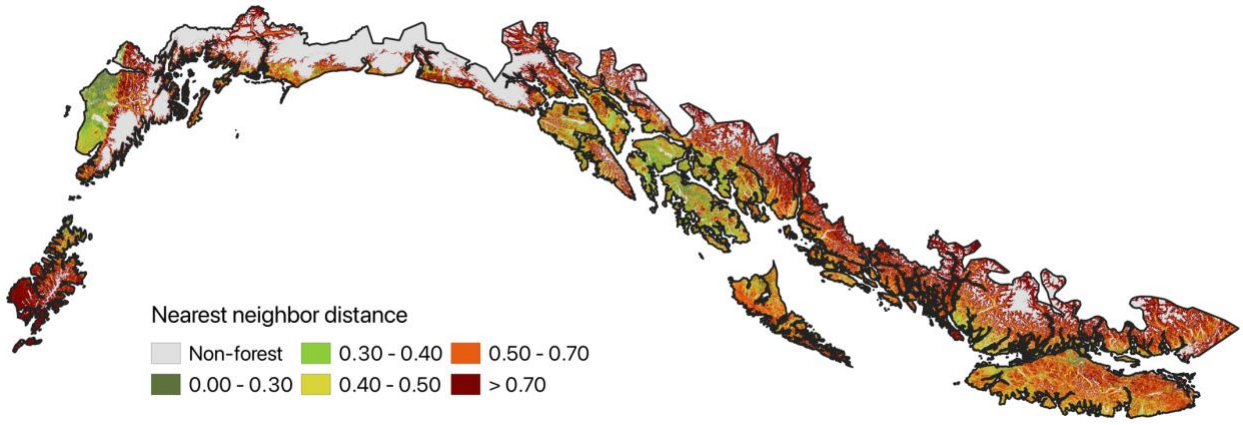


Figure 9. Map of mean nearest-neighbor distances for the k = 5 nearest neighbor predictions. Values in this map represent the mean Euclidean distance from the environmental gradients a pixel represents to the nearest-neighbor imputed by GNN.

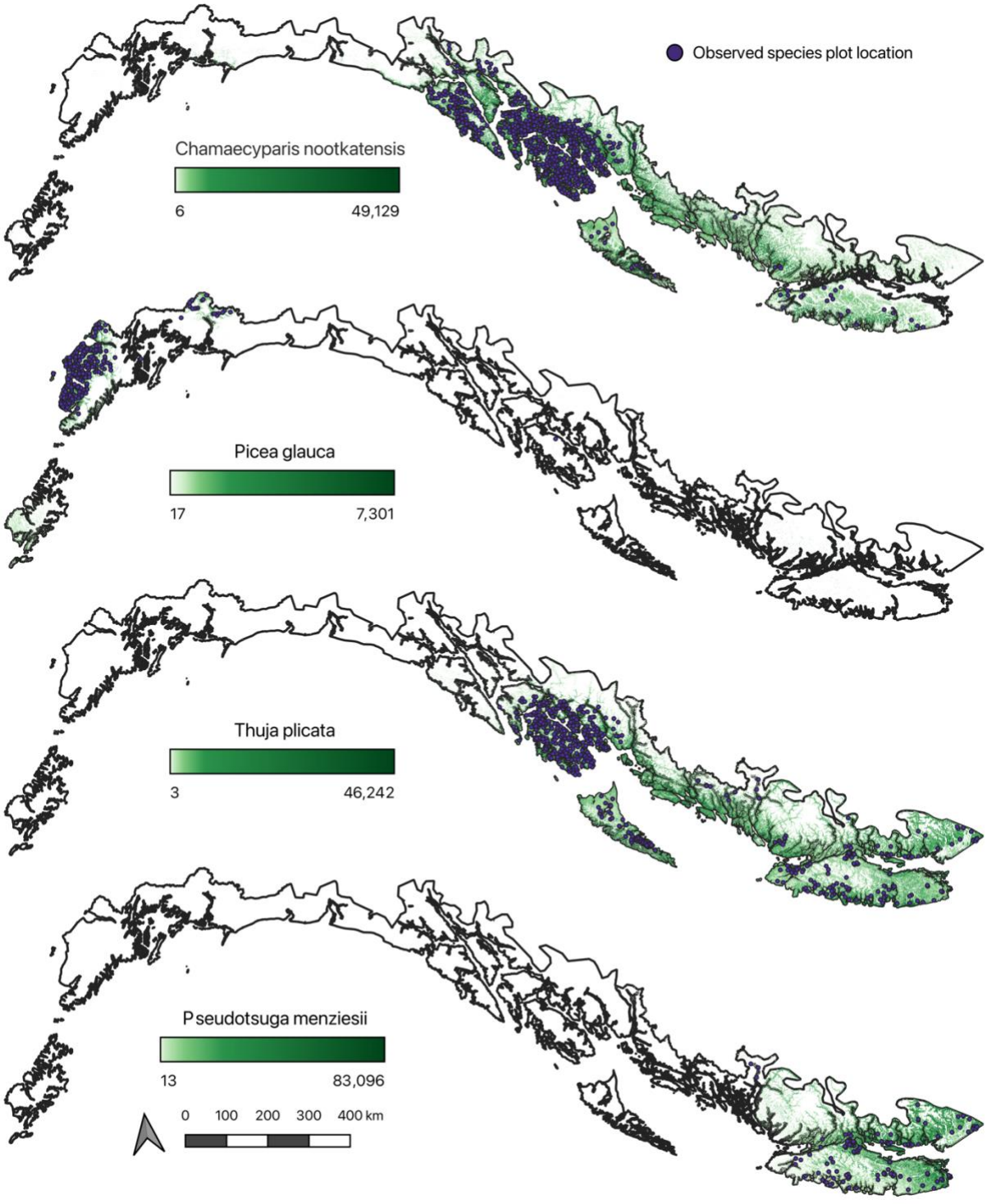


Figure 10. Mapped results of GNN imputation model for the full modeling region of species biomass (gm-2) and extent. The four species select show the spatial constraints around areas of observed presence.

Discussion

Aboveground biomass, age, and species composition across the landscape

Aboveground biomass and stand age

The predicted patterns of forest structure from the GNN analysis matched fairly well with expected patterns from previous publications (Alaback, 1996; Alaback and Juday, 1989; Harris and Farr, 1974; MacKinnon, 2003). Aboveground biomass was shown to have the highest values at lower elevations, however, this trend becomes less apparent at the lowest elevations nearest to the coastline. This is likely due to the management history in this region, with harvesting targeted in high biomass and low elevation stands that were easy to access (Brackley et al., 2009). Stand age was also seen to be affected by elevation, with stand age increasing upslope. However, the trend of stand age increasing with increasing elevation may also be due to these stands being comprised of longer-lived tree species, such as western redcedar and Alaska yellow cedar.

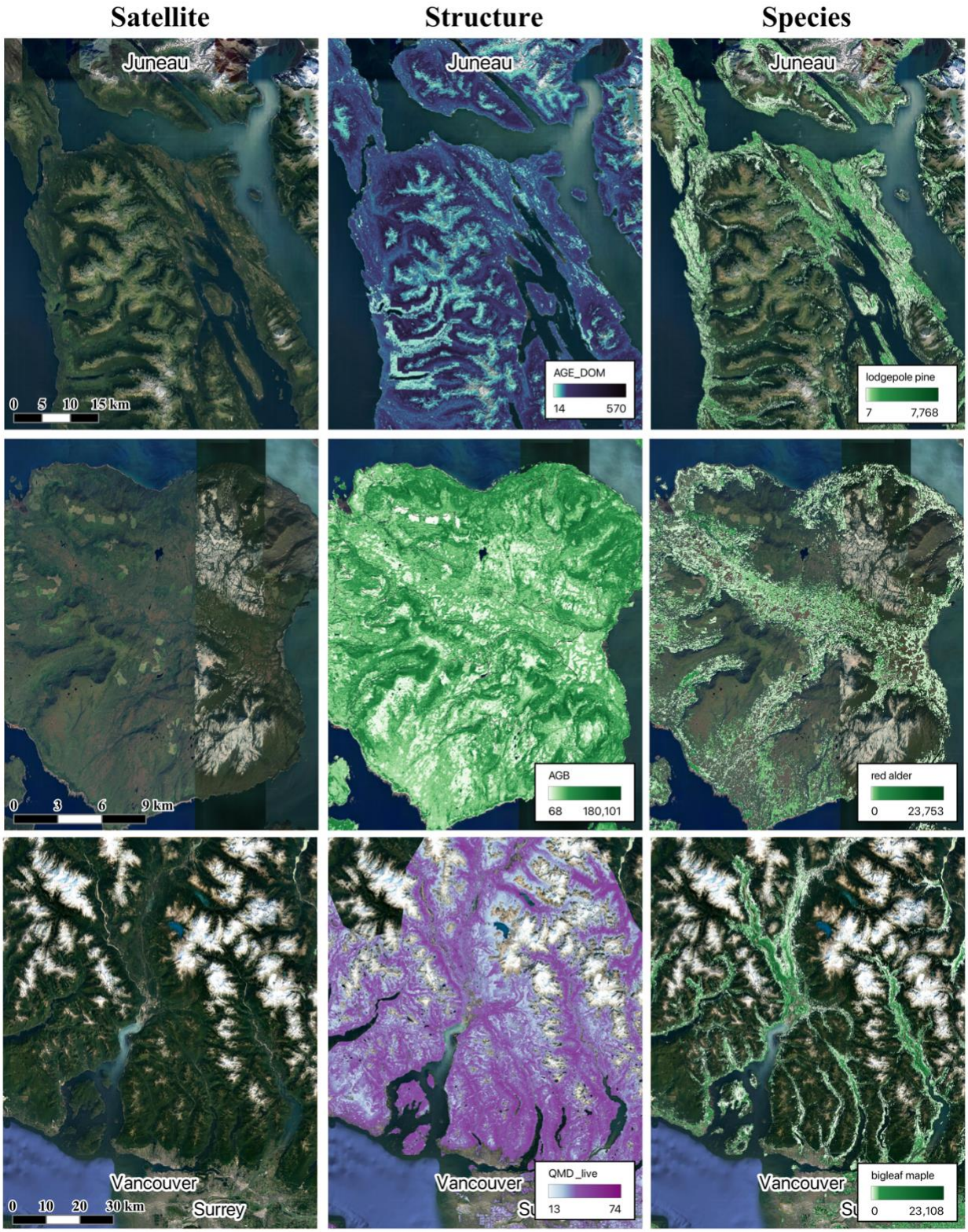


Figure 11. Examples of forest structural predictions. Rows are representative of different places within the study region, with Juneau on top, Zarembo Island in the middle, and Vancouver on the bottom. Columns represent the satellite imagery, structural attribute, and a select individual species prediction.

Individual species predictions

The results for individual species biomass showed relatively good agreement when compared to observed plot data (Figure 10). However, there was a tendency toward commission errors, with individual species being predicted within their known range but in plots where their presence was not actually observed. This issue has been noted in other studies using similar methods to estimate forest structural attributes in the Pacific Northwest (Irvine, 2022; Janet L Ohmann and Gregory, 2002). These errors likely stem from using the mean value from the five nearest neighbors and the reliance on spectral and climate data as predictors. Much like climate envelope modeling, commission errors can result from environmental factors indicating suitable conditions for a species without accounting for limitations such as seed availability or geographic barriers (Elith and Leathwick, 2009). In this study, we addressed these issues by creating separate modeling regions based on environmental and vegetative conditions and the inclusion of spatial location as a predictor variable. Despite these measures, these uncertainties should be considered when using these predictions.

Uses of GNN prediction results

The new GNN data, encompassing Kodiak Island down to the southern border of British Columbia, offer valuable opportunities to inform research, management, or policy decisions across various applications, due to their ability to describe diverse forest attributes across political boundaries. Similar regional vegetation maps have been utilized within the study area to assess regional biomass and carbon storage, monitor disturbance patterns, track land cover changes over time, and study vegetation responses to climatic shifts (Carter and Buma, 2024; Griesbauer and Scott Green, 2010; McNicol et al., 2019; Nowacki and Kramer, 1998). In the

hypermaritime forests of southeast and southcentral Alaska and coastal British Columbia, these data can facilitate research on carbon and nutrient fluxes between terrestrial and aquatic ecosystems, as well as investigations into the spatial patterns of forest structural classes critical for wildlife habitats.

Ecosystems in Alaska and coastal British Columbia are significant carbon reservoirs, storing a substantial portion of terrestrial carbon (Carter and Buma, 2024). Climate change projections suggest complex responses in these ecosystems, with potential increases in emissions in the boreal region, higher sequestration rates in the coastal temperate zone, and changes in the balance of precipitation that falls as snow (Shanley et al., 2015). Forest management practices significantly impact carbon storage and forest characteristics, affecting other management objectives and ecosystem services (Crotteau et al., 2022). Although timber harvest in this region has declined, it still remains actively managed in support of local and global economies. Regardless, Southeast Alaska and coastal British Columbia comprise a significant portion of the Earth's remaining old-growth temperate rainforest, primarily held within Inventoried Roadless Areas (IRAs), Wilderness, and old growth reserves. However, recent changes in policies regarding IRAs present potential future vulnerabilites to these ecosystems and necessitate more comprehensive information about the forests in these areas.

Due to the lack of observation data throughout the region, in places such as wilderness areas and northern regions of coastal British Columbia, predictions from GNN of forest composition and structure can be a valuable tool for forest managers to fill knowledge gaps about the current conditions of these forests. This could prove especially useful with the recent shifts in regional forest management that focus on young growth harvesting, conservation of old growth, and carbon sequestration (DellaSala et al., 2022; Law et al., 2023).

Uncertainty in model results

The amount of uncertainty in forest structural predictions varied by region, as seen in Figure 9. Areas with higher levels of uncertainty can be attributed to various sources, such as the vicinity and density of plot data to a prediction cell, the quality of the spectral data used, how parsimonious the model used may be, and uncertainties in datasets chosen as predictors.

Scarcity of plot data

The FIA program in the United States and Canada's FAIB are both government-led initiatives tasked with monitoring and assessing the status and trends of their respective countries' forest resources. Both programs have comprehensive approaches to forest inventory, collecting data on forest extent, composition, and health, and play crucial roles in providing valuable information to support informed decision-making, policy development, and sustainable forest management practices. However, there are notable differences between the two programs. One significant distinction is the availability of plot data, particularly in coastal British Columbia (Figure 3). While the FIA program in the United States maintains a robust network of permanent sample plots across all forested regions, the FAIB dataset in Canada lacks spatial coverage of the northern portions of the British Columbian coast. This data gap poses challenges for accurately assessing forest conditions and trends in this ecologically diverse and economically significant region.

Furthermore, FAIB employs both fixed and variable radius plots (variable radius plots being a sampling method that allows for flexible plot sizes based on tree diameter; Avery and Burkhart, 1983), whereas FIA primarily uses a series of fixed radius plots at each survey site (Gray et al., 2012). Previous studies show that the FIA fixed-radius plot design may lead to an underestimation of tree density and volume in stands with large, spaced out trees (Gray, 2003),

while variable radius plots may be biased towards trees with higher basal areas (Azuma and Monleon, 2011), and lead to potentially overestimated stand volume. This difference in sampling methodology can present challenges when making regional estimates of forest structure, particularly when those estimates cross political boundaries. Due to the differences in methodologies and resulting plot-level estimates between fixed and variable radius plots, all variable radius plots included in FAIB were omitted and only fixed area plots were used. This also had the effect of further diminishing the plot densities in the southern region of the study area.

Quality of Landsat mosaic

Obtaining a complete Landsat mosaic in the temperate rainforests of North America poses significant challenges due to environmental conditions inherent to these regions. High latitudes, characteristic of temperate rainforests, often result in terrain shadows, particularly in areas with rugged topography, such as coastal mountains (Giles, 2001). These shadows can obscure large portions of the landscape from satellite sensors, leading to incomplete coverage in Landsat imagery (Schulmann et al., 2015). Additionally, consistent cloud cover and snowfall further complicate the acquisition of high-quality satellite data. Complete cloud cover is frequent over the skies of the temperate rainforests, obstructing the view of the Earth's surface and limiting the availability of cloud-free imagery for mosaic creation. Similarly, snow cover, which can persist for extended periods in these regions, adds another layer of complexity by altering surface reflectance properties and reducing the visibility of underlying features. Together these make obtaining remotely sensed imagery over a site within a relatively close timeframe of observed plot data collection a difficult task. Developing methods that better allowed for

temporal matches between observed plot data collection and remotely sensed reflectance values could improve overall model predictions.

Predictor selection

Canonical correspondence analysis (CCA) offers a robust alternative to multiple linear regression, particularly for handling data with numerous null values and non-normal distributions. Unlike multiple linear regression, CCA does not require iterative successional runs to understand the effects of multiple predictors on numerous response variables. However, the careful selection of predictor variables remains crucial for effective model development and to avoid the issues associated with overly complex models (Bell and Schlaepfer, 2016). Previous studies in the Pacific Northwest found that using individual spectral bands from Landsat decreased model performance (Ohmann et al., 2007; Janet L Ohmann and Gregory, 2002). This can be different depending on forest conditions and reflectance values and, for this study, exploratory attempts showed higher agreement in prediction outcomes with all Landsat 8 bands included in the CCA. In the final model, the individual bands showed little explanatory power, while the calculated tasseled cap indices showed stronger relations in predicting forest structure (Figure 4). Choosing appropriate environmental predictors is essential, as community assemblages or structural conditions often correlate with similar environmental factors across the landscape.

Downscaled climate variables

Downscaling CMIP5 global climate model data, particularly in regions characterized by high topographic variability, can introduce significant uncertainties into climate projections (Foley, 2010; Wootten et al., 2017). Global climate models typically have coarse spatial resolutions, which may not adequately capture local-scale variations in terrain, land cover, and

atmospheric dynamics. When downscaling these coarse-resolution climate model outputs to finer spatial scales, such as those relevant for regional or local climate assessments, uncertainties can arise due to the inability of downscaling methods to accurately represent complex topographic features (Ahmadalipour et al., 2018). In areas with high topographic variability, such as mountainous regions, downscaled climate projections may struggle to capture the intricate interactions between elevation, slope, aspect, and microclimatic conditions. Additionally, the choice of downscaling technique, the resolution of input data, and the treatment of physical processes can further contribute to uncertainties in downscaled climate projections. Therefore, careful consideration of these factors should be taken into account when choosing to use any certain downscaled climate variable as a predictor in GNN, particularly in regions with pronounced topographic variability.

CHAPTER 3 – CROSS BORDER MAPPING OF OLD GROWTH AND MATURE FORESTS

Introduction

The late-successional forests in the temperate rainforests of North America are critical ecological, economic, and cultural assets. Coastal British Columbia and southeast Alaska comprise the largest and most intact examples of temperate rainforest in the world (DellaSala et al., 2011). Characterized by their large, old trees, diverse species, and complex structures, they play a crucial role in maintaining biodiversity on the landscape (Orians and Schoen, 2013; Spies, 2004).

Old-growth forests are highly valuable ecologically, economically, and culturally. Ecologically, their complex canopy layers, decaying wood, and varied microhabitats support a diverse range of flora and fauna, fostering unique ecosystems that promote resilience and stability (Carey and Johnson, 1995; Schowalter, 2017; Spies and Cline, 1988; Spies and Franklin, 1996). Economically, these forests play a critical role in carbon sequestration, storing vast amounts of carbon both above and below ground to help offset greenhouse gas emissions (Law et al., 2023; Mildrexler et al., 2020; Suchanek et al., 2004), and historically contributing to local and global economies through extensive timber harvesting in the region (Brackley et al., 2009). Culturally, these forests are significant for Indigenous communities and local populations, being deeply intertwined with their cultural identities, traditions, and histories, and providing essential resources for food, building materials, and medicine (Crone and Mehrkens, 2013).

Conservation of old growth

Forest conservation areas in southeast Alaska and coastal British Columbia play a crucial role in preserving the region's unique ecosystems and biodiversity. Over time, policies governing

these conserved areas have evolved, reflecting changing societal values and ecological understandings (Joeveen Dhari, 2023). Initially established to protect timber resources and watersheds, conservation efforts have increasingly emphasized the intrinsic value of these ecosystems for biodiversity conservation, carbon sequestration, and Indigenous cultural heritage. However, shifting political priorities and economic interests have sometimes led to vulnerabilities in the protections afforded to the forests within the boundaries of certain protected areas (DellaSala et al., 2022; Joeveen Dhari, 2023), with changes in land use regulations, logging practices, and infrastructure development threatening the integrity of these conservation areas.

An example of these shifting policies can be seen in the use of Inventoried Roadless Areas (IRAs) in southeast Alaska. These IRAs are designated regions within national forests that have been identified as lacking roads and exhibiting high conservation value due to their pristine natural conditions (DeVelice and Martin, 2001). These areas, particularly within the Tongass National Forest, represent some of the largest remaining expanses of undeveloped, old-growth temperate rainforests in North America (DellaSala et al., 2022). Their designation has significantly influenced forest management and conservation efforts in southeast Alaska by limiting road construction and prohibiting certain types of development. Through this, IRAs help maintain the ecological functions of these forests, including carbon sequestration, water regulation, and soil conservation. This restriction on road building also reduces the potential for logging and other extractive activities.

During the Trump administration, the protections afforded to IRAs in the Tongass National Forest were revoked. In 2020, the administration finalized a rule that exempted the Tongass from the 2001 Roadless Area Conservation Rule, opening up more than 3.7 million hectares to potential logging, road construction, and other development activities. This move was

aimed at promoting economic development in the region, particularly through the timber and mining industries. However, it sparked significant concern among conservationists, Indigenous communities, and other stakeholders who emphasized the ecological and cultural importance of maintaining these areas in their roadless state. With a change in administration, there was a renewed focus on environmental conservation and the protection of roadless areas. In 2021, the Biden administration announced its intention to restore the protections for IRAs in the Tongass National Forest. By early 2023, the administration had officially reinstated the Roadless Rule protections, once again restricting road construction and development in these critical areas.

To the south in British Columbia, the recent development and implementation of Old Growth Management Areas (OGMAs) mark a significant shift towards preserving the province's remaining old-growth forests. Driven by growing recognition of their ecological, economic, and cultural importance, OGMAs are designated to safeguard these ancient ecosystems and the biodiversity they sustain (Joeveen Dhari, 2023). Following the Old Growth Strategic Review in 2020, which emphasized the need for a conservation-focused approach, the government deferred logging in nearly 1.7 million hectares of at-risk old-growth forests. This initiative reflects a collaborative effort involving the provincial government, Indigenous communities, and stakeholders to update inventories, enhance transparency, and implement science-based management strategies aimed at achieving a sustainable balance between ecological integrity and societal needs.

Major swaths of British Columbia’s coastal forest have already been designated as protected areas, the largest of which is Great Bear Rainforest, a massive area of 8.5 million ha. This vast expanse of temperate rainforest, stretching along the central and northern coast of British Columbia, was the result of decades of collaboration between First Nations,

environmental organizations, the provincial government, and the forestry industry (McGee et al., 2010; Price et al., 2009). Through a series of land use agreements and conservation measures, the Great Bear Rainforest was officially designated in 2016, setting aside approximately 6.4 million hectares of forest for protection.

In recent years, British Columbia has taken further steps to address concerns over old-growth logging through the implementation of management deferrals in key forested areas. These deferrals, announced by the provincial government, temporarily suspend logging activities in specific old-growth forests deemed at risk while long-term management strategies are developed (Old Growth Technical Advisory Panel, 2021). The deferrals are established by the government in collaboration with Indigenous communities, stakeholders, and scientific experts, and are both temporary and short-term protections while First Nations, the Province, and other partners develop long-term approaches for old growth forest management based on the old growth strategic review.

Complexities in defining mature and old growth forests

Defining old growth in the temperate rainforest presents significant challenges due to the complexity and variability of forest ecosystems in the region as well as limits in existing observational data (Gray et al., 2023). Old-growth forests are characterized by a combination of ecological, structural, and biological features, including large, mature trees, diverse species composition, and complex canopy structures (Spies and Franklin, 1996). However, the specific criteria used to define old growth can vary widely among scientists, land managers, and stakeholders, leading to inconsistencies in classification and management strategies. Factors such as stand age, tree size, species diversity, and disturbance history all influence the designation of old-growth status, complicating efforts to establish clear and comprehensive definitions.

Additionally, the cultural and historical significance of old-growth forests further complicates the issue, as different communities may place varying levels of importance on certain attributes or values associated with these ecosystems (Al Gorley and Garry Merkel, 2020). As a result, achieving consensus on old-growth definitions and management approaches requires careful consideration of ecological principles, stakeholder input, and the diverse perspectives of all involved parties (Gray et al., 2023).

In the US, Executive Order 14072, titled "Strengthening the Nation's Forests, Communities, and Local Economies," was signed into law on April 22, 2022. The executive order directed the United States Secretary of Agriculture and the Secretary of the Interior to work collaboratively with other federal agencies, scientific experts, and stakeholders to create consistent and comprehensive definitions of old-growth and mature forests. This effort resulted in the publication of the old growth and mature definitions for each dominant forest type within the ten US Forest Service management regions and were intended to standardize how these forests are identified and managed across various jurisdictions (USFS, 2023). By establishing clear definitions, the order aimed to enhance the protection of these forests, ensuring their ecological integrity and resilience against threats such as climate change, wildfires, and human activities.

Using these new standardized definitions, I will create spatial estimates of old-growth and mature forests across a large landscape spanning from Kodiak Island in Alaska to the southern border of British Columbia. This effort will contextualize where these forests lie within different protected areas, highlighting how current conservation policies could lead to vulnerabilities in the future management of old-growth forests. By integrating spatial analysis with policy evaluation, I aim to provide a comprehensive understanding of the distribution and

protection status of these critical forest ecosystems, offering insights that can inform future conservation strategies and policy developments.

Methods

Study area

This study utilized the modeling regions from Chapter 2 which covered an area of nearly 29.9 million hectares, stretching from Kodiak Island to the border of British Columbia and the state of Washington in the United States. (Figure 2)

Gradient nearest neighbor and explanatory variables

To model the dominant forest type and seral state of these forests, the GNN approach from Chapter 2 was used. Observed vegetation data (i.e. FIA for Alaska and FAIB for British Columbia) and explanatory variables (e.g. climatic and topographic variables, landcover classifications, and Landsat imagery) from Chapter 2 were also used to generate relations in plot data to environmental data in gradient space with CCA. However, instead of imputing mean continuous variables of forest structure and composition from the 5 nearest neighbors in gradient space, the mode categorical variable that classifies a site into dominant forest type and structural classification was used.

Mapped categorical variables

Dominant forest type

To create maps showing which species comprised the highest amount of basal area, we classified each observed plot into dominant species. This was done by assigning a plot an species code based on the calculated basal area for each species. All observed data was filtered for only

living trees, and diameter values were converted to basal area. The species with the maximum basal area was selected and assigned a species code (Table 4).

Table 4. Dominant tree species.

Species Code	*Species*	*Common name*
11	*Abies amabilis*	pacific silver fir
17	*Abies grandis*	grand fir
19	*Abies lasiocarpa*	subalpine fir
42	*Chamaecyparis nootkatensis*	Alaska yellow cedar
94	*Picea glauca*	white spruce
95	*Picea mariana*	black spruce
98	*Picea sitchensis*	Sitka spruce
101	*Pinus albicaulis*	white bark pine
108	*Pinus contorta*	lodgepole pine
119	*Pinus monticola*	western white pine
202	*Pseudotsuga menziesii*	Douglas-fir
231	*Taxus brevifolia*	Pacific yew
242	*Thuja plicata*	western redcedar
263	*Tsuga heterophylla*	western hemlock
264	*Tsuga mertensiana*	mountain hemlock
312	*Acer macrophyllum*	bigleaf maple
351	*Alnus rubra*	red alder
375	*Betula papyrifera*	paper birch
746	*Populus tremuloides*	quaking aspen
747	*Populus trichocarpa*	black cottonwood

Successional classification

To classify forests as either old growth, mature, or other, we utilized the dominant forest type classification mentioned above to determine the seral status of each plot on the observation data. The definitions used in this analysis came from the recent publication of nationwide definitions of old growth and mature forests by US Forest Service (USFS) region in the United States (USDA, 2023). The USFS Alaska Region adopted old-growth forest criteria outlined by Boughton et al. (1992a, 1992b) and translated these criteria into measurable attributes using

available data from FIA plots. Plots were considered old growth if they met specific thresholds of tree density, stand age, and number of large, live, or dead trees. Originally, all criteria had to be met, but regional experts relaxed this requirement to classify a plot as old growth if any one of the criteria was satisfied. This adjustment aligned their results more closely with independent map-based classifications used by the Tongass National Forest (Pelz et al., 2023).

These definitions were used in this analysis based on the calculated plot characteristics of stand age and density of dead standing trees described in Chapter 2 (Table 5). To determine if a plot matched the definition for mature forests, the diameter diversity index (DDI), basal area of standing dead snags (BA dead), and standard deviation of tree height (SD HT) were also calculated. Stands that met the criteria for mature forests were classified as such if they did not meet the old growth definition for a said dominant forest type first.

Table 5. Definitions for old growth and mature classification based on dominant species forest type.

Species		Old Growth		Mature		
Species Code	Species	Stand age	TPH Dead	DDI	BA dead	SD HT
11	*Abies amabilis*	170	4	21.3	4.5	
17	*Abies grandis*	170	4	40.1		14.3
19	*Abies lasiocarpa*	170	4	27.8		12.5
42	*Chamaecyparis nootkatensis*	150	3		14.2	6.9
94	*Picea glauca*	150	22		1.6	6.4
95	*Picea mariana*	200	10		1.6	2.5
98	*Picea sitchensis*	160	1	42.8		12.1
101	*Pinus albicaulis*	170	4	21.3	4.5	
108	*Pinus contorta*	170	2			
119	*Pinus monticola*	170	4	21.3	4.5	
202	*Pseudotsuga menziesii*	150	4	32.6		12.9
242	*Thuja plicata*	170	12	63.8	4.2	17.3
263	*Tsuga heterophylla*	150	2	21.3	4.5	
264	*Tsuga mertensiana*	160	2		1.6	10.2
312	*Acer macrophyllum*	80	6			
351	*Alnus rubra*	80	6			
375	*Betula papyrifera*	80	6			
746	*Populus tremuloides*	80	6			
747	*Populus trichocarpa*	80	6			

Management and conservation extents

The most recently released datasets of protected areas from the two countries, the Canadian Protected and Conserved Area Database for British Columbia (Canada, 2021) and the USGS Protected Area Database for Alaska (Gergely and McKerrow, 2013), contained extents for both the IRAs and the OGMAs. Both datasets were reclassified into shared categories based on the type of land use restriction (i.e., wilderness area, national parks and monuments, wildlife habitat reserve, native reserve, IRA, and OGMA) and then rasterized to the same extent and resolution as the GNN predictions (Figure 12).

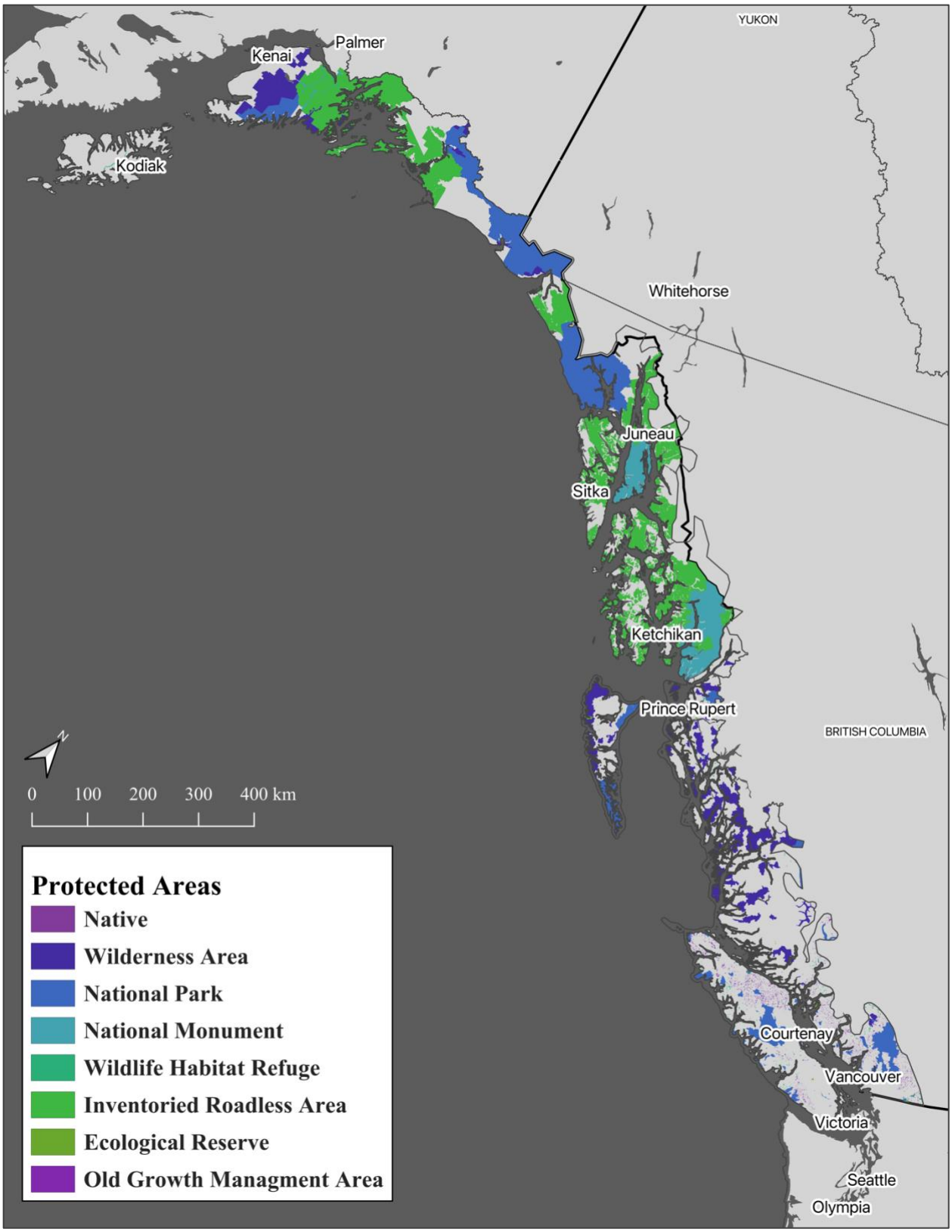


Figure 12. Protected areas of the northern temperate rainforests in Alaska and coastal British Columbia.

Results

Dominant species maps

Dominant overstory species patterns seem to matched regional descriptions of where we would expect to find species on the landscape (Alaback and Juday, 1989; Orians and Schoen, 2013). The species that shows dominance in the largest amount of area is western hemlock, covering an area over 5 million hectares (Table 6, Figure 13). Western hemlock stands tended to be in low-elevation areas nearest to the coastline. This coastal area is also interspersed with populations of Sitka spruce in the north and western redcedar in the mid and southern parts of the study region, although at lower levels of canopy dominance (14 percent for both species). The second most dominant species on the landscape is mountain hemlock, which can be seen at higher elevations up to tree line and covers more than 4.8 million hectares (23 percent) of southeast Alaska and coastal British Columbia. Douglas-fir, an important commercial species in the Pacific Northwest, covers over 1.4 million hectares and is mostly constrained to the southeastern areas of Vancouver Island and more inland forests north of Washington state.

Conifer species with lower levels of canopy dominance were lodgepole pine, Alaska yellow cedar, Pacific silver fir, white spruce, and black spruce. For lodgepole pine, dominant populations tended to be in low lying areas near the coast that are associated with waterlogged soils (muskegs) or areas of low productivity. White and black spruce are dominant forests (1.4 and 1.3 percent) only in the Kenai Peninsula, which resembles the more boreal environments found to the north. Western white pine and subalpine fir both were seldom dominant on the landscape, covering less than 1.000 hectares combined, likely due to very low occurrence in the observation data.

Hardwood species had relatively low dominance, with all hardwood species representing less than 3 percent total area as a dominant forest type. However, where they did occur matches where we would expect to find them. For example, bigleaf maple made up large components of forested areas near the edges of rivers to the south while aspen occurred in similar areas to the north.

Table 6. Dominant overstory species extent and percent cover of total study region.

Species	SPCD	Total area (ha)	Percent area
Tsuga heterophylla	263	5,206,934	25
Tsuga mertensiana	264	4,805,966	23
Thuja plicata	242	3,046,853	14
Picea sitchensis	98	2,883,049	14
Pseudotsuga menziesii	202	1,405,777	6.6
Chamaecyparis nootkatensis	42	1,215,076	5.7
Pinus contorta	108	731,461	3.4
Betula papyrifera	375	499,956	2.4
Abies amabilis	11	347,135	1.6
Picea glauca	94	293,468	1.4
Picea mariana	95	285,372	1.3
Populus trichocarpa	747	205,428	1.0
Alnus rubra	351	164,933	0.8
Acer macrophyllum	312	96,010	0.5
Populus tremuloides	746	27,706	0.1
Pinus monticola	119	8,112	0.04
Abies lasiocarpa	19	2,164	0.01

Old growth and mature classifications

The results from classifying the forests into seral states show that a total of 1,176,903 hectares are classified as productive old growth forests while 2,291,309 hectares can be classified as mature forests. In southeast Alaska, highly productive old growth and mature stands comprise nearly 23 percent of all forests within the Tongass National Forest boundary. Throughout much of this region, old growth and mature forests are under different forms of protection from harvest. There are many national parks and monuments throughout southeast

Alaska and British Columbia, covering a combined area of over 5.9 million hectares of forested land. This analysis shows that 230,345 hectares of productive old growth and 309,949 hectares of mature forests are held within these national parks and monuments (Table 7). Designated wilderness areas, while having a slightly smaller footprint on the landscape at over 2.3 million hectares, also contain large amounts of productive old growth. In British Columbia, OGMAs hold substantial amounts of old growth compared to their dispersed nature and relatively small spatial coverage, with over 20 percent of the forests being classified as either old growth or mature. The largest stores of older forests reside within IRAs in southeast Alaska, with a total of 832,500 hectares combined.

The mean amount of aboveground biomass varied among the different administratively protected areas. Some of the highest values of forest biomass density are held within national monuments, wildlife habitat refuges, and ecological reserves (Table 7). National parks and indigenously managed land also showed high levels of biomass density. Wilderness areas showed lower overall biomass densities, which is likely due to their inclusion of forests with lower productivity and at higher elevations. The highest levels of biomass were seen in the OGMAs of British Columbia, with a mean aboveground biomass density of 45,972 gm^{-2}.

Table 7. Administrative protective areas with the total area (ha) of old growth and mature forest contained within each. Mean aboveground biomass (gm^{-2}) within each protected area is also reported.

Protected area	Old growth	Mature	Mean AGB
No administrative protection	136,258	336,298	27,332
Indigenously managed	553	805	36,409
Wilderness Area	82,744	175,588	31,118
National Park	73,682	162,190	37,385
National Monument	156,663	147,759	40,432
Wildlife Habitat Refuge	2,143	6,047	40,946
IRA	372,290	460,210	32,855
Ecological Reserve	388	2,056	40,793
OGMA	7,398	23,725	45,972

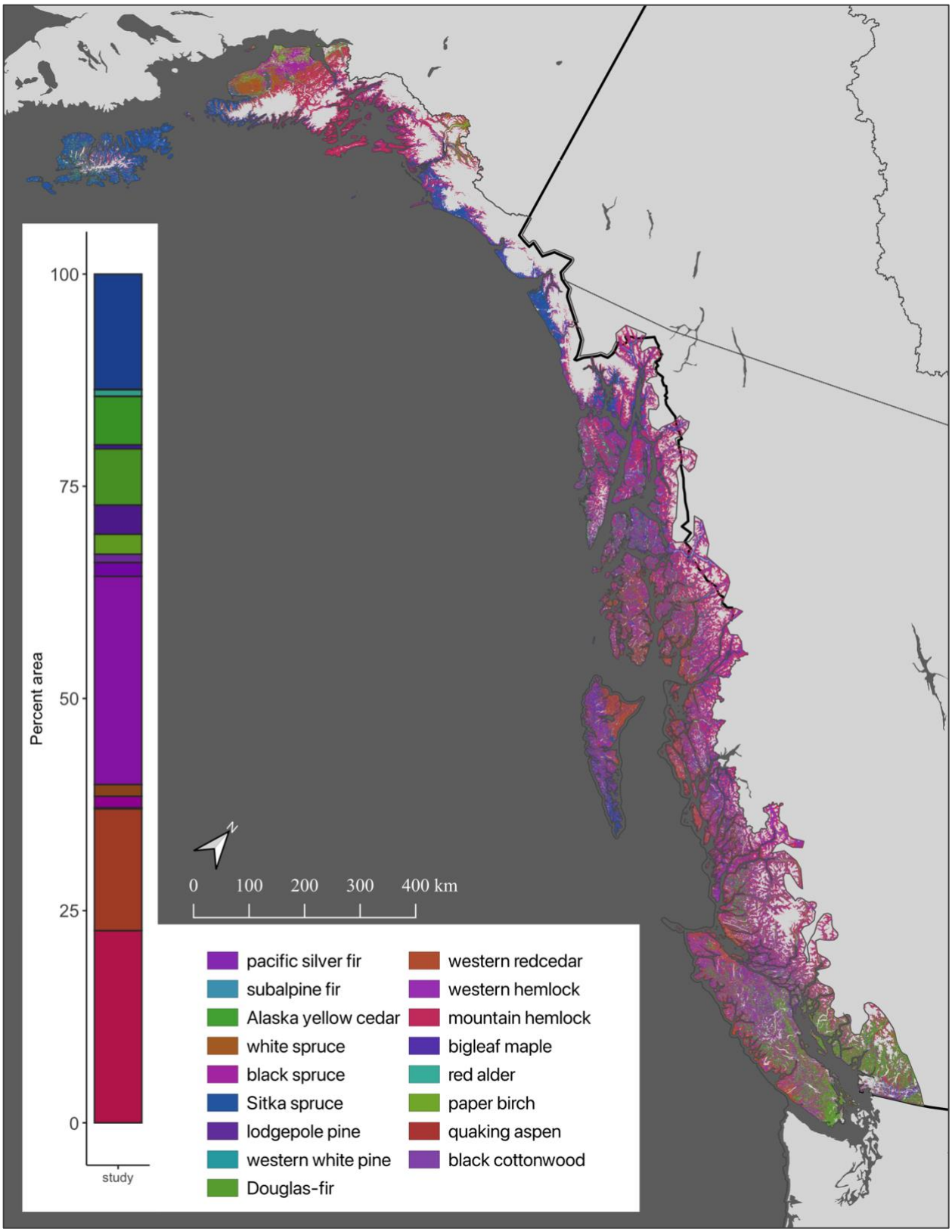


Figure 13. Dominant species classification map. Percent of total area by species is also displayed on the left of the map.

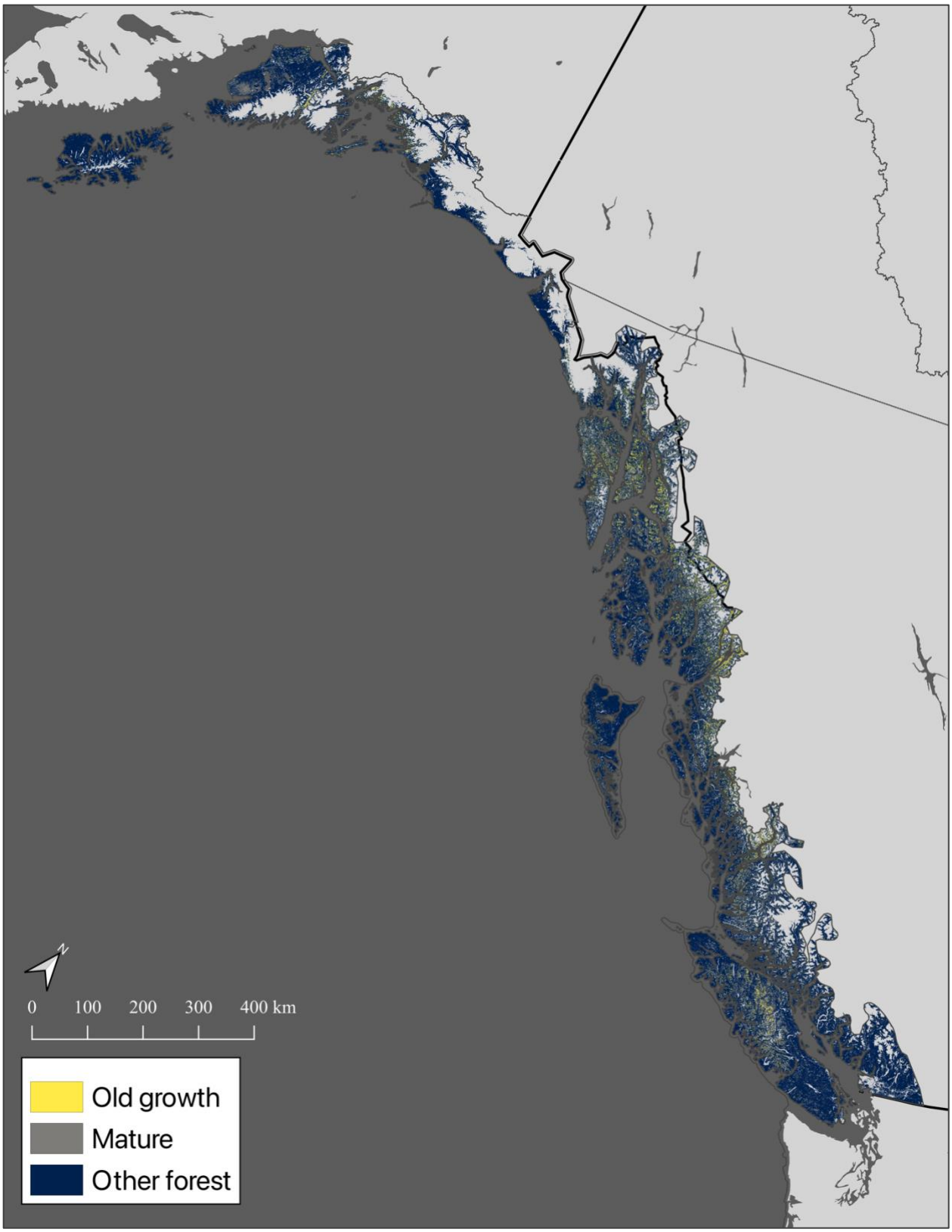


Figure 14. Map showing the spatial predictions of old growth and mature forests.

Discussion

Dominant Species Extent Maps

The dominant species extent maps produced in this study provide a detailed and harmonized view of overstory species distribution across Southeast Alaska and coastal British Columbia. The results indicate that western hemlock (*Tsuga heterophylla*) is the most dominant species, covering over 5 million hectares, predominantly in low elevation areas near the coastline. Mountain hemlock (*Tsuga mertensiana*) is the second most dominant species, occupying higher elevations and covering more than 4.8 million hectares. Other significant species include Sitka spruce (*Picea sitchensis*) and western redcedar (*Thuja plicata*), which are interspersed throughout the region, with notable presence in the northern and southern parts of the study area, respectively. These patterns align well with regional ecological descriptions, confirming the reliability of the mapping approach used. Comparatively, the work by Shang et al., 2020 in British Columbia also maps dominant species using remote sensing and modeling techniques, achieving high accuracy with localized models.

In southeast Alaska, there has been less focus on spatially complete estimates of forest composition and structure. A synthesis of the fire regimes in the region used the LANDFIRE Biophysical Settings (BpSs) maps (Rogers et al., 2011). These maps of biophysical settings describe both species assemblage and environmental factors (such as productivity and drainage), much like the British Columbia biogeoclimatic ecosystem classification (BEC) maps (Meidinger and Pojar, 1991). However, the dominant species predictions presented in this study are the first attempt at creating a harmonized map that crosses the jurisdictional boundaries of the US and British Columbia, providing a seamless view of forest composition across a vast and ecologically diverse region. This integration is crucial for transboundary conservation efforts and forest

management strategies, offering a unified dataset that can inform policy and management decisions on both sides of the border.

Multiple regional definitions

The management and conservation of old-growth forests are complicated by varying definitions of what constitutes an old-growth forest across different jurisdictions. This inconsistency can lead to significant challenges in policy implementation, ecological conservation, and forest management. One major issue is the discrepancy between defining old-growth forests by age versus their capacity to support large trees, as discussed in Price et al., 2021. In British Columbia, for example, the provincial government often defines old-growth forests primarily based on the age of the trees, typically those older than 140 years in coastal regions and 250 years in interior regions. While age is a straightforward criterion, it does not necessarily capture the ecological complexity and productivity of these forests. They argue that an age-based definition can be misleading because it includes large areas of low-productivity forests, such as subalpine and bog forests, that do not support large, ecologically significant trees. This approach can result in a skewed perception of old-growth forest abundance, potentially underrepresenting the more productive, biologically rich areas that are crucial for biodiversity and carbon storage. For instance, highly productive old-growth forests constitute less than 1% of BC's forests but are critical for maintaining biodiversity and ecological functions.

The definitions for old growth and mature forests provided by the USFS were chosen for this study because they offer a comprehensive and standardized approach suitable for all forest types within the study region (*USFS*, 2023). These definitions are the most recent and incorporate detailed criteria that account for both age and site productivity, ensuring a nuanced understanding of forest dynamics.

Future vulnerabilities to late-successional forests.

Inventoried Roadless Areas (IRAs) are a significant component of protected old-growth forests in the United States, particularly within the Tongass National Forest where they hold the highest extents of late-successional forests (Table 7). IRAs are designated to restrict road construction and logging, thereby preserving large tracts of undeveloped land. DellaSala et al., 2022 highlights the critical role of IRAs in maintaining biodiversity, ecological functions, and carbon storage in the Tongass, noting that an estimated 1,060,035 hectares of productive old growth are held within IRAs. However, the predictions in this study show much lower extents of old growth in IRAs, with only 372,290 hectares classified as old growth and 460,210 hectares as mature. This discrepancy could be attributed to the broader definition of old growth used in DellaSala et al., 2022 (wood standing volume > 46.6 m^3/ha and stand age > 150 years) and the inclusion of a mature forest classification in this analysis. When combining the estimates of old growth and mature forests within IRA boundaries, the two estimates are more closely aligned, with a total of 832,500 hectares classified as being in a late-successional stage.

Different types of protective designations offer varying degrees of security for old-growth forests. Some protections are more permanent, such as national parks and wilderness areas, which typically require legislative action to alter their status. In contrast, other protections, such as administrative designations like IRAs and old-growth management areas (OGMAs) in British Columbia, can be more easily modified or revoked by government agencies. These areas are shown to have some of the highest levels of aboveground biomass (Table 7) and are vulnerable to policy reversals and exemptions that can open them to logging and development (DellaSala et al., 2022; Dietz et al., 2021; Joeveen Dhari, 2023; Price et al., 2021). The recent history of the Roadless Rule, which governs IRAs, illustrates this vulnerability. The rule has

been subject to multiple legal challenges and administrative changes, reflecting its impermanence and the ongoing debate over land use priorities.

Implications

The research presented here offers valuable insights into the distribution and extent of dominant overstory species and the classification of old growth and mature forests across Southeast Alaska and coastal British Columbia. By providing detailed and harmonized maps that cross jurisdictional boundaries, this study offers a comprehensive view of forest composition and structure that is crucial for effective transboundary conservation and forest management strategies. For land managers and policymakers, these findings are instrumental in guiding conservation efforts and policy decisions. The detailed spatial data on dominant species and forest seral stages can inform targeted management practices to preserve biodiversity, enhance carbon storage, and maintain ecosystem functions. Additionally, understanding the distribution of biomass across different protected areas helps in prioritizing regions that require stricter conservation measures. The harmonized dataset facilitates coordinated efforts between the US and British Columbia, ensuring that conservation and management strategies are implemented seamlessly across borders. Overall, this research supports informed decision-making and promotes sustainable forest management practices that can adapt to future environmental challenges.

CHAPTER 4 – MODELING FUTURE CARBON VULNERABILITIES WITH NATURAL DISTURBANCE, MANAGEMENT AND CLIMATE CHANGE

Introduction

Although mostly undeveloped, the coastal temperate rainforests of North America are known for their highly productive timber industry, where vast expanses of forests have long been instrumental in sustaining local economies and global wood product markets (Harris and Farr, 1974). Historically, silvicultural methods focused on clearcutting stands containing large, commercially valuable, old-growth conifers such as Sitka spruce, western red-cedar, western hemlock, and Douglas-fir (Brackley et al., 2009). However, as these timber harvesting practices have continued alongside growing environmental awareness, managing old-growth forests has become a subject of intense debate. Discussions among the United States, British Columbia, indigenous communities, and large non-profits (e.g., The Nature Conservancy's Emerald Edge Project) have recently shifted regional policies away from clearcutting old-growth to preserving old-growth stands in the region.

The Tongass National Forest, located in the coastal temperate rainforests of the U.S. is the nation's largest national forest. In 2016, the Tongass Land and Resource Management Plan outlined guidelines for the U.S. Forest Service to design integrated forest management projects that support a "diverse economies, enhance community resilience, conserve natural resources, and retain climate-resilient forests through integrated forest management practices". One of the main objectives of the plan was to end large-scale, old-growth timber harvest and to focus resources in support of forest restoration, recreation, climate resilience, and sustainable young-growth management (i.e. rotational harvest in areas that have been historically logged every 55-60 years).

In combination with the reenactment of the 2001 Roadless Area Conservation Rule in January of 2023 (Fed Reg. Vol 88, No. 18, 2023), the shift to a young-growth harvesting plan has the potential to provide a sustainable and economically viable source of timber to local and global economies while also conserving large areas of undisturbed forests.

Natural disturbance and succession

Within the Tongass and throughout the southeastern coast of Alaska, the predominant disturbance of windstorms is extratropical cyclones (ETCs) (Mesquita et al., 2010). These ETCs can span over 1000 km and typically persist over a period of days, bringing heavy rainfall and high winds to coastal and inland regions (Clifford Mass and Brigid Dotson, 2010; Read, 2015). From autumn to late winter, potent and sizable ETCs, with the potential to generate hurricane-force winds, can quickly form in the eastern Pacific Ocean through a phenomenon known as explosive cyclogenesis (Bullock and Gyakum, 1993; M. G. Kramer et al., 2001). These cyclones are often associated with strong winds, which can occasionally reach or exceed 40 meters per second. These storms generate substantial precipitation that contributes to the region's overall high levels of moisture. These ETCs also affect forest stand and soil developmental trajectories, ultimately leaving long-lasting legacies on stand conditions, disturbance patch size, and distribution of stand types across the landscape.

In addition to forest overstory dynamics, windthrow also has a profound and long-term effect on coarse woody debris (CWD) and forest soil dynamics. Much like other forest disturbances, windthrow takes standing live trees and converts them to standing dead and broken or downed coarse woody debris (Yatskov, 2016). Standing dead and fallen trees also play a crucial role in forest ecosystems by offering habitat and support for plant, insect, microbial, and animal communities as they go through various stages of decomposition (Bouget and Duelli, 2004; Feller,

2003; Song, 1997; Spies and Cline, 1988). Wind-felled trees produce upturned root systems and expose large volumes of mineral soil and forest floor (Mitchell, 2013). However, in the absence of disturbance in this region, organic matter will accumulate in the soil profile over long periods of time and impair soil drainage over long periods of time. The increase in organic matter can lead to an increase in peat formation and a decline in forest productivity, causing an ecosystem shift from forest to bog (Simard et al., 2007). Frequent wind, snow, and ice storms occurring from fall through early spring (Alaback et al., 2013a)limit the growing seasons for vegetation, but also exert significant impacts on associated soil carbon dynamics (D'Amore and Hennon, 2006), nutrient cycling (D'Amore et al., 2010), and rates of forest regeneration (Alaback, 1982). For instance, the decline of Alaska yellow-cedar (*Callitropsis nootkatensis*) appears to be closely linked to changes in transient snow — reduced snowpacks affect soil insulation, leading to damage and mortality of fine roots in poorly drained areas (Hennon et al., 2012).

The shift from old growth to young-growth management in Alaska present uncertainties about how the spatial legacies of historical harvests will influence the carbon storage capacities of these forests. In this region, the highest aboveground carbon stocks are found in areas of moderate slopes (Buma et al., 2016a), and the highest belowground stocks found in relatively flat areas (McNicol et al., 2019). Previous harvests were often located in stands within areas that were both highly productive and easily accessible. These areas also tend to be protected from windstorms (Marc G Kramer et al., 2001). Therefore, areas with the highest productivity are most vulnerable to wind. Conversely, areas with the lowest risk of natural disturbance are also being managed for future timber harvests. Essentially, logging over the past several decades is opposite to natural disturbance patterns (Alaback et al., 2013a), diverging from current management initiatives designed to emulate natural disturbance regimes (Lindenmayer and Franklin, 2013; North and

Keeton, 2008).

Future climate and vegetation

In the forests of southeast Alaska, climatic warming has affected ecosystems primarily through changes in precipitation (Mote and Salathé, 2010; NOAA, 2023). Historically, this region has average winter temperatures near 0°C along with long growing seasons. In the past few decades, the region has experienced a 1.7 °C increase in average annual temperatures and an 8% increase in annual precipitation (Karger and Zimmermann, 2018). Moderate warming due to climate change is projected to increase rain, reduce snow, and increase growing season length (Figure 15, Figure 16). These climatic shifts are expected to alter thethe distribution of individual species and ecological communities (Hamann and Wang, 2006; Wolken et al., 2011). Species with wide distributions and genetic diversity, such as western hemlock (*Tsuga heterophylla*) and Sitka spruce (*Picea sitchensis*), are expected to rapidly colonize new habitats (Gavin et al., 2006; Harris and Farr, 1974). However, other species, like yellow-cedar and many understory plants, are anticipated to change at a slower pace due to specific regeneration requirements (Bunnell and Kremsater, 2012; Gilliam, 2007), potentially leading to the formation of novel plant communities (Oakes et al., 2014).

This study creates a better understanding of how the shift from old growth to young growth management may interact with ETCs and climate change on the landscape. To do this, I used a spatially-explicit forest landscape model to project how shifting the spatial distribution of management from areas protected by wind or exposed to large wind events affects the carbon and species trajectories on Zarembo Island, Alaska.

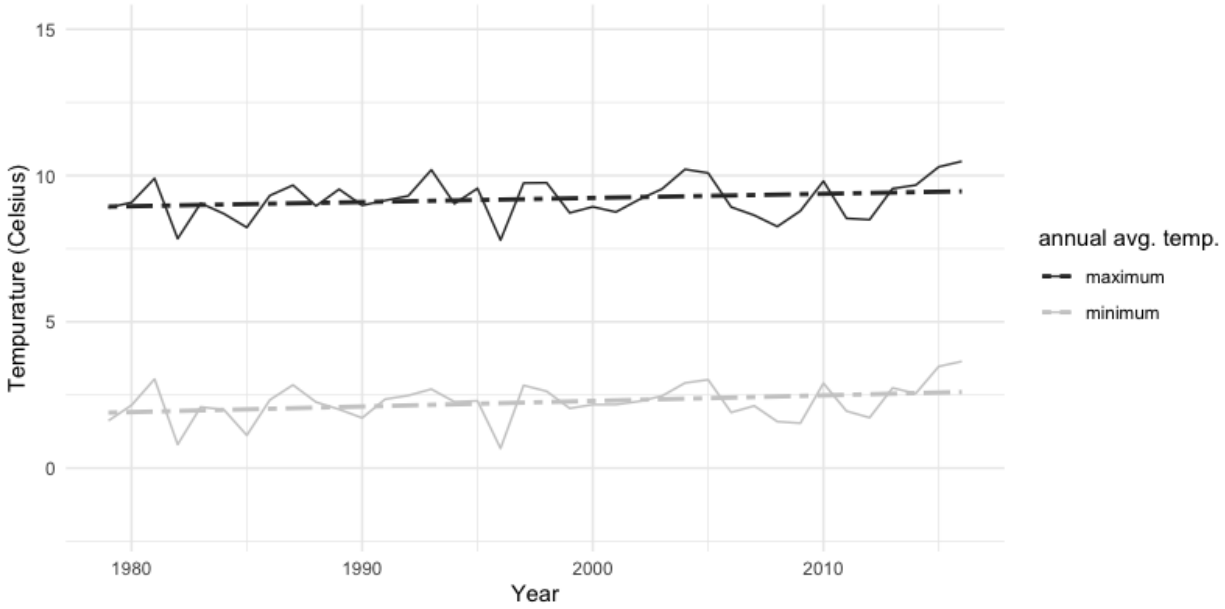


Figure 15. Average annual minimum and maximum aboveground air temperature across the perhumid forests of southeast Alaska and British Columbia from the years 1979 to 2016. Dashed lines are linear regressions fitted to monthly temperature records and show a general increase in both minimum and maximum temperatures. Historical data obtained from CHELSA (Karger and Zimmermann 2018)

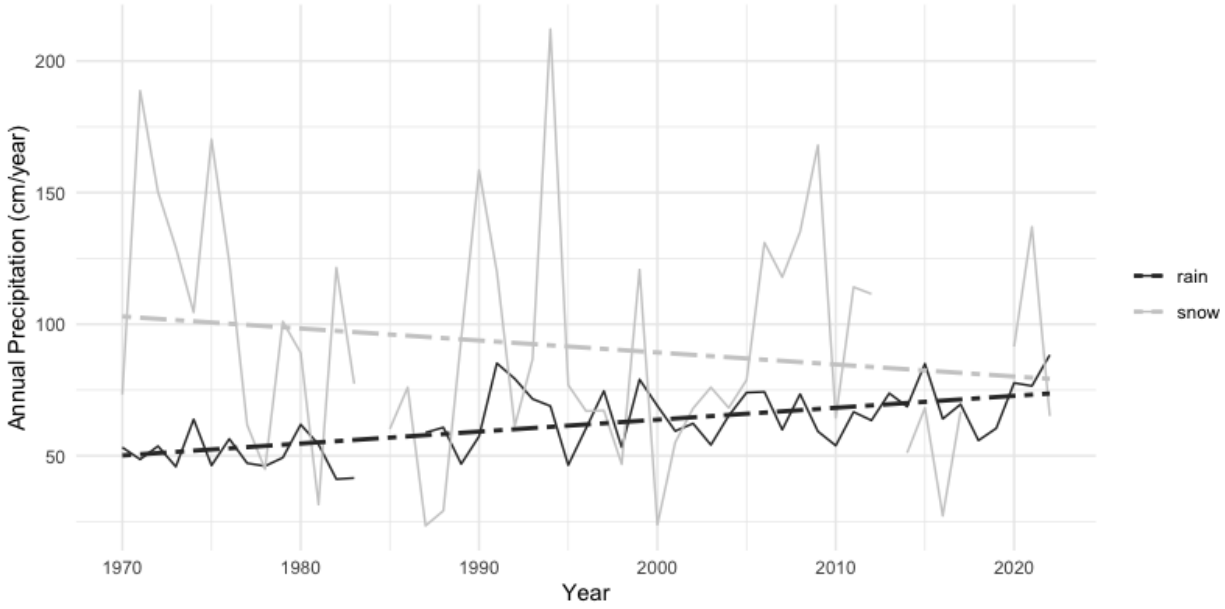


Figure 16. Annual rain and snow precipitation at the Juneau International Airport weather station from 1970 – 2022. Dashed lines are linear regressions fitted to monthly temperature records and show a general increase in both minimum and maximum temperatures. Historical data obtained from Climate Data Online *(NOAA 2023)*.

Methods

Study area

The modeling region for this analysis consists of Zarembo Island, a 48,407 hectare island located in the Alexander Archipelago of southeastern Alaska (Figure 1). It is characterized by its temperate rainforest ecosystem and is located within the Tongass National Forest. The island's landscape is dominated by dense coniferous forests primarily composed of Sitka spruce (*Picea sitchensis*), western redcedar (*Thuja plicata*) and western hemlock (*Tsuga heterophylla*), interspersed with muskegs, wetlands, small alpine meadows and consists of elevations ranging from sea level to 950 meters. Muskegs and hydric soils, which comprise 57% of the landscape, are predominantly located in broad glacial valleys and higher-elevation benches (Kramer et al., 2001). The island receives substantial rainfall, averaging between 2500 to 3800 millimeters (100 to 150 inches) annually. Temperatures are moderate throughout the year, with average winter temperatures ranging from -1 to 4°C (30 to 40°F) and summer temperatures ranging from 10 to 16°C (50 to 60°F) (Karger and Zimmermann, 2018).

The island is frequently affected by ETCs, especially during the fall and winter months (Read, 2015). These storms, often originating from the south and southwest, bring heavy rainfall and strong winds to the region. This island was chosen as a representative subset of the larger Tongass ecoregion because it is affected by frequent ETCs and includes large areas classified as suitable young growth, available for timber harvests under the young growth management plan of the Tongass National Forest.

LANDIS-II landscape model

LANDIS-II (v. 7) was used to simulate forest succession, windstorms, and forest management under three climate change scenarios at a high spatial resolution (90m). LANDIS-II

is an open source spatially-explicit, process-based, simulation model (Scheller et al., 2007) that forecasts the interactive effects of climate, succession, management, and natural disturbances on the spatial distributions of tree species and carbon dynamics. It operates on grid cells containing species-age cohorts, which can grow and compete within a cell over time based on species-specific traits, such as longevity, shade tolerance, seeding distances, and post-fire regeneration strategies (e.g., serotiny and resprouting). Each cell can contain multiple cohorts of each species, allowing for complex age structures. LANDIS-II extensions are typically calibrated using historical reference data, but simulations follow no single successional pathway once executed. Processes like regeneration (e.g., seed dispersal and resprouting) and disturbances (e.g., fire, wind, insects) are stochastic and interact spatially across the landscape. LANDIS-II is modular, with a variety of extensions available to represent ecosystem processes such as forest growth as well as disturbances such as wildfire, pests, and wind (https://www.landis-ii.org/extensions), which offers flexibility in the complexity that can be captured. Multiple extensions may be implemented with LANDIS-II simultaneously to simulate multiple processes.

Description of NECN extension

We used the Net Ecosystem Carbon Nitrogen (NECN) succession extension (Scheller et al., 2011), which simulates monthly growth rates, competition, mortality, and regeneration in each raster cell containing multiple species and age cohorts and tracks changes in aboveground biomass, soil organic carbon stocks and forest composition (Figure 17). The map of overstory vegetation composition and age from the GNN imputations described in Chapter 2 was used as the starting conditions for LANDIS-II and NECN. Species growth and mortality were calibrated using observed FIA plot data (Gray et al., 2012).

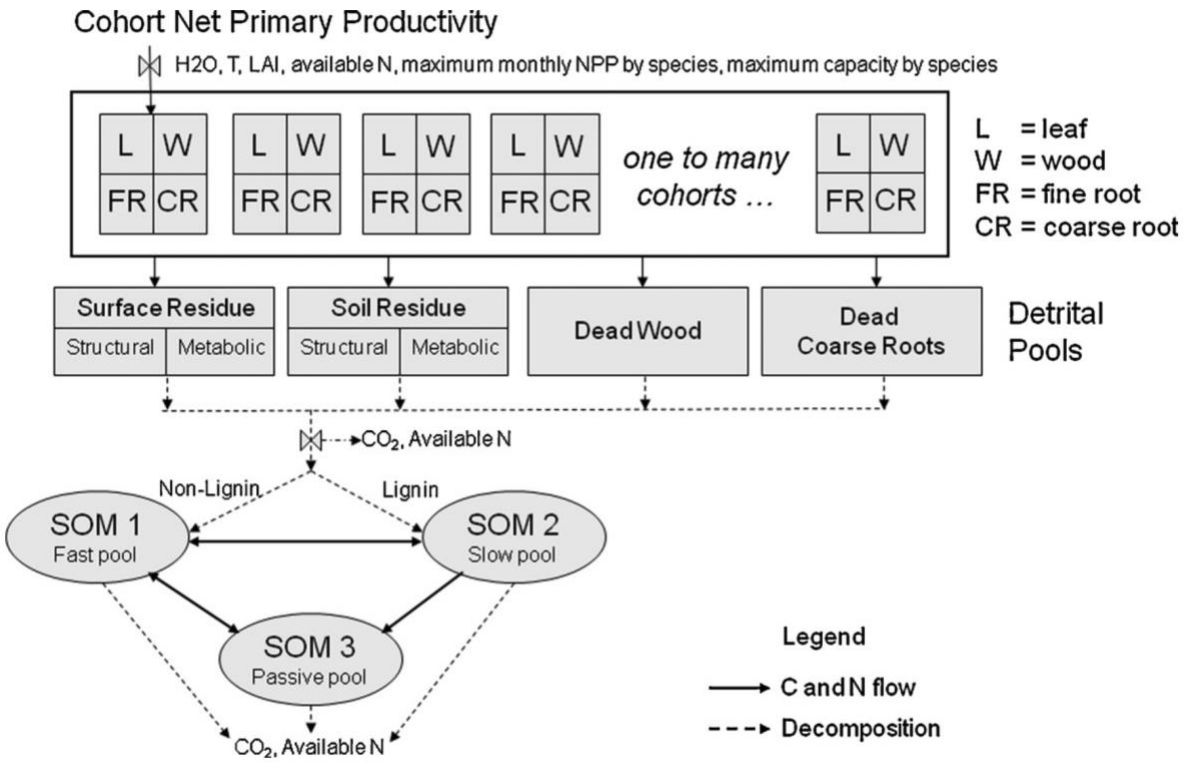


Figure 17. Schematic diagram of the NECN succession extension for LANDIS-II. In the top panel, species and age cohorts with leaf, wood, fine root, and coarse root components are represented. Following mortality, this biomass is transferred to one of the detrital pools. Foliage is transferred to the surface residue pool; fine roots to the soil residue pool. As decay progresses, carbon and nitrogen are transferred to and among the fast, slow, and passive soil organic matter (SOM) pools, with some loss to the atmosphere and through leaching. (Scheller et al., 2011)

Natural Disturbance

To simulate windthrow from regional cyclonic storms, a modified version of Base Hurricane was used in LANDIS-II (Schrum et al., 2020). The new extension, called Biomass Hurricane, generates storms that lead to mortality at a site depending on species-specific windthrow probabilities and can be calibrated with annual storm frequencies, landfall wind speeds, and storm direction (Figure 18). Simulated maximum sustained windspeeds (sMSWS) are modified using regional wind exposure maps generated from methods described in Kramer et al., 2001, with sMSWS decreasing in areas of less exposure to the storm based on its track. Due to this, disturbance is limited to areas that experience higher levels of wind exposure and are not

sheltered by topographic features. The extension also creates spatial outputs of maximum wind speeds and associated tree mortality at a site level for each modeled storm affecting the study area.

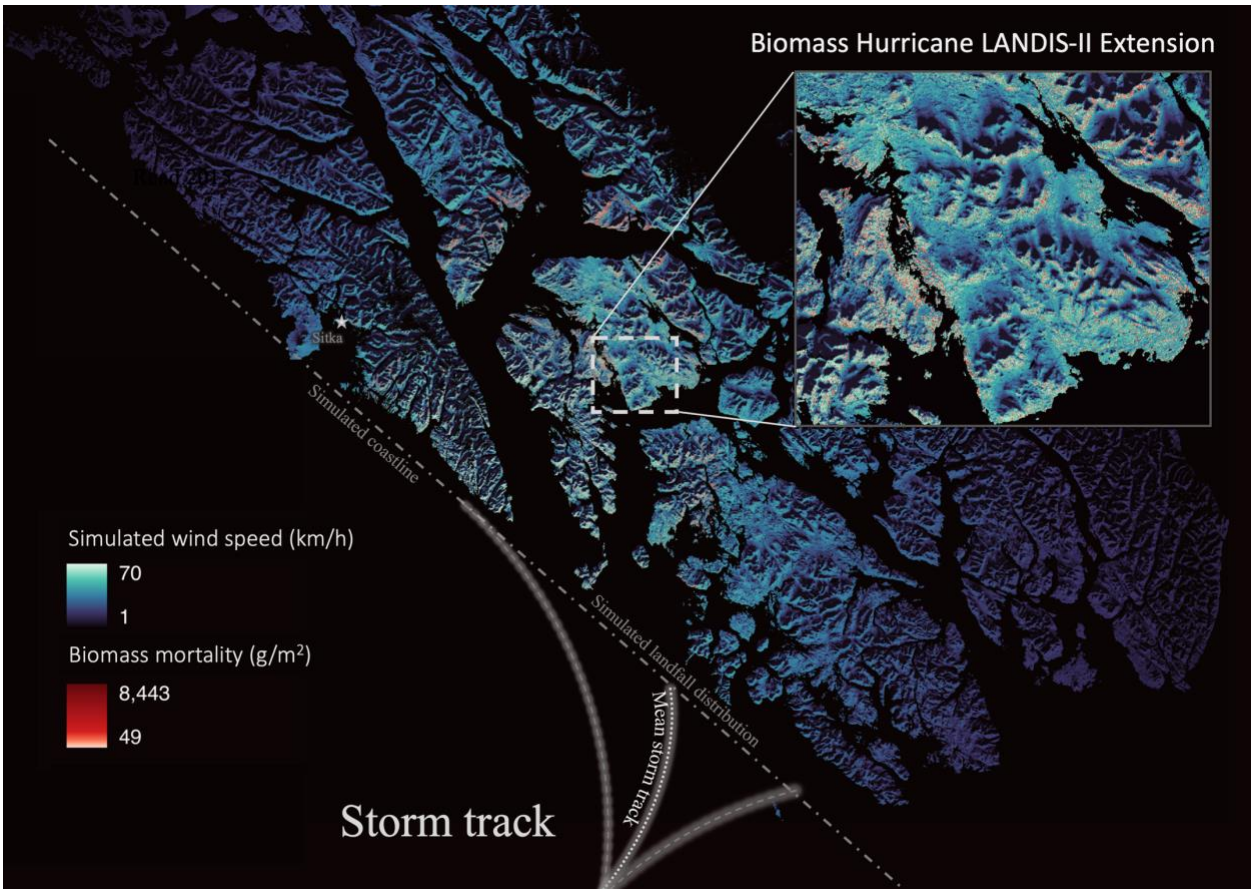


Figure 18. Conceptual diagram of the Biomass Hurricane extension in LANDIS-II used in this study. Simulated coastline is represented as a linear line with a fixed axis. Simulated wind speed (increasing brightness of blue color), mean and deviations of the storm track, and biomass removed (red) in each cell are also shown.

Biophysical inputs

Maps of soil texture were obtained from OpenLandMap (CITE) and processed in Google Earth Engine (GEE). Field capacity and permanent wilting point were calculated from soil texture for each cell using methods from Saxton et al., 1986. Soil carbon maps were obtained from McNicol et al., 2019 down to a meter in depth and SoilGrids (Hengl et al., 2017) were used for soil carbon data down to two meters. Downed woody debris maps were obtained through the

analysis from Carter et al. in prep. Maximum gross primary productivity data across a range of soil water contents and soil temperature (10 cm depth) from a British Columbia Ameriflux site (Black, 1997) was used to fit nonlinear temperature and soil moisture response functions for five species functional groups: low-elevation conifers, high-elevation conifers, hardwoods, lodgepole pine, and red alder. For functional groups that did not have representative flux tower data, soil moisture and gross primary productivity data were obtained from the Soil Moisture Active Passive (SMAP) satellite using Google Earth Engine (Chan et al., 2016).

Climate scenarios

Three climate scenarios were used, representing historical climate (1979 to 2016), moderate warming (CMIP5, RCP 4.5), and severe warming (CMIP5, RCP-8.5) at monthly timesteps. These downscaled climate data were sourced from the CHELSA online climate portal (https://chelsa-climate.org, Karger and Zimmermann, 2018) and summarized into homogenous climate regions using k-means clustering analysis of average projected precipitation and temperature using the 'cluster' package in R (Maechler et al., 2023). While updated climate models (CMIP6) are available, there has not been an effort to downscale these global models in our region and therefore they do not adequately capture local climatic gradients experienced in this highly topographic and coastal system. The two climate change scenarios were bias-corrected to produce a smooth transition between past weather streams and future climate streams (Figure 19).

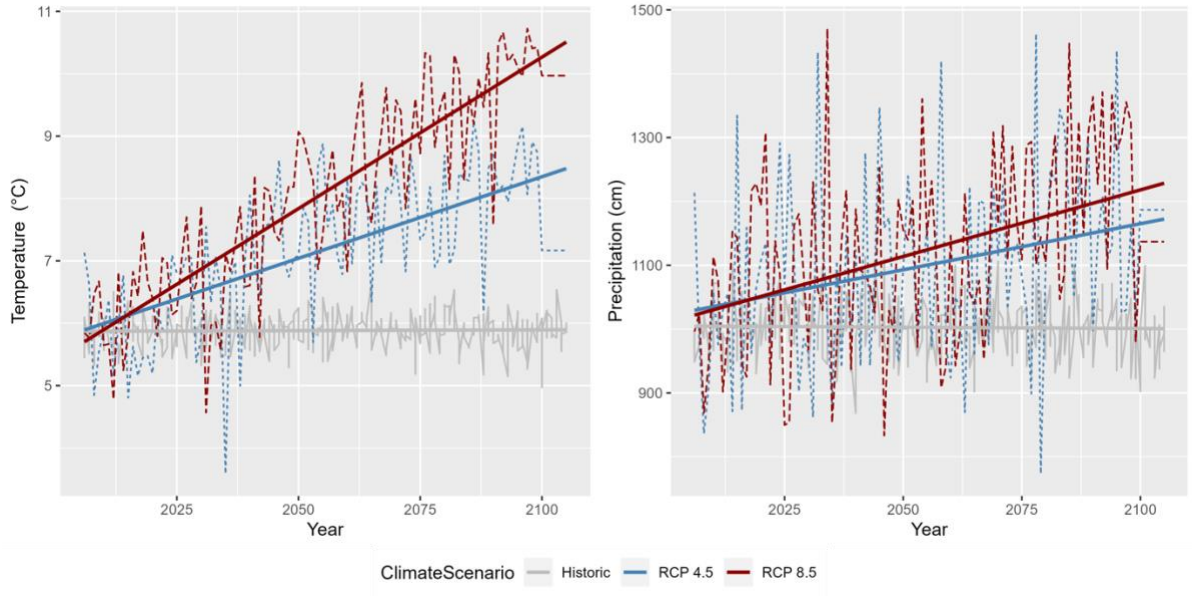


Figure 19. Simulated climate scenarios.

Management scenarios

The Biomass Harvest extension v. 4.6 (Gustafson et al., 2000) was used to simulate young growth management activities on Zarembo Island. This extension simulates biomass removal (including partial biomass removal of individual cohorts) and the planting of tree species following harvesting. Harvesting is controlled by prescriptions targeted to specific forest types that specify how much biomass is removed from which species and ages within a forest stand. In the Tongass national forests, clearcutting is often preceded by an initial pre-commercial thinning treatment when a stand is between 15-35 years of age. As such, our simulations include both a clearcutting prescription and a pre-commercial thinning prescription. Scenarios were calibrated to have equal amounts of biomass removed annually.

Three forest management scenarios were developed to explore the effects of harvesting practices of young growth under varying conditions of wind exposure in southeastern Alaska. The first scenario, "unconstrained," involves harvesting occurring anywhere within the suitable young-growth boundaries as defined by the Tongass National Forest, without any restrictions

related to wind exposure. The second scenario, "wind-protected," restricts harvesting to areas within the young-growth boundaries that are shielded from high wind events, thereby aiming to minimize the impact of wind disturbance on forest regeneration. The third scenario, "wind-exposed," limits harvesting to areas that fall within the young-growth boundaries but are susceptible to high wind events (Figure 20).

In all three harvest scenarios, two different prescriptions were applied. I implemented two distinct harvest prescriptions. The first was a clearcut harvest targeting stands aged between 60-80 years. These clearcuts were restricted to a maximum size of 40 hectares, ensuring that 11% of the standing biomass was retained post-harvest. The second prescription involved pre-commercial thinning in younger stands aged 15-35 years, with a follow-up clearcut harvest 65 years later. Both prescriptions start at the beginning and run until the end of each scenario.

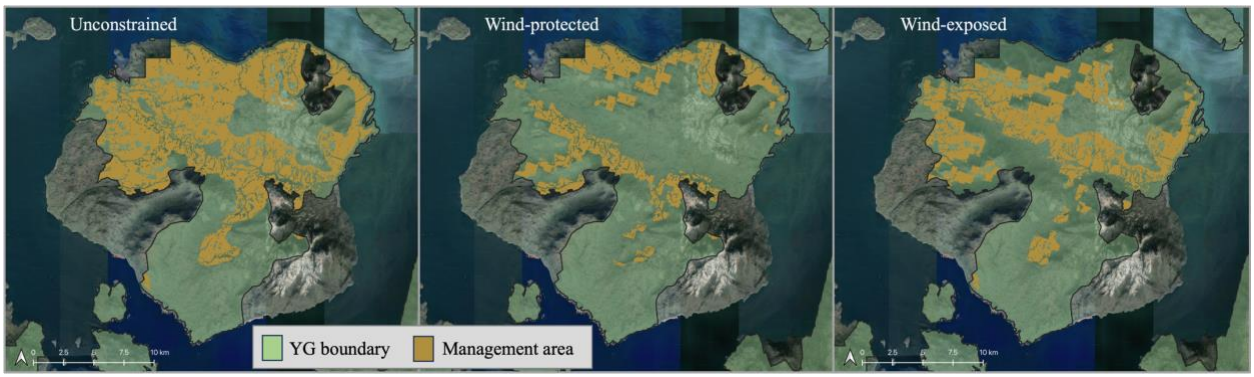


Figure 20. Maps of unconstrained, wind-protected, and wind-exposed management areas used in LANDIS-II.

Results

The Biomass Hurricane extension in LANDIS-II simulated storm conditions comparable to local observations data from the Sitka Airport weather station (NOAA, 2023, Figure 21). Simulated maximum sustained wind speeds fell within the distribution of those experienced in Sitka, ranging from 50 to 92 km/h. This was also true for the simulated storm track, which showed a pattern of storm directions similar to the observed wind directions from the airport

weather station. However, it is worth mentioning that making comparisons between storm track and local wind speed is difficult being that local wind speeds are affected by a number of different factors, such as local terrain, vegetation structure, and attributes of the human built environment near the station.

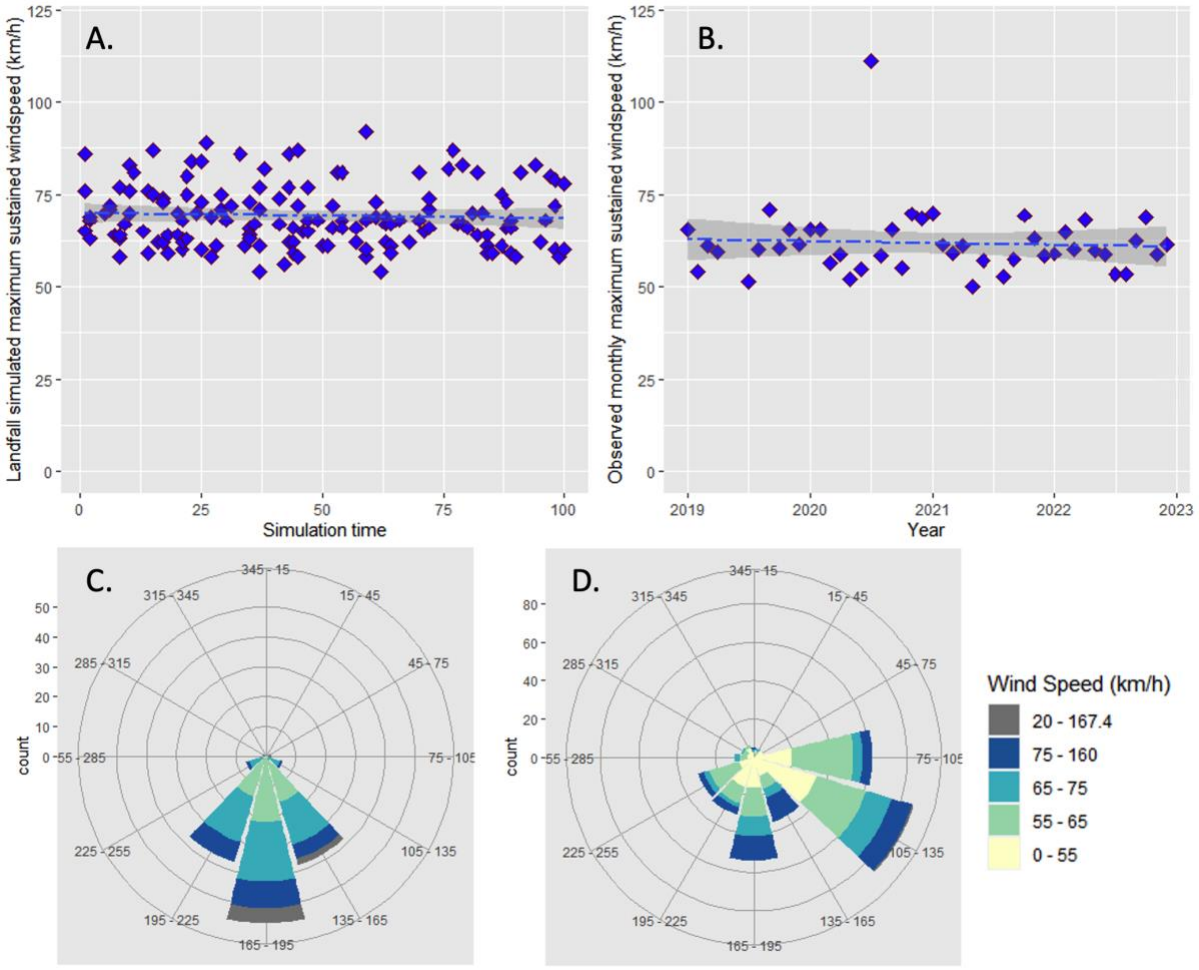


Figure 21. Comparison of simulated and observed maximum sustained wind speed and wind direction: A. Simulated MSWS, B. Observed (Sitka airport) MSWS, C. Simulated wind direction by windspeed, D. Observed (Sitka airport) wind direction by windspeed.

Simulated storm intensity and direction caused a range of wind damage to a site. High-intensity storms showed higher mortality levels over a larger extent, while moderate storms showed more localized mortality events (Figure 22). Storm track direction also modified which

sites were more exposed or protected from an individual storm, resulting in variability of site disturbance based on individual storm events.

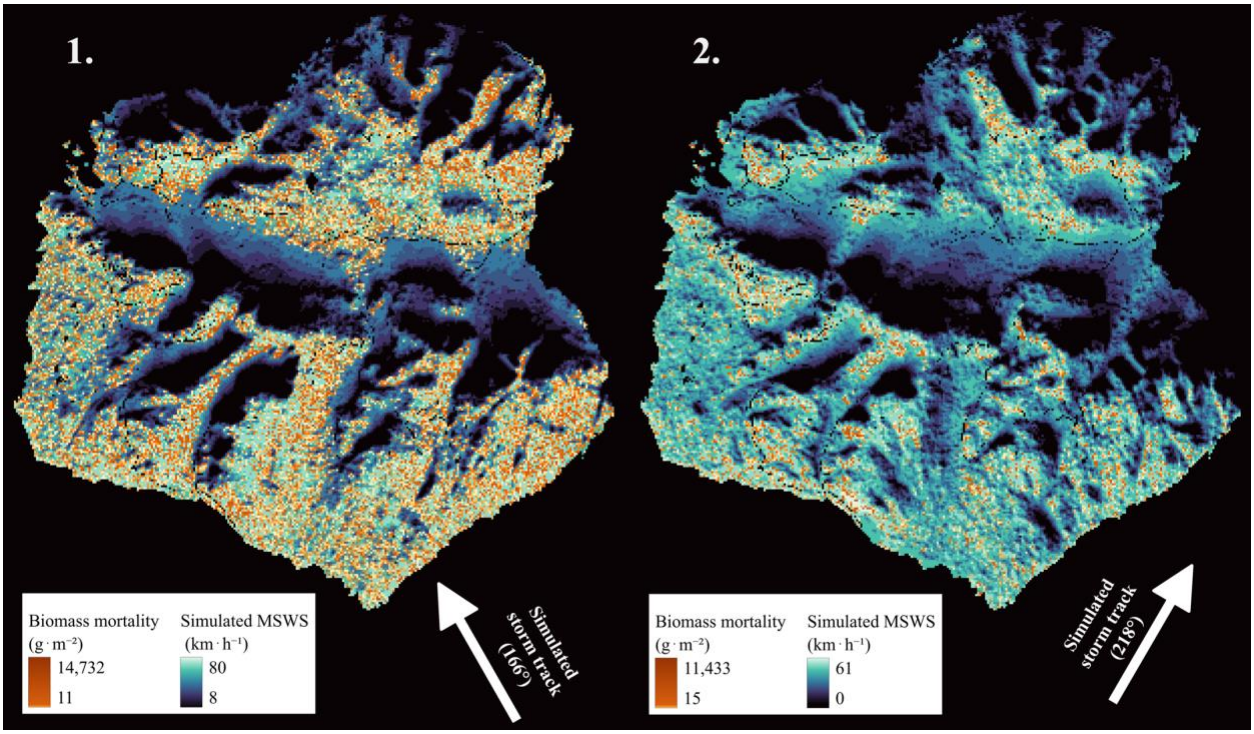


Figure 22. Two simulated storms and associated biomass mortality: 1. Severe storm from the southeast with widespread tree mortality, 2. moderate storm from the southwest with more localized tree mortality.

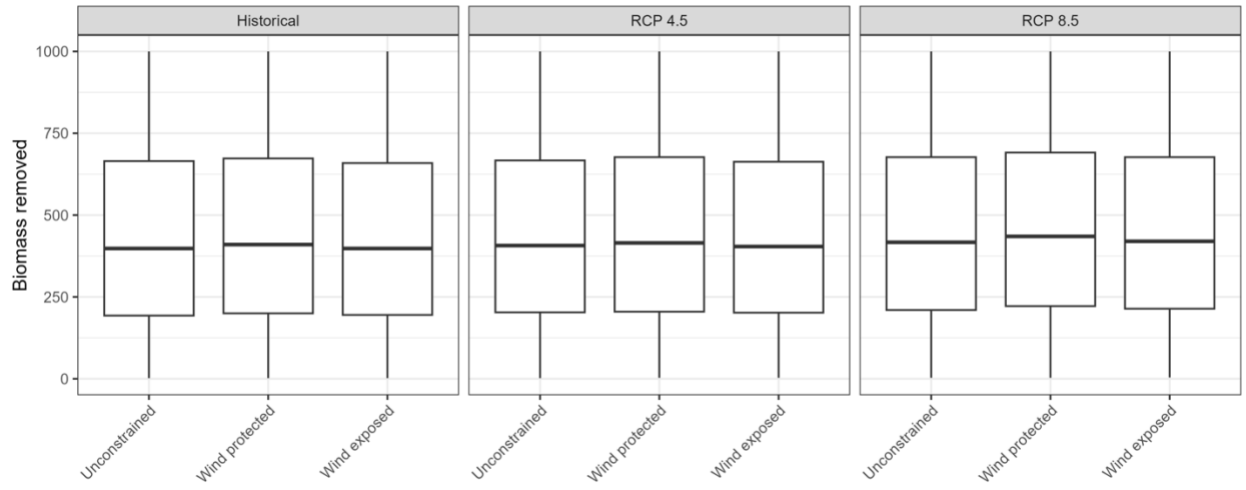


Figure 23. Boxplots showing biomass removed (g•m^{-2}) from ETC events across all management and climate scenarios. Outliers which represent larger blowdown events are not shown.

Biomass removed remained consistent across all management and climate scenarios (Figure 23), with mean biomass removed values of 1,072 – 1,205 $g \cdot m^{-2}$ across sites within the managed areas of Zarembo Island. However, sites of different levels of exposure to simulated storms showed different trajectories in the future accumulation of aboveground biomass (Figure 24). Sites that were largely protected from high wind events steadily increased over time, resulting in higher increases in aboveground biomass at the end of the scenarios. In areas of high wind exposure, sites increased only slightly in aboveground biomass by the end of the scenarios. However, the rate of biomass accumulation was more variable over time. Sites with moderate wind exposure had similar accumulation trends as areas of low wind exposure.

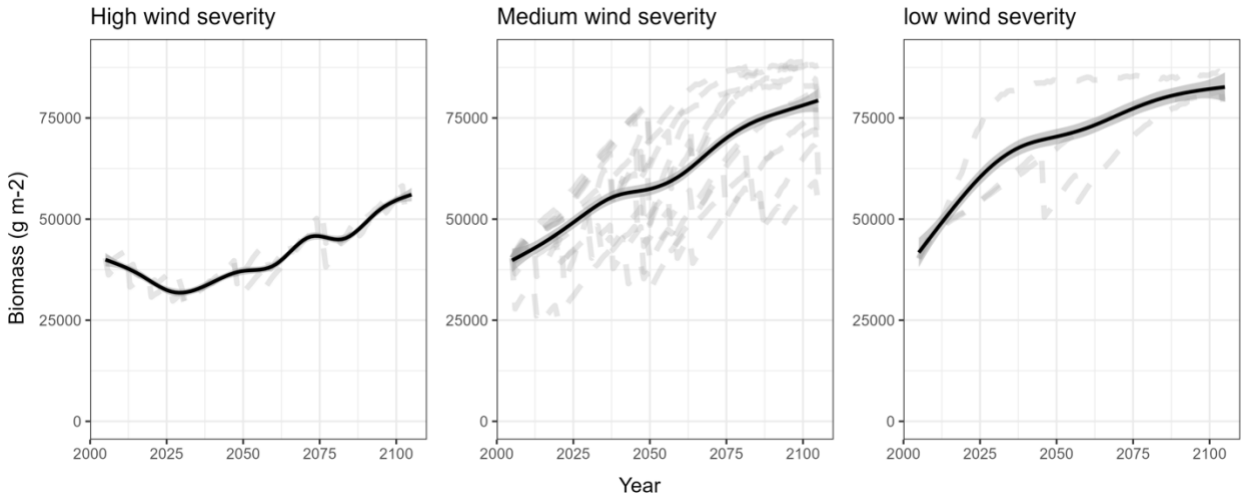


Figure 24. Aboveground biomass trajectories in stands of high, medium, and low wind exposure. Sites shown here had similar aboveground starting conditions but different exposure levels to large regional storm events.

Although set to the same harvesting targets, management scenarios with harvests in wind protected areas had the highest levels of aboveground biomass removed annually under historical climate (Figure 25). This is likely due to the compounding effect that sites in wind protected areas had higher overall biomass in initial conditions and the stochastic nature of how harvesting

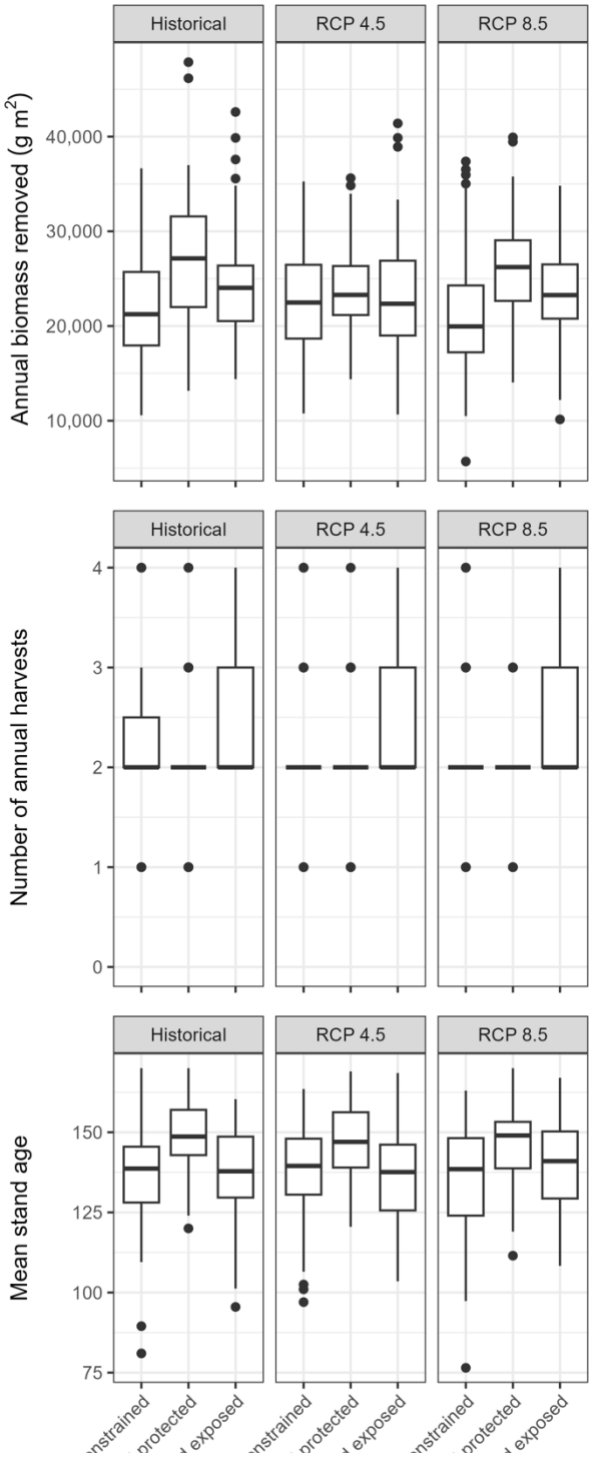


Figure 25. Summarized results from unconstrained, wind-protected, and wind-exposed harvest scenarios under historical, moderate, and severe climate change.

sites were ranked and selected for management. . In scenarios where harvesting occurred only in sites of high wind exposure, higher annual harvest treatments were required to meet harvest targets because of the lower aboveground biomass. The mean age of harvested stands differed between management scenarios, with older stands being harvested within wind-protected areas and younger stands being harvested in wind-exposed areas. Climate showed minimal effect on harvest outcomes, with annual biomass removed, number of harvests, and mean stand age of harvest staying consistent between climate scenarios.

Species composition shifts were observed from initial starting conditions to end of scenario, with the largest increases in biomass of Alaska yellow cedar (*Callitropsis nootkatensis*), lodgepole pine (*Pinus contorta*), and Sitka spruce. (*Picea sitchensis*) under all harvest and climate scenarios (Figure 26). This is consistent with predictions of vegetative shifts from climate in the region by Shanley et al., 2015. However, the biomass of western hemlock (*Tsuga heterophylla*) declined across all scenarios. While red alder

holds a relatively minor contribution to the aboveground biomass in this region, its biomass stayed consistent in all harvest and climate scenarios.

Differences in biomass were primarily due to climate change with the most severe warming scenario showing the highest overall levels of aboveground biomass (Figure 26). There was little observed variation in species biomass across management scenarios for a given climate scenario, however, management in the young-growth boundary of Zarembo Island without spatial constraints from wind exposure showed slightly higher mean aboveground biomass regardless of climate scenario.

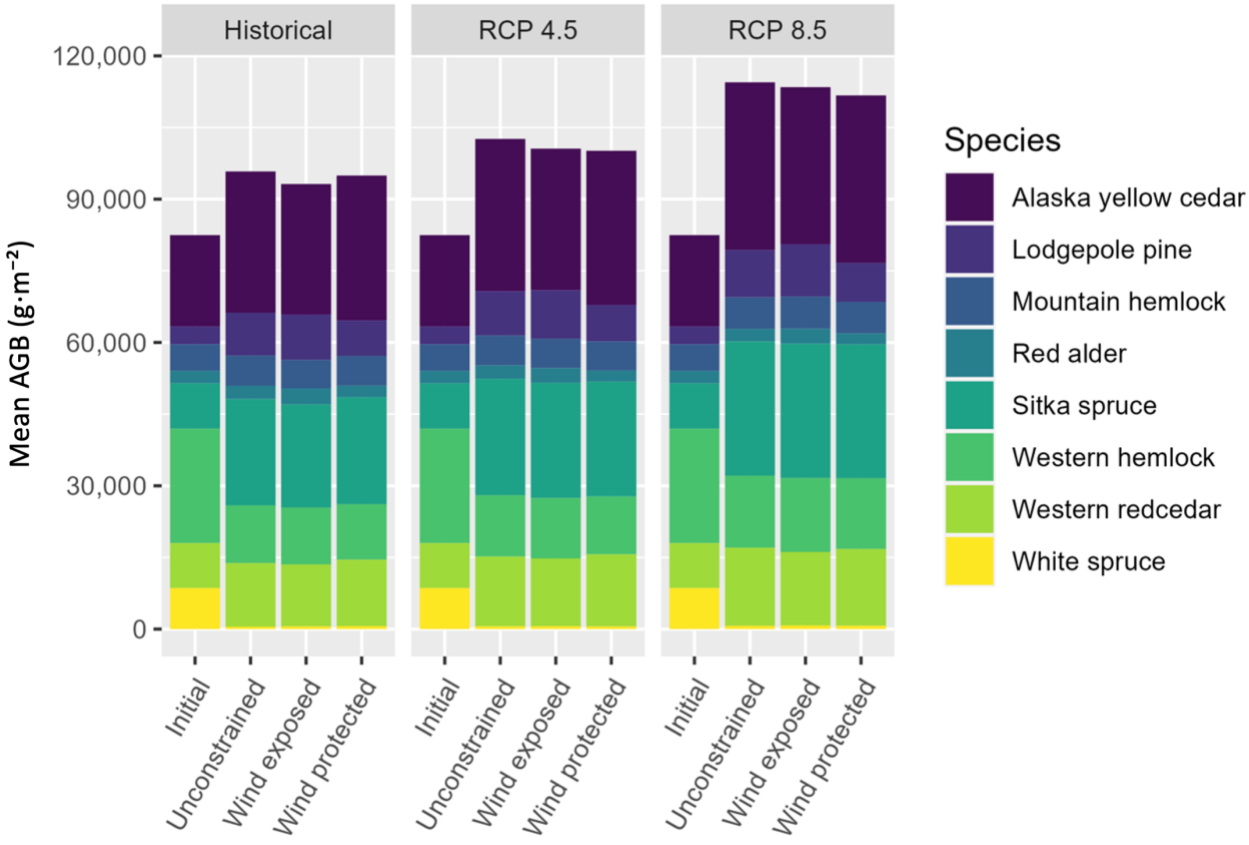


Figure 26. Mean biomass per species, within the young-growth management area of Zarembo Island, under simulated management and climate scenarios. The first bar in each climate scenario represents the initial starting conditions, followed by the end scenario species biomass of each harvest scenario.

At the end of the century, stand age distribution was similar across climate and management scenarios. Patterns of age distributions showed consistent end-of-scenario results, with the 50 to 220-year cohorts shifting into older stand ages later in the scenario. Most of the forest, both initially and at the end-of-century, were comprised of young cohorts (30 – 100 years old), showing successful regeneration of young trees into the future. However, in the warmest climate scenario (RCP 8.5), there was a decrease in the youngest cohorts (1-20 years old), which may be representative of lower levels of establishment late into the next century under extreme climate warming.

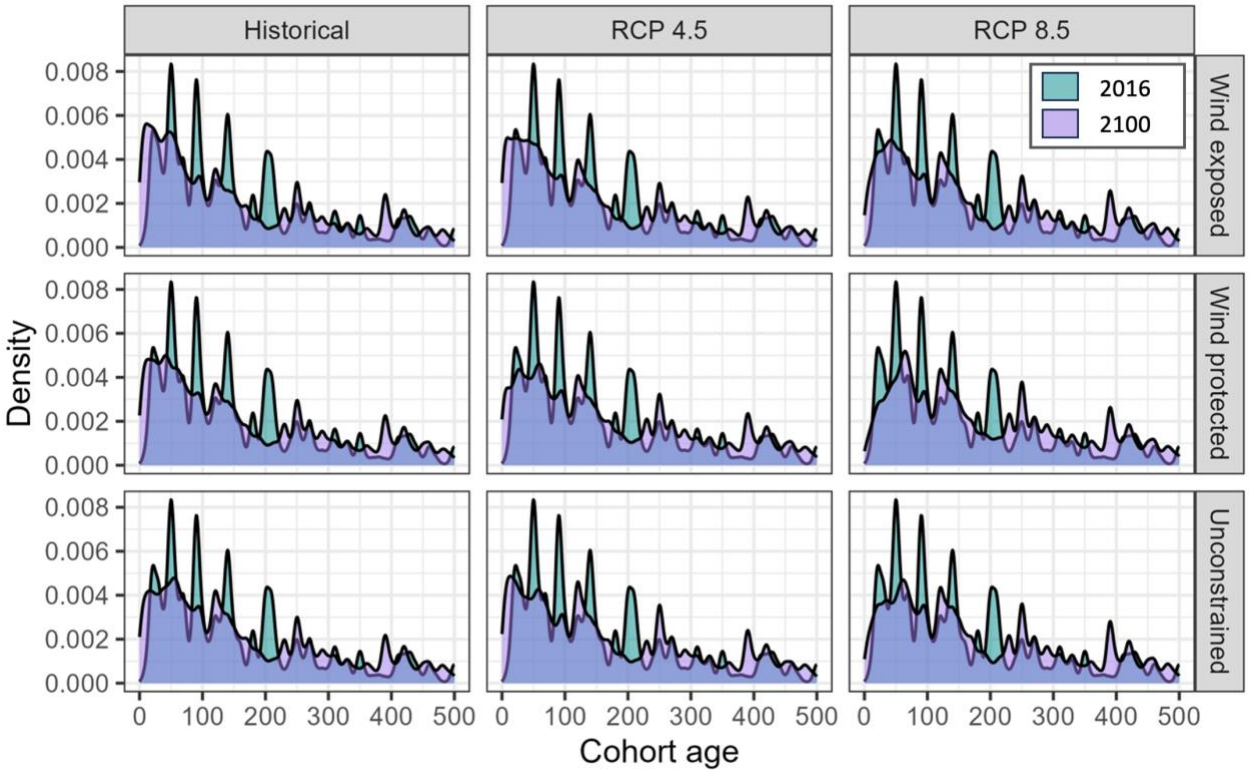


Figure 27. Density plot showing age distribution within the young-growth management area of Zarembo Island under simulated management and climate scenarios.

Management had little influence on annual net primary productivity (ANPP) within managed forests; climate was the main driver of ANPP (Figure 28). Under historical climate,

average ANPP was1,600 g/m^2/yr while warmer scenarios had higher mean ANPP (1,730 and 1,870 g/m^2/yr respectively).

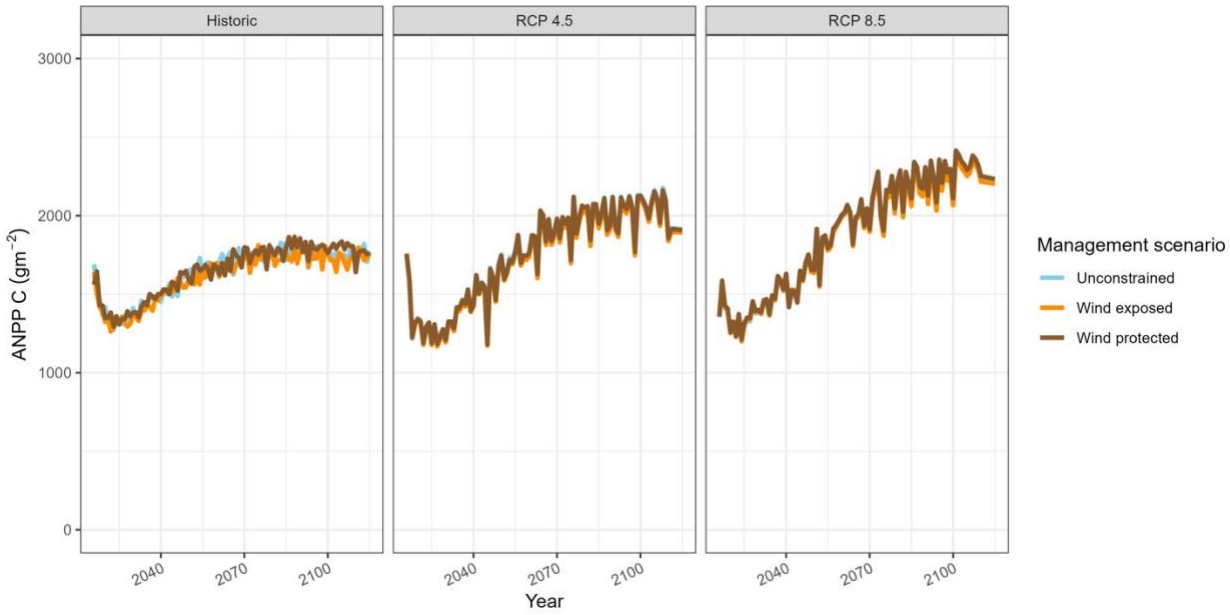


Figure 28. Annual net primary productivity (ANPP) of the three different management scenarios by climate scenario.

Discussion

Patterns of natural disturbance

Gap-phase disturbance processes are critical in regulating forest biomass and age dynamics in the coastal temperate rainforests of North America (Alaback et al., 2013a; Lertzman et al., 1996). In our study, patterns of windthrow disturbance matched those found on Zarembo Island in Kramer et al. 2001 (Figure 29), with most damage from windstorms constrained to high ridgelines with a southeast aspect. Regional studies state that mean canopy gaps size is ca. 50 m^2, making the scale of gap-phase disturbance smaller than that of an individual cell in this model

(Ott, 1997). However, based on the amount of biomass removed at a site level (90 m^2), the new extension is accurately representing gap-phase disturbance dynamics across the landscape.

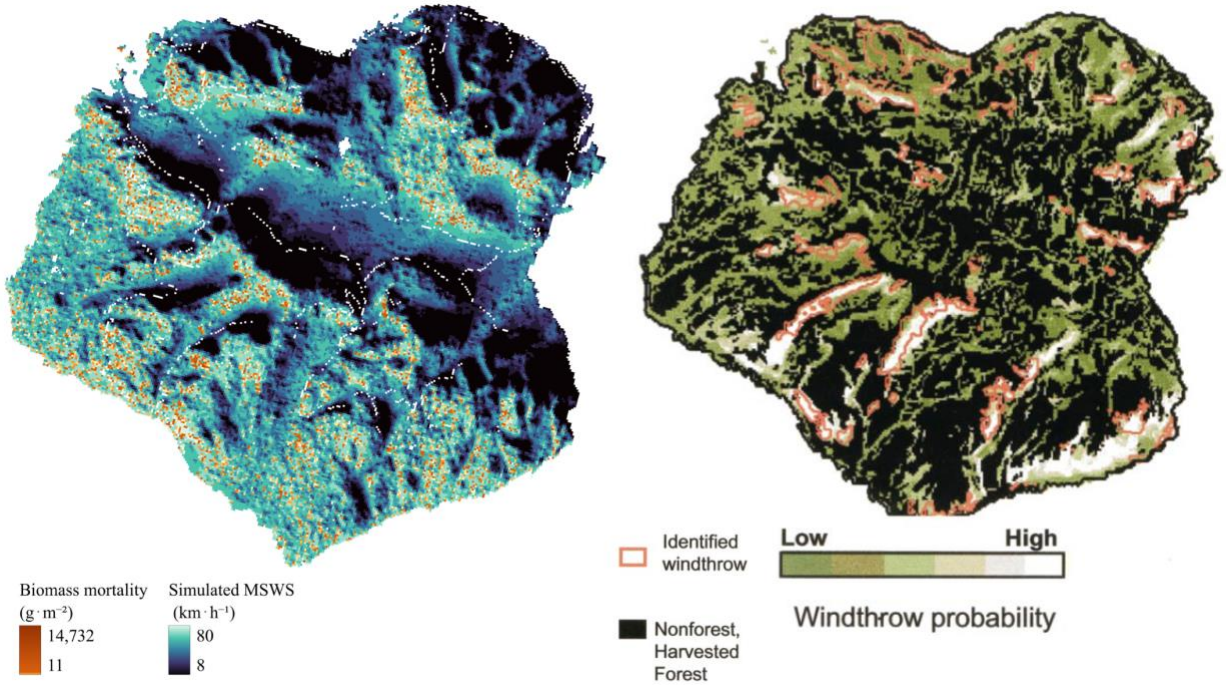


Figure 29. Modelled wind disturbance from a moderate storm using the Biomass Hurricane extension in LANDIS-II (left). Modelled windthrow probabilities and areas of identified windthrow from aerial observations (Kramer et al., 2001)

Harvest interactions with natural disturbance

Altering the spatial arrangement of management on the landscape based on patterns of natural disturbance was shown to have little effect on end-of-century biomass accumulation. One explanation for this outcome could be the way harvests were implemented in this study, with all scenarios calibrated to similar levels of biomass removal each year. This would likely also be the case in terms of actual implementation of harvests on the landscape, given that harvest targets are

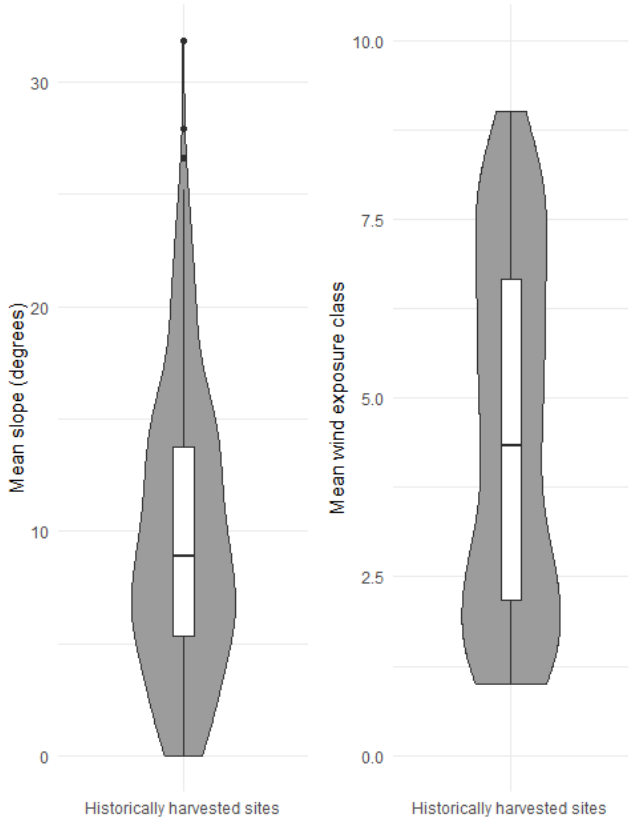


Figure 30. Mean slope and wind exposure class of historical harvest boundaries on Zarembo Island.

on a volume basis and would stay consistent regardless of how management was spatially implemented. However, there was a slight difference in the total number of harvests occurring each year between management scenarios, with managing in wind exposed environments showing greater numbers of harvests (Figure 23).

Another reason why end-of-century biomass outcomes were similar between management scenarios may be our assumption that historic harvests are located mainly in places easily accessible and sheltered by large wind events. Although this may be the case in other areas of southeast Alaska (Alaback et al., 2013b; Kramer et al., 2001), an analysis of where historical harvest areas reside in terms of wind exposure class shows no strong trend toward historical harvests being located in wind-protected locations on Zarembo Island (Figure 30). This finding is also supported by an analysis of harvests in both the Tongass National Forest and coastal British Columbia by Carter and Buma (2024).

Although this study shows that altering the spatial pattern of harvests shows minimal effect on landscape-level carbon, there may be other reasons besides carbon to harvest in areas that are naturally disturbed. Black bears prefer to select dens in wind-protected landscapes DeGayner et al 2005). Most bear dens (58%) were located in forests most protected from

catastrophic storm effects, while only a small percentage (6%) were found in storm-prone areas. Wind protected forests may provide a more suitable overwinter habitat for black bears, suggesting that harvest would be less detrimental to bears if constrained to wind exposed areas.

The cultural use of forest resources by native Alaskan communities should also be considered when designing the amount and spatial configuration of management. Large-diameter trees, particularly redcedar and yellow cedar, are essential for creating traditional items such as totem poles, canoes, longhouses, and ceremonial objects (ref or maybe add the Johnson ref here). These items hold deep cultural, spiritual, and historical significance for Indigenous communities in Southeast Alaska (Johnson et al., 2021). The introduction of commercial logging and other resource extraction activities significantly disrupted traditional practices. The large-scale removal of old-growth trees not only impacted the availability of culturally significant wood but also altered the forest structure and ecosystem dynamics (Crone and Mehrkens, 2013). Altering harvest practices to prioritize the retention of forested ecosystems that can retain large-diameter trees while fostering collaborative management with local communities may better facilitate access to necessary resources for cultural practices.

The future of aboveground biomass and climate change

Ecosystems in this region are likely to experience shifts in forest composition, with lowland and subalpine forests expanding in altitude and latitude while alpine habitats shrink as the climate changes. Projected increases in mean annual temperature (MAT) are expected to drive shifts in species distributions and ecological communities. Species with wide genetic diversity, such as western hemlock and Sitka spruce, are likely to colonize new habitats rapidly. In contrast, species like cedars may experience slower changes due to regeneration requirements and low genetic diversity (Shanley et al., 2015). The results from this follow the predicted trends

from other studies, with shifts in mean aboveground biomass favoring species such as Sitka spruce, western redcedar, and Alaska yellow cedar. However, outcomes in this model also show a decline in western hemlock across all scenarios. This may be due to western redcedar and Sitka spruce outcompeting western hemlock near coastal areas. On Zarembo Island, these species occupy similar ecotones and this decline of western hemlock may not be observed in areas outside of the ranges of western redcedar and Sitka spruce.

Our results show that climate change is the predominant driver of increases in stored biomass at the end of the century (Figure 26), with increasingly warm scenarios resulting in higher average biomass values. With climate change, the coastal temperate rainforest is expected to experience a combination of warmer temperatures with higher levels of precipitation, leading to longer growing seasons (Littell et al., 2018; Mote and Salathé, 2010; Shanley et al., 2015). This can also be seen in the substantial increases in ANPP with increasing amounts of climate warming. The future biomass trajectories presented here are supported by similar studies , where climate projections indicate that southeast Alaska is expected to remain a stable carbon sink or even increase in the future due to climate change (Law et al., 2023; McGuire et al., 2018; Zhu and Woodcock, 2014). A potential caveat to this can be seen in the modeled outputs of mean stand age distributions (Figure 27), with a decline in the youngest cohorts at the end of the century under extreme climate change. This decrease could be a symptom of an increase in competition from older cohorts leading to overall less establishment of younger cohorts late in the scenario. It also could be from climatic conditions reaching a point where establishment becomes difficult.

Limitations

First, this study was done on a relatively small subset of a much larger landscape. Although patterns of natural disturbance and succession are similar across the Tongass National Forest, our analysis was restricted to Zarembo Island. A future modeling endeavor would benefit from simulating the entire region. Secondly, the wind extension of LANDIS-II did not simulate more complicated wind dynamics, such as unusual storm wind directions, eddies, wind channeling through valleys, and other complex wind-topography interactions, such as downslope winds, which cause extensive windthrow. However, a majority of observed windthrow on Zarembo Island occurred on exposed windward hillslopes (Kramer et al., 2001; Figure 29), which was simulated by LANDIS-II. Although Alaska yellow cedar was projected to increase with climate change in our simulations, this is not likely realistic given empirical studies that show warmer winters and reduced snow cover leads to declines in this species. Without adequate snow insulation, the tree roots are exposed to freezing temperatures, causing root damage and increasing vulnerability to drought and disease (Beier et al., 2008; D'Amore and Hennon, 2006; Hennon et al., 2006). The inability of NECN to adequately represent the effect of snow dynamics, particularly at a monthly scale, may be responsible.

CONCLUSION

The temperate rainforests of the Pacific coast of North America, covering nearly 29.9 million hectares from Southeast Alaska to Coastal British Columbia, represent almost half of all temperate rainforests on Earth. These forests are globally significant for their high carbon storage capacities and local ecological, cultural, and economic values. Despite their importance, there is a lack of consistent spatial data and predictive models to inform management decisions and recent shifts in land management policies and climate change introduce uncertainties about future forest conditions. The research presented here addresses these gaps by utilizing Gradient Nearest Neighbor (GNN) modeling to map forest structure and composition, examining the distribution of old-growth and mature forests, and modeling future carbon vulnerabilities under different disturbance and climate scenarios.

Predicted patterns of forest structure from the GNN analysis matched fairly well with expected patterns from previous studies (Alaback, 1996; Alaback and Juday, 1989; Harris and Farr, 1974; MacKinnon, 2003). Elevation, mean annual temperature, and annual precipitation, as well as latitudinal and longitudinal gradients, were shown to be the strongest drivers of forest structure and composition in this region. Aboveground biomass was shown to have the highest values at lower elevations; however, this trend becomes less apparent at the lowest elevations nearest to the coast. Also, the results for individual species biomass showed relatively good agreement when compared to observed plot data. However, there was a tendency toward commission errors, with species being predicted in areas where their presence was not observed, a pattern observed in other studies using GNN to predict structural attributes in the Pacific Northwest (Irvine, 2022; Ohmann and Gregory, 2002)

Based on the reclassification of GNN analysis, a total of 1,176,903 hectares were classified as old growth forests while 2,291,309 hectares were classified as mature forests. In British Columbia, OGMAs contain the largest amounts of old growth despite their dispersed nature and relatively small spatial coverage, with over 20 percent of the forests being within OGMAs classified as either old growth or mature. The largest stores of older forests reside within IRAs in southeast Alaska, with a total of 832,500 hectares. Both IRAs and OGMAs are vulnerable to policy reversals and exemptions that can open them to logging and development (DellaSala et al., 2022; Dietz et al., 2021; Joeveen Dhari, 2023; Price et al., 2021). This is especially concerning as these areas are also home to some of the region's highest stores of biomass.

We also explored how the spatial pattern of young-growth management and windstorms would affect biomass and species composition on Zamembo Island in the Tongass National Forest in Alaska. A new LANDIS-II extension was developed to model windthrow from the large wind disturbance events experienced in this region which modifies the exposure of a site to an individual storm based on topography and storm direction while creating spatial maps of disturbance. Stands that experience different levels of wind exposure to simulated storms showed different trajectories in the future accumulation of aboveground biomass, with wind-protected stands steadily increasing over time and areas of high exposure showing slower accumulation rates by the end of the century. Our results found that altering the spatial arrangement of management on the landscape based on patterns of natural disturbance was shown to have little effect on end-of-century biomass accumulation. Instead, we found that climate change was the predominant driver of biomass accumulation rates by the end of the century, with increasingly warm scenarios resulting in higher average biomass values.

REFERENCES

Ahmadalipour, A., Moradkhani, H., Rana, A., 2018. Accounting for downscaling and model uncertainty in fine-resolution seasonal climate projections over the Columbia River Basin. Clim Dyn 50, 717–733. https://doi.org/10.1007/s00382-017-3639-4

Al Gorley, Garry Merkel, 2020. A New Future for Old Forests: A Strategic Review of How British Columbia Manages for Old Forests Within its Ancient Ecosystems. Old Growth Review Panel.

Alaback, P., Nowacki, G., Saunders, S., 2013a. Natural disturbance patterns in the temperate rainforests of southeast Alaska and adjacent British Columbia. North Pacific temperate rainforests: ecology and conservation 73–88.

Alaback, P., Nowacki, G., Saunders, S., 2013b. Natural disturbance patterns in the temperate rainforests of southeast Alaska and adjacent British Columbia. North Pacific temperate rainforests: ecology and conservation 73–88.

Alaback, P.B., 1996. Biodiversity Patterns in Relation to Climate: The Coastal Temperate Rainforests of North America, in: Lawford, R.G., Fuentes, E., Alaback, P.B. (Eds.), High-Latitude Rainforests and Associated Ecosystems of the West Coast of the Americas, Ecological Studies. Springer New York, New York, NY, pp. 105–133. https://doi.org/10.1007/978-1-4612-3970-3_7

Alaback, P.B., 1982. Dynamics of Understory Biomass in Sitka Spruce-Western Hemlock Forests of Southeast Alaska. Ecology 63, 1932. https://doi.org/10.2307/1940131

Alaback, P.B., Juday, G.P., 1989. Structure and composition of low elevation old-growth forests in research natural areas of Southeast Alaska. Natural areas journal 9, 27–39.

Avery, T.E., Burkhart, H.E., 1983. Forest measurements. McGraw-Hill Book Company.

Azuma, D., Monleon, V.J., 2011. Differences in forest area classification based on tree tally from variable- and fixed-radius plots. Can. J. For. Res. 41, 211–214. https://doi.org/10.1139/x10-200

Beamish, A., Raynolds, M.K., Epstein, H., Frost, G.V., Macander, M.J., Bergstedt, H., Bartsch, A., Kruse, S., Miles, V., Tanis, C.M., 2020. Recent trends and remaining challenges for optical remote sensing of Arctic tundra vegetation: A review and outlook. Remote Sensing of Environment 246, 111872.

Beier, C.M., Sink, S.E., Hennon, P.E., D'Amore, D.V., Juday, G.P., 2008. Twentieth-century warming and the dendroclimatology of declining yellow-cedar forests in southeastern Alaska. Can. J. For. Res. 38, 1319–1334. https://doi.org/10.1139/X07-240

Bell, D.M., Schlaepfer, D.R., 2016. On the dangers of model complexity without ecological justification in species distribution modeling. Ecological Modelling 330, 50–59.

Bell, D.M., Wilson, B.T., Werstak, C.E., Oswalt, C.M., Perry, C.H., 2022. Examining k-Nearest Neighbor Small Area Estimation Across Scales Using National Forest Inventory Data. Frontiers in Forests and Global Change 5, 25. https://doi.org/10.3389/FFGC.2022.763422/BIBTEX

Black, A., 1997. CA-Ca1: British Columbia - 1949 Douglas-fir stand. https://doi.org/0.17190/AMF/1480300

Blackard, J.A., Finco, M.V., Helmer, E.H., Holden, G.R., Hoppus, M.L., Jacobs, D.M., Lister, A.J., Moisen, G.G., Nelson, M.D., Riemann, R., 2008. Mapping US forest biomass using nationwide forest inventory data and moderate resolution information. Remote sensing of Environment 112, 1658–1677.

Bouget, C., Duelli, P., 2004. The effects of windthrow on forest insect communities: a literature review. Biological Conservation 118, 281–299. https://doi.org/10.1016/j.biocon.2003.09.009

Braaten, J.D., Cohen, W.B., Yang, Z., 2015. Automated cloud and cloud shadow identification in Landsat MSS imagery for temperate ecosystems. Remote Sensing of Environment 169, 128–138. https://doi.org/10.1016/j.rse.2015.08.006

Brackley, A.M., Haynes, R.W., Alexander, S.J., 2009. Timber harvests in Alaska: 1910-2006 (No. PNW-RN-560). U.S. Department of Agriculture, Forest Service, Pacific Northwest Research Station, Portland, OR. https://doi.org/10.2737/PNW-RN-560

Bullock, T.A., Gyakum, J.R., 1993. A Diagnostic Study of Cyclogenesis in the Western North Pacific Ocean. Monthly Weather Review 121, 65–75. https://doi.org/10.1175/1520-0493(1993)121<0065:ADSOCI>2.0.CO;2

Buma, B., Krapek, J., Edwards, R.T., 2016a. Watershed-scale forest biomass distribution in a perhumid temperate rainforest as driven by topographic, soil, and disturbance variables. Can. J. For. Res. 46, 844–854. https://doi.org/10.1139/cjfr-2016-0041

Buma, B., Krapek, J., Edwards, R.T., 2016b. Watershed-scale forest biomass distribution in a perhumid temperate rainforest as driven by topographic, soil, and disturbance variables. Canadian Journal of Forest Research 46, 844–854. https://doi.org/10.1139/CJFR-2016-0041/SUPPL_FILE/CJFR-2016-0041SUPPL.PDF

Bunnell, F., Kremsater, L.L., 2012. Migrating like a herd of cats – climate change and emerging forests in British Columbia. Journal of Ecosystems and Management 13. https://doi.org/10.22230/jem.2012v13n2a131

Canada, G. of, 2021. Canadian protected and conserved areas database.

Caouette, J.P., Steel, E.A., Hennon, P.E., Cunningham, P.G., Pohl, C.A., Schrader, B.A., 2016. Influence of elevation and site productivity on conifer distributions across Alaskan temperate rainforests. Can. J. For. Res. 46, 249–261. https://doi.org/10.1139/cjfr-2015-0283

Carey, A.B., Johnson, M.L., 1995. Small Mammals in Managed, Naturally Young, and Old-Growth Forests. Ecological Applications 5, 336–352. https://doi.org/10.2307/1942026

Carter, T.A., Buma, B., 2024. The Distribution of Tree Biomass Carbon within the Pacific Coastal Temperate Rainforest, a Disproportionally Carbon Dense Forest. Can. J. For. Res. cjfr-2024-0015. https://doi.org/10.1139/cjfr-2024-0015

Chan, S.K., Bindlish, R., O'Neill, P.E., Njoku, E., Jackson, T., Colliander, A., Chen, F., Burgin, M., Dunbar, S., Piepmeier, J., Yueh, S., Entekhabi, D., Cosh, M.H., Caldwell, T., Walker, J., Wu, X., Berg, A., Rowlandson, T., Pacheco, A., McNairn, H., Thibeault, M., Martínez-Fernández, J., González-Zamora, Á., Seyfried, M., Bosch, D., Starks, P., Goodrich, D., Prueger, J., Palecki, M., Small, E.E., Zreda, M., Calvet, J.-C., Crow, W.T., Kerr, Y., 2016. Assessment of the SMAP Passive Soil Moisture Product. IEEE Transactions on Geoscience and Remote Sensing 54, 4994–5007. https://doi.org/10.1109/TGRS.2016.2561938

Clifford Mass, Brigid Dotson, 2010. Major Extratropical Cyclones of the Northwest United States: Historical Review, Climatology, and Synoptic Environment. American Meteorological Society 138, 2499–2527. https://doi.org/10.1175/2010MWR3213.1

Cohen, W.B., Spies, T.A., 1992. Estimating structural attributes of Douglas-fir/western hemlock forest stands from Landsat and SPOT imagery. Remote sensing of environment 41, 1–17.

Crone, L.K., Mehrkens, J.R., 2013. Indigenous and commercial uses of the natural resources of the north pacific rainforest with a focus on southeast Alaska and Haida Gwaii, in: North Pacific Temperate Rainforests: Ecology and Conservation. University of Washington Press Seattle, pp. 89–126.

Crotteau, J.S., D'amore, D.V., Barnard, J.C., Lawton, G., Mcfarland, J., 2022. Commercial thinning strategies in southeast Alaska: establishment and effects of the Prince of Wales Commercial Thinning Study, Gen. Tech. Rep. PNW-GTR-1012. Portland, OR: U.S. Department of Agriculture, Forest Service, Pacific Northwest Research Station. 77 p. (Online only). https://doi.org/10.2737/PNW-GTR-1012

D'Amore, D.V., Fellman, J.B., Edwards, R.T., Hood, E., 2010. Controls on dissolved organic matter concentrations in soils and streams from a forested wetland and sloping bog in southeast Alaska. Ecohydrology 3, 249–261. https://doi.org/10.1002/eco.101

D'Amore, D.V., Hennon, P.E., 2006. Evaluation of soil saturation, soil chemistry, and early spring soil and air temperatures as risk factors in yellow-cedar decline. Global Change Biology 12, 524–545. https://doi.org/10.1111/j.1365-2486.2006.01101.x

Davis, R.J., Bell, D.M., Gregory, M.J., Yang, Z., Gray, A.N., Healey, S.P., Stratton, A.E., 2022. Northwest Forest Plan—the first 25 years (1994–2018): status and trends of late-successional and old-growth forests, Gen. Tech. Rep. PNW-GTR-1004. Portland, OR: U.S. Department of Agriculture, Forest Service, Pacific Northwest Research Station. 82 p. https://doi.org/10.2737/PNW-GTR-1004

DeGayner, E.J., Kramer, M.G., Doerr, J.G., Robertsen, M.J., 2005. Windstorm Disturbance Effects on Forest Structure and Black Bear Dens in Southeast Alaska. Ecological Applications 15, 1306–1316. https://doi.org/10.1890/03-5385

DellaSala, D.A., Gorelik, S.R., Walker, W.S., 2022. The Tongass National Forest, Southeast Alaska, USA: A Natural Climate Solution of Global Significance. Land 11, 717. https://doi.org/10.3390/land11050717

DellaSala, D.A., Moola, F., Alaback, P., Paquet, P.C., Schoen, J.W., Noss, R.F., 2011. Temperate and Boreal Rainforests of the Pacific Coast of North America, in: DellaSala, D.A. (Ed.), Temperate and Boreal Rainforests of the World: Ecology and Conservation. Island Press/Center for Resource Economics, Washington, DC, pp. 42–81. https://doi.org/10.5822/978-1-61091-008-8_2

DeVelice, R.L., Martin, J.R., 2001. Assessing the Extent to Which Roadless Areas Complement the Conservation of Biological Diversity. Ecological Applications 11, 1008–1018. https://doi.org/10.1890/1051-0761(2001)011[1008:ATETWR]2.0.CO;2

Dietz, M.S., Barnett, K., Belote, R.T., Aplet, G.H., 2021. The importance of US national forest roadless areas for vulnerable wildlife species. Global Ecology and Conservation 32, e01943.

Elith, J., Leathwick, J.R., 2009. Species Distribution Models: Ecological Explanation and Prediction Across Space and Time. Annu. Rev. Ecol. Evol. Syst. 40, 677–697. https://doi.org/10.1146/annurev.ecolsys.110308.120159

Falkowski, M.J., Hudak, A.T., Crookston, N.L., Gessler, P.E., Uebler, E.H., Smith, A.M.S., 2010. Landscape-scale parameterization of a tree-level forest growth model: A k-nearest neighbor imputation approach incorporating LiDAR data. Canadian Journal of Forest Research 40, 184–199. https://doi.org/10.1139/X09-183

Feller, M.C., 2003. Coarse woody debris in the old-growth forests of British Columbia. Environ. Rev. 11, S135–S157. https://doi.org/10.1139/a03-008

Foley, A.M., 2010. Uncertainty in regional climate modelling: A review. Progress in Physical Geography: Earth and Environment 34, 647–670. https://doi.org/10.1177/0309133310375654

Gavin, D.G., Hu, F.S., Lertzman, K., Corbett, P., 2006. Weak Climatic Control of Stand-Scale Fire History During the Late Holocene. Ecology 87, 1722–1732. https://doi.org/10.1890/0012-9658(2006)87[1722:WCCOSF]2.0.CO;2

Gergely, K.J., McKerrow, A., 2013. PAD-US—National inventory of protected areas. US Geological Survey.

Giles, P.T., 2001. Remote sensing and cast shadows in mountainous terrain. Photogrammetric engineering and remote sensing 67, 833–840.

Gilliam, F.S., 2007. The ecological significance of the herbaceous layer in temperate forest ecosystems. BioScience 57, 845–858.

Gorelick, N., Hancher, M., Dixon, M., Ilyushchenko, S., Thau, D., Moore, R., 2017. Google Earth Engine: Planetary-scale geospatial analysis for everyone. Remote Sensing of Environment. https://doi.org/10.1016/j.rse.2017.06.031

Gray, A., 2003. Monitoring stand structure in mature coastal Douglas-®r forests: effect of plot size. Forest Ecology and Management.

Gray, A.N., Brandeis, T.J., Shaw, J.D., McWilliams, W.H., Miles, P.D., 2012. Forest inventory and analysis database of the United States of America (FIA). Biodiversity, Evolution and Ecology of Plants.

Gray, A.N., Pelz, K., Hayward, G.D., Schuler, T., Salverson, W., Palmer, M., Schumacher, C., Woodall, C.W., 2023. Perspectives: The wicked problem of defining and inventorying mature and old-growth forests. Forest Ecology and Management 546, 121350.

Griesbauer, H.P., Scott Green, D., 2010. Assessing the climatic sensitivity of Douglas-fir at its northern range margins in British Columbia, Canada. Trees 24, 375–389. https://doi.org/10.1007/s00468-009-0407-z

Gustafson, E.J., Shifley, S.R., Mladenoff, D.J., Nimerfro, K.K., He, H.S., 2000. Spatial simulation of forest succession and timber harvesting using LANDIS. Can. J. For. Res. 30, 32–43. https://doi.org/10.1139/x99-188

Hamann, A., Wang, T., 2006. Potential Effects of Climate Change on Ecosystem and Tree Species Distribution in British Columbia. Ecology 87, 2773–2786. https://doi.org/10.1890/0012-9658(2006)87[2773:PEOCCO]2.0.CO;2

Harris, A., Farr, W., 1974. The forest ecosystem of southeast Alaska (No. PNW-25). USDA Forest Service, Pacific Northwest Research Station.

Hengl, T., De Jesus, J.M., Heuvelink, G.B.M., Gonzalez, M.R., Kilibarda, M., Blagotić, A., Shangguan, W., Wright, M.N., Geng, X., Bauer-Marschallinger, B., Guevara, M.A., Vargas, R., MacMillan, R.A., Batjes, N.H., Leenaars, J.G.B., Ribeiro, E., Wheeler, I.,

Mantel, S., Kempen, B., 2017. SoilGrids250m: Global gridded soil information based on machine learning. PLOS ONE 12, e0169748. https://doi.org/10.1371/JOURNAL.PONE.0169748

Hennon, P., D'Amore, D., Wittwer, D., Johnson, A., Schaberg, P., Hawley, G., Beier, C., Sink, S., Juday, G., 2006. Climate warming, reduced snow, and freezing injury could explain the demise of yellow-cedar in southeast Alaska, USA. World Resource Review. 18(2): 427-450. 18, 427–450.

Hennon, P.E., D'Amore, D.V., Schaberg, P.G., Wittwer, D.T., Shanley, C.S., 2012. Shifting Climate, Altered Niche, and a Dynamic Conservation Strategy for Yellow-Cedar in the North Pacific Coastal Rainforest. BioScience 62, 147–158. https://doi.org/10.1525/BIO.2012.62.2.8

Hijmans, R.J., 2023. terra: Spatial Data Analysis.

Hurni, K., Heinimann, A., Würsch, L., 2017. Google earth engine image pre-processing tool: background and methods.

Irvine, D., 2022. Wall-to-Wall Forest Mapping in Southeast and Southcentral Alaska: A New Application of the Gradient Nearest Neighbor Approach. Oregon State University.

Jenkins, J.C., Chojnacky, D.C., Heath, L.S., Birdsey, R.A., 2003. National-scale biomass estimators for United States tree species. Forest Science 49, 12–35. https://doi.org/10.1093/forestscience/49.1.12

Joeveen Dhari, 2023. Old growth protections in British Columbia: A comparative analysis. Simon Fraser University.

Johnson, A., Clavijo, A.E., Hamar, G., Head, D.-A., Thoms, A., Price, W., Lapke, A., Crotteau, J., Cerveny, L.K., Wilmer, H., Petershoare, L., Cook, A., Reid, S., 2021. Wood Products for Cultural Uses: Sustaining Native Resilience and Vital Lifeways in Southeast Alaska, USA. Forests 12, 90. https://doi.org/10.3390/f12010090

Kane, V.R., Gillespie, A.R., McGaughey, R., Lutz, J.A., Ceder, K., Franklin, J.F., 2008. Interpretation and topographic compensation of conifer canopy self-shadowing. Remote sensing of Environment 112, 3820–3832.

Karger, D.N., Conrad, O., Böhner, J., Kawohl, T., Kreft, H., Soria-Auza, R.W., Zimmermann, N.E., Linder, H.P., Kessler, M., 2017. Climatologies at high resolution for the earth's land surface areas. Sci Data 4, 170122. https://doi.org/10.1038/sdata.2017.122

Karger, D.N., Zimmermann, N.E., 2018. CHELSAcruts—high resolution temperature and precipitation timeseries for the 20th century and beyond. EnviDat.

Kennedy, R.E., Andréfouët, S., Cohen, W.B., Gómez, C., Griffiths, P., Hais, M., Healey, S.P., Helmer, E.H., Hostert, P., Lyons, M.B., Meigs, G.W., Pflugmacher, D., Phinn, S.R., Powell, S.L., Scarth, P., Sen, S., Schroeder, T.A., Schneider, A., Sonnenschein, R., Vogelmann, J.E., Wulder, M.A., Zhu, Z., 2014. Bringing an ecological view of change to landsat-based remote sensing. Frontiers in Ecology and the Environment 12, 339–346. https://doi.org/10.1890/130066

Kennedy, R.E., Yang, Z., Gorelick, N., Braaten, J., Cavalcante, L., Cohen, W.B., Healey, S., 2018. Implementation of the LandTrendr Algorithm on Google Earth Engine. Remote Sensing 2018, Vol. 10, Page 691 10, 691. https://doi.org/10.3390/RS10050691

Kozak, A., Munro, D.D., Smith, J.H.G., 1969. Taper Functions and their Application in Forest Inventory. The Forestry Chronicle 45, 278–283. https://doi.org/10.5558/TFC45278-4

Kramer, M., Andrew J. Hansen, Mark L. Taper, Everett J. Kissinger, 2001. Abiotic Controls on Long-Term Windthrow Disturbance and Temperate Rain Forest Dynamics in Southeast Alaska. Ecology 82, 2749–2768. https://doi.org/10.1890/0012-9658(2001)082[2749:ACOLTW]2.0.CO;2

Kramer, M.G., Hansen, A.J., Taper, M.L., Kissinger, E.J., 2001. Abiotic controls on long-term windthrow disturbance and temperate rain forest dynamics in southeast Alaska. Ecology 82, 2749–2768.

Kramer, M.G., Sollins, P., Sletten, R.S., 2004. Soil Carbon Dynamics Across a Windthrow Disturbance Sequence in Southeast Alaska. Ecology 85, 2230–2244. https://doi.org/10.1890/02-4098

Krumlik, J.G., 1974. Biomass and nutrient distribution in two old growth forest ecosystems in south coastal British Columbia. University of British Columbia. https://doi.org/10.14288/1.0075432

Law, B.E., Berner, L.T., Wolf, C., Ripple, W.J., Trammell, E.J., Birdsey, R.A., 2023. Southern Alaska's Forest Landscape Integrity, Habitat, and Carbon Are Critical for Meeting Climate and Conservation Goals. AGU Advances 4, e2023AV000965. https://doi.org/10.1029/2023AV000965

Lertzman, K.P., Sutherland, G.D., Inselberg, A., Saunders, S.C., 1996. Canopy Gaps and the Landscape Mosaic in a Coastal Temperate Rain Forest. Ecology 77, 1254–1270. https://doi.org/10.2307/2265594

Lindenmayer, D.B., Franklin, J.F., 2013. Conserving forest biodiversity: a comprehensive multiscaled approach. Island press.

Littell, J.S., McAfee, S.A., Hayward, G.D., 2018. Alaska Snowpack Response to Climate Change: Statewide Snowfall Equivalent and Snowpack Water Scenarios. Water 10, 668. https://doi.org/10.3390/w10050668

Lorenz, T.J., Raphael, M.G., Young, R.D., Lynch, D., Nelson, S.K., McIver, W.R., 2021. Status and trend of nesting habitat for the Marbled Murrelet under the Northwest Forest Plan, 1993 to 2017. US Department of Agriculture, Forest Service, Pacific Northwest Research Station.

Loudermilk, E.L., Scheller, R.M., Weisberg, P.J., Kretchun, A., 2017. Bending the carbon curve: fire management for carbon resilience under climate change. Landscape Ecology 32, 1461–1472. https://doi.org/10.1007/S10980-016-0447-X/TABLES/2

Lucash, M.S., Marshall, A.M., Weiss, S.A., McNabb, J.W., Nicolsky, D.J., Flerchinger, G.N., Link, T.E., Vogel, J.G., Scheller, R.M., Abramoff, R.Z., 2023a. Burning trees in frozen soil: Simulating fire, vegetation, soil, and hydrology in the boreal forests of Alaska. Ecological Modelling 481, 110367.

Lucash, M.S., Williams, N.G., Srikrishnan, V., Keller, K., Scheller, R.M., Hegelson, C., Nicholas, R.E., Smithwick, E.A.H., 2023b. Balancing multiple forest management objectives under climate change in central Wisconsin, U.S.A. Trees, Forests and People 14, 100460. https://doi.org/10.1016/j.tfp.2023.100460

MacKinnon, A., 2003. West coast, temperate, old-growth forests. The Forestry Chronicle 79, 475–484. https://doi.org/10.5558/tfc79475-3

Maechler, M., original), P.R. (Fortran, original), A.S. (S, original), M.H. (S, Hornik [trl, K., maintenance(1999-2000)), ctb] (port to R., Studer, M., Roudier, P., Gonzalez, J., Kozlowski, K., pam()), E.S. (fastpam options for, Murphy (volume.ellipsoid({d >= 3})), K., 2023. cluster: “Finding Groups in Data”: Cluster Analysis Extended Rousseeuw et al.

Mature and Old-Growth Forests: Definition, Identification, and Initial Inventory on Lands Managed by the Forest Service and Bureau of Land Management (No. FS-1215a), 2023. . USDA Forest Service.

McGee, G., Cullen, A., Gunton, T., 2010. A new model for sustainable development: a case study of The Great Bear Rainforest regional plan. Environment, development and sustainability 12, 745–762.

McGuire, A.D., Genet, H., Lyu, Z., Pastick, N., Stackpoole, S., Birdsey, R., D’Amore, D., He, Y., Rupp, T.S., Striegl, R., Wylie, B.K., Zhou, X., Zhuang, Q., Zhu, Z., 2018. Assessing historical and projected carbon balance of Alaska: A synthesis of results and policy/management implications. Ecological Applications 28, 1396–1412. https://doi.org/10.1002/eap.1768

McNicol, G., Bulmer, C., D’Amore, D., Sanborn, P., Saunders, S., Giesbrecht, I., Arriola, S.G., Bidlack, A., Butman, D., Buma, B., 2019. Large, climate-sensitive soil carbon stocks mapped with pedology-informed machine learning in the North Pacific coastal temperate rainforest. Environmental Research Letters 14, 014004. https://doi.org/10.1088/1748-9326/AAED52

Meidinger, D., Pojar, J., 1991. Ecosystems of British Columbia. Special Report Series-Ministry of Forests, British Columbia.

Mesquita, M.S., Atkinson, D.E., Hodges, K.I., 2010. Characteristics and Variability of Storm Tracks in the North Pacific, Bering Sea, and Alaska. Journal of Climate 23, 294–311. https://doi.org/10.1175/2009JCLI3019.1

Mildrexler, D.J., Berner, L.T., Law, B.E., Birdsey, R.A., Moomaw, W.R., 2020. Large trees dominate carbon storage in forests east of the cascade crest in the United States Pacific Northwest. Frontiers in Forests and Global Change 3, 594274.

Mitchell, S.J., 2013. Wind as a natural disturbance agent in forests: a synthesis. Forestry: An International Journal of Forest Research 86, 147–157. https://doi.org/10.1093/FORESTRY/CPS058

Moeur, M., Stage, A.R., 1995. Most similar neighbor: an improved sampling inference procedure for natural resource planning. Forest science 41, 337–359.

Mote, P.W., Salathé, E.P., 2010. Future climate in the Pacific Northwest. Climatic Change 102, 29–50. https://doi.org/10.1007/s10584-010-9848-z

NOAA, 2023. Juneau Airport, AK Daily Summaries.

North, M.P., Keeton, W.S., 2008. Emulating Natural Disturbance Regimes: an Emerging Approach for Sustainable Forest Management, in: Lafortezza, R., Sanesi, G., Chen, J., Crow, T.R. (Eds.), Patterns and Processes in Forest Landscapes. Springer Netherlands, Dordrecht, pp. 341–372. https://doi.org/10.1007/978-1-4020-8504-8_19

Nowacki, G., Kramer, M., 1998. The Effects of Wind Disturbance on Temperate Rain Forest Structure and Dynamics of Southeast Alaska (General Technical Report No. PNW-GTR-42). USDA Forest Service, Pacific Northwest Research Station.

Nowacki, G.J., Spencer, P., Fleming, M., Brock, T., Jorgenson, T., 2003. Unified ecoregions of Alaska: 2001. US Geological Survey.

Oakes, L.E., Hennon, P.E., O'Hara, K.L., Dirzo, R., 2014. Long-term vegetation changes in a temperate forest impacted by climate change. Ecosphere 5, art135. https://doi.org/10.1890/ES14-00225.1

Ohmann, Janet L., Gregory, M.J., 2002. Predictive mapping of forest composition and structure with direct gradient analysis and nearest-neighbor imputation in coastal Oregon, U.S.A. Canadian Journal of Forest Research 32, 725–741. https://doi.org/10.1139/x02-011

Ohmann, Janet L, Gregory, M.J., 2002. Predictive mapping of forest composition and structure with direct gradient analysis and nearest-neighbor imputation in coastal Oregon, U.S.A. https://doi.org/10.1139/X02-011

Ohmann, J.L., Gregory, M.J., Henderson, E.B., Roberts, H.M., 2011. Mapping gradients of community composition with nearest-neighbour imputation: extending plot data for landscape analysis. J Vegetation Science 22, 660–676. https://doi.org/10.1111/j.1654-1103.2010.01244.x

Ohmann, J.L., Gregory, M.J., Roberts, H.M., 2014. Scale considerations for integrating forest inventory plot data and satellite image data for regional forest mapping. Remote sensing of environment 151, 3–15.

Ohmann, J.L., Gregory, M.J., Spies, T.A., 2007. Influence of Environment, Disturbance, and Ownership on Forest Vegetation of Coastal Oregon. Ecological Applications 17, 18–33. https://doi.org/10.1890/1051-0761(2007)017[0018:IOEDAO]2.0.CO;2

Ohmann, J.L., Spies, T.A., 1998. Regional Gradient Analysis and Spatial Patterns of Woody Plant Communities of Oreon Forests. Ecological Monographs 68, 151–182. https://doi.org/10.1890/0012-9615(1998)068[0151:RGAASP]2.0.CO;2

Old Growth Technical Advisory Panel, 2021. Priority Deferrals, An Ecological Approach. British Columbia Ministry of Forests.

Orians, G.H., Schoen, J.W. (Eds.), 2013. North Pacific temperate rainforests: ecology & conservation. Audubon Alaska and the Nature Conservancy of Alaska in association with University of Washington Press, Seattle.

Ott, R.A., 1997. Natural disturbance at the site and landscape levels in temperate rainforests of southeast Alaska. University of Alaska Fairbanks.

Pelz, K.A., Hayward, G., Gray, A.N., Berryman, E.M., Woodall, C.W., Nathanson, A., Morgan, N.A., 2023. Quantifying old-growth forest of United States Forest Service public lands. Forest Ecology and Management 549, 121437. https://doi.org/10.1016/j.foreco.2023.121437

Pierce, K.B., Ohmann, J.L., Wimberly, M.C., Gregory, M.J., Fried, J.S., 2009. Mapping wildland fuels and forest structure for land management: A comparison of nearest neighbor imputation and other methods. Canadian Journal of Forest Research 39, 1901–1916. https://doi.org/10.1139/X09-102

Price, K., Holt, R.F., Daust, D., 2021. Conflicting portrayals of remaining old growth: the British Columbia case. Can. J. For. Res. 51, 742–752. https://doi.org/10.1139/cjfr-2020-0453

Price, K., Roburn, A., MacKinnon, A., 2009. Ecosystem-based management in the Great Bear Rainforest. Forest Ecology and Management 258, 495–503.

R Core Team, 2023. R: A Language and Environment for Statistical Computing. R Foundation for Statistical Computing, Vienna, Austria.

Read, W.A., 2015. The climatology and meteorology of windstorms that affect southwest British Columbia, Canada, and associated tree-related damage to the power distribution grid. University of British Columbia. https://doi.org/10.14288/1.0166485

Riemann, R., Wilson, B.T., Lister, A., Parks, S., 2010. An effective assessment protocol for continuous geospatial datasets of forest characteristics using USFS Forest Inventory and Analysis (FIA) data. Remote Sensing of Environment 114, 2337–2352. https://doi.org/10.1016/j.rse.2010.05.010

Rogers, B.M., Neilson, R.P., Drapek, R., Lenihan, J.M., Wells, J.R., Bachelet, D., Law, B.E., 2011. Impacts of climate change on fire regimes and carbon stocks of the U.S. Pacific Northwest. J. Geophys. Res. 116, G03037. https://doi.org/10.1029/2011JG001695

Saxton, K.E., Rawls, W.J., Romberger, J.S., PAPENDiCK, R.I., 1986. Estimating Generalized Soil-water Characteristics from Texture. SOIL SCI. SOC. AM. J. 50.

Scheller, R.M., Domingo, J.B., Sturtevant, B.R., Williams, J.S., Rudy, A., Gustafson, E.J., Mladenoff, D.J., 2007. Design, development, and application of LANDIS-II, a spatial landscape simulation model with flexible temporal and spatial resolution. Ecological Modelling 201, 409–419. https://doi.org/10.1016/j.ecolmodel.2006.10.009

Scheller, R.M., Hua, D., Bolstad, P.V., Birdsey, R.A., Mladenoff, D.J., 2011. The effects of forest harvest intensity in combination with wind disturbance on carbon dynamics in Lake States Mesic Forests. Ecological Modelling 222, 144–153. https://doi.org/10.1016/j.ecolmodel.2010.09.009

Schowalter, T., 2017. Arthropod diversity and functional importance in old-growth forests of North America. Forests 8, 97.

Schrum, P., Scheller, R.M., Duveneck, M.J., Lucash, M.S., 2020. Base-Hurricane: A new extension for the Landis-II forest landscape model. Environmental Modelling & Software 133, 104833. https://doi.org/10.1016/J.ENVSOFT.2020.104833

Schulmann, T., Katurji, M., Zawar-Reza, P., 2015. Seeing through shadow: Modelling surface irradiance for topographic correction of Landsat ETM+ data. ISPRS Journal of Photogrammetry and Remote Sensing 99, 14–24. https://doi.org/10.1016/j.isprsjprs.2014.10.004

Shang, C., Coops, N.C., Wulder, M.A., White, J.C., Hermosilla, T., 2020. Update and spatial extension of strategic forest inventories using time series remote sensing and modeling. International Journal of Applied Earth Observation and Geoinformation 84, 101956. https://doi.org/10.1016/j.jag.2019.101956

Shanley, C.S., Pyare, S., Goldstein, M.I., Alaback, P.B., Albert, D.M., Beier, C.M., Brinkman, T.J., Edwards, R.T., Hood, E., MacKinnon, A., McPhee, M.V., Patterson, T.M., Suring, L.H., Tallmon, D.A., Wipfli, M.S., 2015. Climate change implications in the northern

coastal temperate rainforest of North America. Climatic Change 130, 155–170. https://doi.org/10.1007/s10584-015-1355-9

Simard, M., Lecomte, N., Bergeron, Y., Bernier, P.Y., Paré, D., 2007. Forest productivity decline caused by successional paludification of boreal soils. Ecological Applications 17, 1619–1637. https://doi.org/10.1890/06-1795.1

Smithwick, E.A.H., Harmon, M.E., Remillard, S.M., Acker, S.A., Franklin, J.F., 2002. Potential Upper Bounds of Carbon Stores in Forests of the Pacific Northwest. Ecological Applications 12, 1303–1317. https://doi.org/10.1890/1051-0761(2002)012[1303:PUBOCS]2.0.CO;2

Song, X., 1997. Relationships between coarse woody debris and understory vegetation in six forest ecosystems in British Columbia. University of British Columbia. https://doi.org/10.14288/1.0075189

Special Areas; Roadless Area Conservation; National Forest System Lands in Alaska, 2023. , Fed. Reg.

Spies, T.A., 2004. Ecological Concepts and Diversity of Old-Growth Forests. Journal of Forestry 102, 14–20. https://doi.org/10.1093/jof/102.3.14

Spies, T.A., Cline, S.P., 1988. Coarse woody debris in forests and plantations of coastal Oregon. From the forest to the sea: a story of fallen trees. Gen. Tech. Rep. PNW-GTR-229. Portland, OR: Pacific Northwest Research Station, Forest Service, US Department of Agriculture 5–23.

Spies, T.A., Franklin, J.F., 1996. The diversity and maintenance of old-growth forests. Biodiversity in managed landscapes: theory and practice. Oxford University Press, New York, New York, USA 296–314.

Stow, D.A., Hope, A., McGuire, D., Verbyla, D., Gamon, J., Huemmrich, F., Houston, S., Racine, C., Sturm, M., Tape, K., 2004. Remote sensing of vegetation and land-cover change in Arctic Tundra Ecosystems. Remote sensing of environment 89, 281–308.

Suchanek, T.H., Mooney, H.A., Franklin, J.F., Gucinski, H., Ustin, S.L., 2004. Carbon dynamics of an old-growth forest. Ecosystems 7, 421–426.

Suttles, W., Ames, K., Schoonmaker, P.K., von Hagen, B., Wolf, E.C., 1997. Pre-European history. The rain forests of home 255–274.

Tadono, T., Nagai, H., Ishida, H., Oda, F., Naito, S., Minakawa, K., Iwamoto, H., 2016. Generation of the 30 m-mesh global digital surface model by ALOS PRISM. The international archives of the photogrammetry, remote sensing and spatial information sciences 41, 157–162.

Ter Braak, C.J.F., 1986. Canonical correspondence analysis: a new eigenvector technique for multivariate direct gradient analysis. Ecology 67, 1167–1179. https://doi.org/10.2307/1938672

USDA Forest Service, 2022. Southeast Alaska Sustainability Strategy, Forest Management. US Department of Agriculture, Forest Service.

Vogeler, J.C., Cohen, W.B., 2016. A review of the role of active remote sensing and data fusion for characterizing forest in wildlife habitat models. Revista de Teledetección 1–14. https://doi.org/10.4995/raet.2016.3981

Walsh, S.J., 2018. Multi-scale Remote Sensing of Introduced and Invasive Species: An Overview of Approaches and Perspectives, in: Torres, M.D.L., Mena, C.F. (Eds.), Understanding Invasive Species in the Galapagos Islands, Social and Ecological Interactions in the Galapagos Islands. Springer International Publishing, Cham, pp. 143–154. https://doi.org/10.1007/978-3-319-67177-2_8

Wang, J.A., Sulla-Menashe, D., Woodcock, C.E., Sonnentag, O., Keeling, R.F., Friedl, M.A., 2019. ABoVE: Landsat-derived Annual Dominant Land Cover Across ABoVE Core Domain, 1984-2014. ORNL DAAC, Oak Ridge, Tennessee, USA.

Weiss, S.A., Marshall, A.M., Hayes, K.R., Nicolsky, D.J., Buma, B., Lucash, M.S., 2023. Future transitions from a conifer to a deciduous-dominated landscape are accelerated by greater wildfire activity and climate change in interior Alaska. Landsc Ecol 38, 2569–2589. https://doi.org/10.1007/s10980-023-01733-8

William Bourgeois, Clark Brinley, Valerie LeMay, Ian Moss, Nick Reynolds, 2018. British Columbia Forest Inventory Review Panel Technical Background Report. Office of the Chief Forester Division, British Columbia Ministry of Forests, Lands, Natural Resource Operations and Rural Development.

Wolken, J.M., Hollingsworth, T.N., Rupp, T.S., Chapin III, F.S., Trainor, S.F., Barrett, T.M., Sullivan, P.F., McGuire, A.D., Euskirchen, E.S., Hennon, P.E., Beever, E.A., Conn, J.S., Crone, L.K., D'Amore, D.V., Fresco, N., Hanley, T.A., Kielland, K., Kruse, J.J., Patterson, T., Schuur, E.A.G., Verbyla, D.L., Yarie, J., 2011. Evidence and implications of recent and projected climate change in Alaska's forest ecosystems. Ecosphere 2, art124. https://doi.org/10.1890/ES11-00288.1

Wootten, A., Terando, A., Reich, B.J., Boyles, R.P., Semazzi, F., 2017. Characterizing Sources of Uncertainty from Global Climate Models and Downscaling Techniques. Journal of Applied Meteorology and Climatology 56, 3245–3262. https://doi.org/10.1175/JAMC-D-17-0087.1

Wulder, M.A., Kurz, W.A., Gillis, M., 2004. National level forest monitoring and modeling in Canada. Progress in Planning 61, 365–381. https://doi.org/10.1016/S0305-9006(03)00069-2

Yatskov, M.A., 2016. The Impact of Disturbance on Carbon Stores and Dynamics in Forests of Coastal Alaska. Oregon State University.

Yatskov, M.A., Harmon, M.E., Barrett, T.M., Dobelbower, K.R., 2019. Carbon pools and biomass stores in the forests of Coastal Alaska: Uncertainty of estimates and impact of disturbance. Forest Ecology and Management 434, 303–317. https://doi.org/10.1016/J.FORECO.2018.12.014

Zhu, Z., Woodcock, C.E., 2014. Continuous change detection and classification of land cover using all available Landsat data. Remote Sensing of Environment 144, 152–171. https://doi.org/10.1016/j.rse.2014.01.011